EXPRESSION OF PERFORIN AND GRANZYME VARIANTS IN ADULT RAT

TESTES AFTER ETHYLENE DIMETHANE SULFONATE (EDS)-INDUCED

TESTOSTERONE DEPLETION

A DISSERTATION

SUBMITTED IN PARTIAL FULFILLMENT OF THE REQUIREMENTS

FOR THE DEGREE OF DOCTOR OF PHILOSOPHY

IN THE GRADUATE SCHOOL OF THE

TEXAS WOMAN'S UNIVERSITY

DEPARTMENT OF BIOLOGY

COLLEGE OF ARTS AND SCIENCES

BY

DIBYENDU DUTTA, B.Sc., M.Sc.

DENTON, TEXAS

AUGUST, 2011
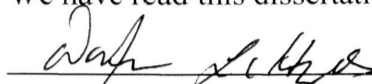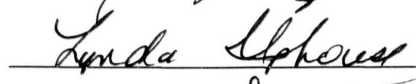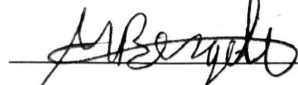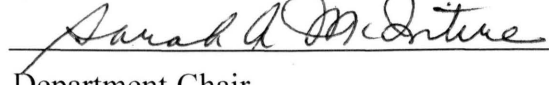
TEXAS WOMAN'S UNIVERSITY
DENTON, TEXAS

06/28/2011

To the Dean of the Graduate School:

I am submitting herewith a dissertation written by Dibyendu Dutta entitled "Expression of Perforin and Granzyme Variants in Adult Rat Testes after Ethylene Dimethane Sulfonate (EDS)-Induced Testosterone Depletion." I have examined this dissertation for form and content and recommend that it be accepted in partial fulfillment of the requirements for the degree of Doctor of Philosophy with a major in Molecular Biology.

Nathaniel Mills
Dr. Nathaniel Mills, Major Professor

We have read this dissertation and recommend its acceptance:

_____

_____

_____

_____

_____

_____
Department Chair

Accepted:

Jennifer Martin
_____
Dean of the Graduate School

DEDICATION

To my parents, Mr. Dilip Kumar Dutta and Mrs. Jayanti Dutta

ACKNOWLEDGEMENTS

I deem it a great pleasure to have the outstanding opportunity of executing this dissertation under the supervision of Dr. Nathaniel Mills (Professor), Dept. of Biology, Texas Woman's University, Texas, USA. He helped me whole-heartedly to develop myself and prepared me to attain success in future. His patient advice and challenging me in every aspect of my work helped me build my basics that are necessary for success.

I am also grateful to Dr. Lynda Uphouse (Professor), Dept. of Biology, Texas Woman's University, Texas, USA, for her cordial help in every moment of my difficulties. Besides helping me in a host of matters, she also taught me how to write scientifically and how to conceptualize problems.

I would like to thank my committee members, Dr. Sarah McIntire, Dr. Michael Bergel, Dr. Huanbiao Mo, and Dr. DiAnna Hynds for their support, inputs and critical evaluations of my dissertation.

I would also like to thank Dr. Laura Hanson and Dr. Brian Beck for helping me with various ideas and tools without which this work would not have been successful.

With equal felicity I thank my lab-mates, students and friends, especially, Teresa Brown and Karishma Patel for their support and help during such an important phase of my life. Without them it would have been impossible for me to live away from my home and family for such a long period.

ABSTRACT

DIBYENDU DUTTA

EXPRESSION OF PERFORIN AND GRANZYME VARIANTS IN ADULT RAT TESTES AFTER ETHYLENE DIMETHANE SULFONATE (EDS)-INDUCED TESTOSTERONE DEPLETION

AUGUST 2011

Testosterone is essential for regulation of spermatogenesis and testosterone withdrawal results in germ cell apoptosis. However, the mechanism for germ cell apoptosis is unknown. In testes, mature Leydig cells produce testosterone. Using ethane dimethane sulfonate (EDS), a Leydig cell-specific toxicant, to deplete testosterone, we investigated the relationship between granzyme and perforin, and germ cell apoptosis. To confirm effects of testosterone depletion, EDS-treated rats were compared with testosterone-replaced and testosterone-supplemented rats. At 5 and 7 days post-EDS treatment, rats were euthanized for tissue collection. Leydig cell loss was confirmed by the significant reduction in mRNA for *Lhr* (90%) and *Insl3* (99%), and testosterone depletion was confirmed by the undetectable level of testosterone in serum and testes of EDS-treated rats. Due to ablation of testosterone, there was testicular weight loss (18%) along with a significant increase in germ cell apoptosis (135 cells/mm^2 of testicular cross-section). However, no difference in testicular weight or numbers of apoptotic germ cells was observed in testosterone-replaced and testosterone-supplemented rats. Hence, although EDS eliminated Leydig cells, testosterone replacement maintained testicular

weight and germ cell viability. In addition to increased germ cell apoptosis, the mRNA levels for *grankyme K* (*GzmK*) and *perforin* (*Prf*) were also significantly higher (2- and 2.5-fold, respectively) in EDS-treated rats compared to controls. After testosterone replacement, the levels of *GzmK* and *Prf* mRNAs were restored. The mRNA levels for *Cd4* and *Cd8* were also significantly elevated (2- and 5-fold, respectively) following EDS treatment, whereas testosterone replacement partially reversed it. Therefore, it was hypothesized that testosterone depletion resulted in disruption of the blood-testis barrier allowing CD4$^+$ and CD8$^+$ T cells to migrate inside the seminiferous tubule. With recruitment of CD8$^+$ T cells inside the seminiferous tubule, *GzmK* and *Prf* were released to induce germ cell apoptosis. However, CD8$^+$ T cells were detected in the interstitium, whereas GZMK and PRF were detected inside the seminiferous tubule. This indicated that GZMK and PRF expression in testes may not be associated with CD8$^+$ T cells. Moreover, detection of GZMK and PRF proximal to residual bodies indicated their possible role in germ cell release during spermiation.

TABLE OF CONTENTS

LIST OF TABLES

LIST OF FIGURES

CHAPTER I

INTRODUCTION

Environmental exposure-induced male infertility is a matter of great concern in the developed world. The Third National Report from the Centers for Disease Control and Prevention (CDC) mentioned that humans are constantly exposed to hundreds of environmental chemicals, of which many are known as endocrine disrupting chemicals (Diamanti-Kandarakis *et al.* 2009). Chemicals such as phthalates and polychlorinated biphenyls that are used in making personal care products (perfumes and cosmetics) and lubricants for electrical insulators induce male infertility (Diamanti-Kandarakis *et al.* 2009). Infertility in men is due to a reduction in semen quality, sperm quantity, urogenital tract abnormalities and testicular germ cell cancer. All four of these conditions, either by themselves or collectively, constitute testicular dysgenesis syndrome (Skakkebaek *et al.* 2001). Constant exposure to endocrine disrupting chemicals results in androgen deficiency and impaired germ cell development (Boisen *et al.* 2001) resulting in testicular dysgenesis syndrome. Therefore, to find possible treatments for male infertility, it is important to understand the roles of androgens in testes and germ cell production and development.

Testes are the part of the male reproductive system from which sperm and androgen (testosterone) are secreted (Setchell & Breed 2006). The testicular capsule is composed of three distinct layers. The outermost layer is called the tunica vaginalis; the

middle layer is called tunica albuginea; and, the third and innermost layer is called tunica vasculosa (Steinberger & Steinberger 1975). Inside each testis, highly coiled tubules called seminiferous tubules form convoluted structures that empty their contents into the epididymis via the rete testis and the efferent ducts (Setchell & Breed 2006). Sperm are produced inside seminiferous tubules by the process called spermatogenesis.

Inside the seminiferous tubules, spermatogenesis begins from the primordial germ cells that give rise to the testicular germ cells, also called gonocytes, in the basal epithelium layer of the seminiferous tubules (Steinberger & Steinberger 1975). Gonocytes give rise to spermatogonia, which divide by mitosis and differentiate to become type A-spermatogonia (Fig. 1). Type A-spermatogonia proliferate to become type B-spermatogonia, which, in turn, differentiate to become more specialized meiotic cells called spermatocytes. Spermatocytes undergo meiotic divisions and give rise to haploid round spermatids, which later undergo morphological differentiation into elongated spermatids and then spermatozoa (de Rooij 2001). There are approximately 350,000 stem cells in the rat testis and, from each stem cell, approximately 17,000 sperm are made (de Rooij 2001). During this division and differentiation process, germ cells constantly move from the basal layer towards the lumen via the adluminal compartment of the seminiferous tubule. The migration, division and differentiation of germ cells during spermatogenesis require strict regulatory activities of different cells present inside and outside the seminiferous tubules.
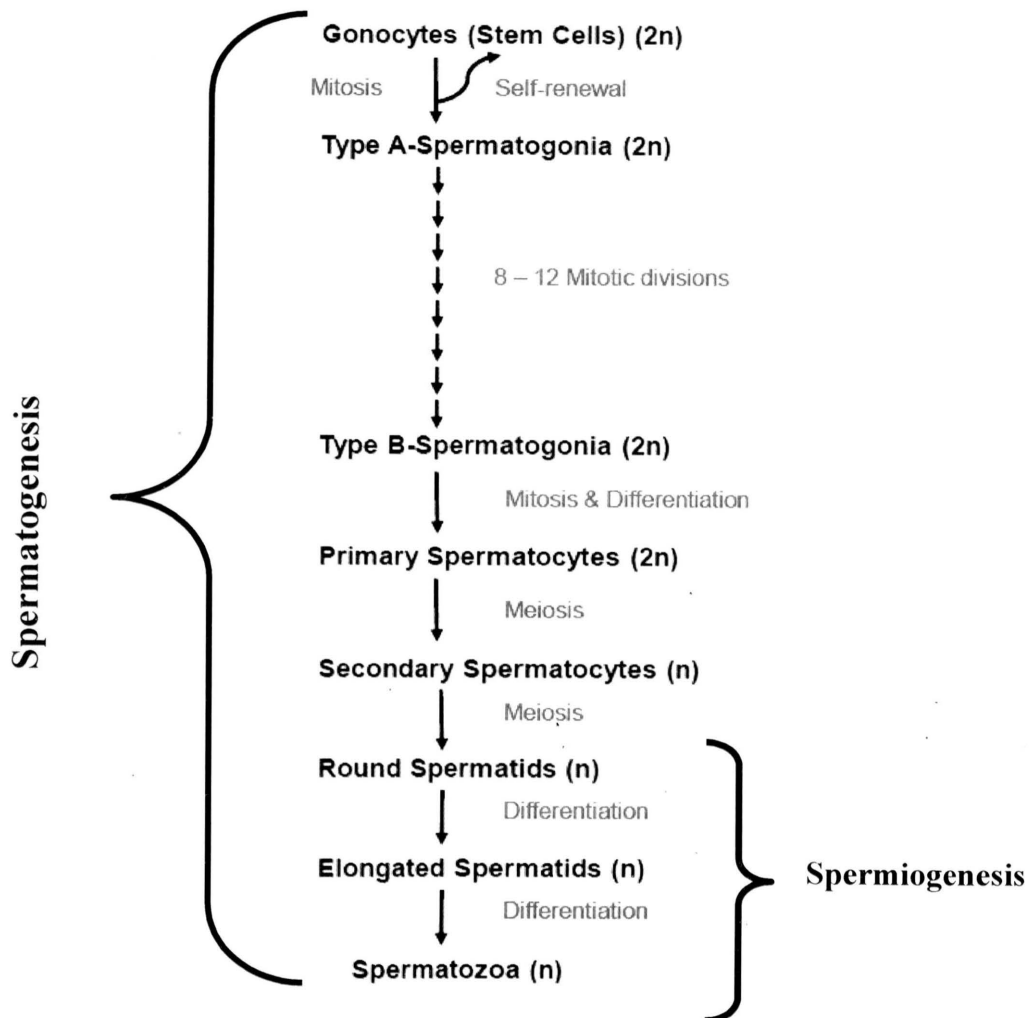
Figure 1: The process of spermatogenesis. Testicular stem cells undergo mitosis to become type A-spermatogonia or self-renew to maintain the stem cell population. Type A-spermatogonia undergo 8 – 12 mitotic divisions to increase the number of potential sperm. Each type B-spermatogonia divides and subsequently differentiates to become meiotic spermatocytes. Spermatocytes undergo meiosis to become haploid, round spermatids. Through morphological differentiation, round spermatids metamorphose to elongated spermatids which eventually become sperm. This morphological differentiation process is called spermiogenesis [modified from (de Rooij 2001)]. Diploid (2n), Haploid (n).

Regulation of spermatogenesis occurs in three concentric circles – intrinsic, interactive and extrinsic (Eddy 2002). Intrinsic regulation is managed by an evolutionarily conserved genetic program that determines specific and unique sequential events of spermatogenesis. Extrinsic regulation of spermatogenesis is governed by secretions from the anterior pituitary (luteinizing hormone and follicle stimulating hormone) and from Leydig cells (testosterone). Sertoli cells act as the interactive regulator of spermatogenesis by modulating the endocrine signals via androgen receptors.

Sertoli cells are irregularly shaped, columnar cells that extend from the basal to the adluminal compartment of the seminiferous tubule and occupy a volume of approximately 17 to 19% of the total seminiferous epithelium of adult rats (Griswold 1998). During puberty, immature Sertoli cells permanently cease all divisional activities and become mature Sertoli cells (Griswold 1998). The number of mature Sertoli cells remains constant in mammalian species at approximately 16×10^6 cells/gram of testis (Mori & Christensen 1980). Sertoli cells express androgen receptors and secrete various proteins and luminal fluid to modulate spermatogenesis (Mruk & Cheng 2004). The Sertoli cell occupies a large area inside the seminiferous tubule and the plasma membrane of each Sertoli cell remains in direct surface contact with about 50 developing germ cells at a time (Russell 1993). Such direct surface contact helps Sertoli cells to form barriers for maintaining a secluded, immune-privileged environment for the developing germ cells. The junctional barrier between adjacent Sertoli cells constitutes the blood-testis barrier (BTB) and the junction between a Sertoli cell and a germ cell is called the ectoplasmic specialization (Mruk & Cheng 2004). Inside the seminiferous epithelium,

4

germ cells are embedded in the surface area of Sertoli cells and are held in their location by the blood-testis barrier. The Sertoli cell to germ cell ratio in every species is fixed (Sharpe 1994). Just before the onset of puberty, the density of spermatogenic stem cells in the testis is achieved through an early and massive apoptosis in the seminiferous tubule (Eddy 2002). Apoptosis is also observed after the attainment of puberty. During normal spermatogenesis, mistimed cell division and improper differentiation may lead to defective sperm formation. Defective germ cells are eliminated from the testis by apoptosis (Sharpe 1994) and apoptotic germ cells are phagocytosed by Sertoli cells (Mruk & Cheng 2004).

Although apoptosis is essential in maintaining a viable germ cell population in the testes, abnormally high apoptosis of germ cells may lead to male infertility. Testosterone depletion, physiological abnormalities, toxic insults and chemotherapy can increase germ cell apoptosis and, therefore, induce sterility (Nandi *et al.* 1999, Woolveridge *et al.* 1999, Woolveridge *et al.* 2001, Show *et al.* 2004, O'Shaughnessy *et al.* 2008, Show *et al.* 2008). In this study, we are particularly interested in understanding how depletion of testosterone induces germ cell apoptosis in adult rats.

Testosterone is produced by Leydig cells that are located in the interstitium of the testis and occupy approximately 2.7% of the total testicular volume (Mori & Christensen 1980). In rats, approximately 22 million Leydig cells are present per gram of testis (Mori & Christensen 1980) and each Leydig cell is estimated to produce approximately 0.4 pg of testosterone per day. Therefore, in an adult rat, approximately 6.1 ng of testosterone is produced per gram of testis in one minute (Free & Tillson 1973). The enzymes involved

in the biosynthesis of testosterone are predominantly located in the smooth endoplasmic reticulum of the Leydig cells and follow the Δ^4 pathway of steroidogeneis (Stocco & McPhaul 2006).

Testosterone production and the functioning of Sertoli and Leydig cells are dependent on the hypothalamus and pituitary gland secretions. Gonadotropin releasing hormone (GnRH) from the hypothalamus stimulates the anterior pituitary to secrete luteinizing hormone (LH) and follicle stimulating hormone (FSH) (Sharpe 1994). Leydig cells synthesize testosterone under the influence of LH by increasing cholesterol desmolase activity (Stocco & McPhaul 2006); FSH upregulates receptors for LH on Leydig cells to facilitate testosterone synthesis (Stocco & McPhaul 2006). Follicle stimulating hormone also acts on Sertoli cells to control the opening and closing of the blood-testis barrier and leads to synthesis of various hormones and peptides, such as activin and inhibin (Griffin 2004). Activin acts as a positive feedback regulator for FSH secretion, and inhibin negatively regulates FSH production from the anterior pituitary (Griffin 2004) (Fig. 2). Inside the seminiferous tubule, FSH supports development of spermatogonia and entry of spermtocytes into meiosis (O'Donnell *et al.* 2006). Follicle stimulating hormone, in cooperation with testosterone, helps in survival of spermatocytes, production of round spermatids and release of sperm (spermiation) (O'Donnell *et al.* 2006).
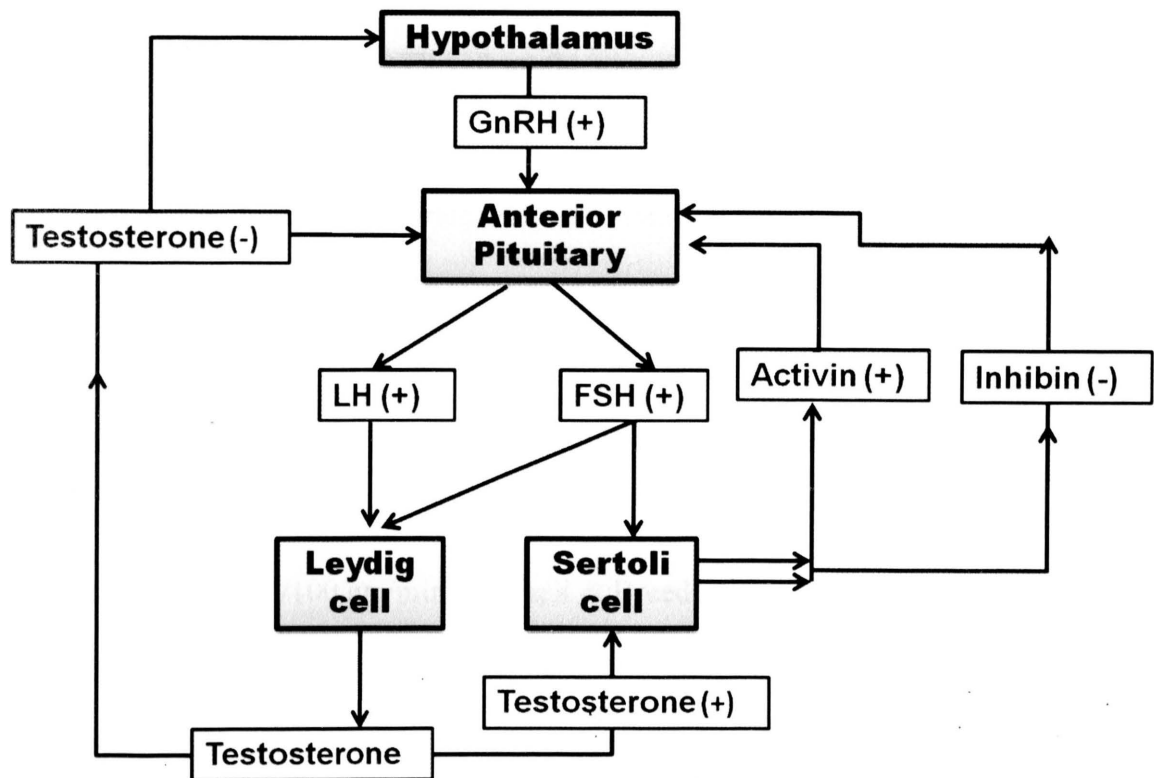
Figure 2: Hypothalamic-pituitary-testicular axis. Schematic representation of hormone interrelationships; (+) indicates positive effect; (-) indicates negative effect [modified from (Griffin 2004)].

Testosterone produced by Leydig cells is not stored but is secreted into the interstitial fluid (Sharpe 1994). Therefore, the transport of testosterone to its receptor is governed by the testicular blood flow. The veins in the testis run parallel to the arteries but in the opposite direction and drain arterial contents in the interstitium (Setchell & Breed 2006). Capillaries inside the testis are confined to the intersitium and are not perforated (Setchell & Breed 2006). These capillaries form networks that run parallel to the seminiferous tubules and around the tubules (Setchell & Breed 2006). Blood flow is comparatively lower in the testis compared to other organs. In rats, testicular blood flow is approximately 30 ml/100 gm/min (Setchell & Breed 2006). Along with blood vessels, 11 to 15 lymphatic vessels are also present in the testicular interstitium and then contents are emptied into the epididymis via efferent ducts (Setchell & Breed 2006). Secreted testosterone is transported to the germ cells and into seminiferous tubular fluid via Sertoli cells (Sharpe 1994). From the interstitium, testosterone enters into the lymphatic spaces and capillaries of the interstitium (Setchell & Breed 2006). Through these capillaries, testosterone is transported into the testicular vein (Setchell & Breed 2006), where the testosterone concentration is approximately equal to that of the seminiferous tubular fluid (50 – 100 ng/ml) (Sharpe 1994). As the testicular venous blood with high testosterone starts to leave the testis, testosterone is exchanged back into the arterial blood through the countercurrent exchange mechanism (Sircar 2008) (Fig. 3). This countercurrent testosterone exchange mechanism is believed to be responsible for maintaining approximately a 40-fold higher testosterone concentration in the testis compared to the circulating blood (Sharpe 1994).

8
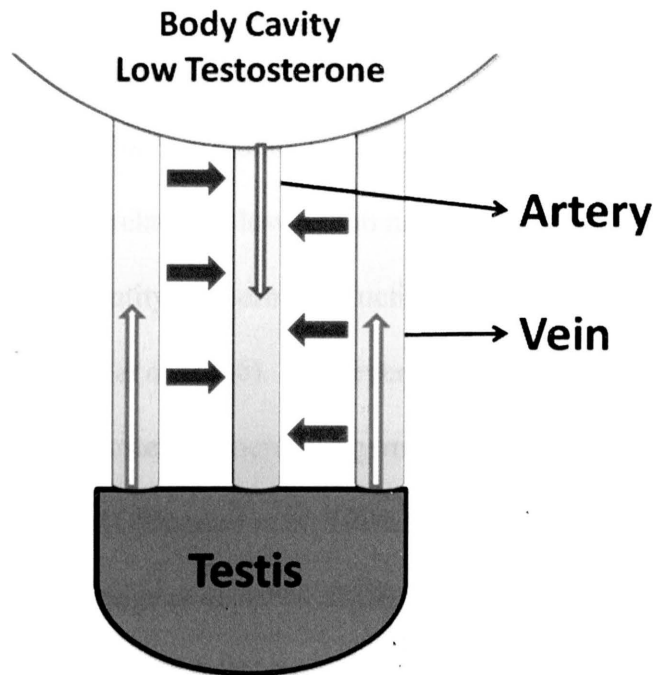
Figure 3: Countercurrent exchange of testosterone in the testis. Testosterone made in the testis goes into venous blood that is destined to be taken inside the body cavity. While blood moves upwards, testosterone is exchanged from the venous blood to the arterial blood that goes inside the testis. Thus, a high concentration of testosterone is always maintained inside the testis compared to other body parts or circulating blood [modified from (Sircar 2008)].

Although maintenance of testosterone concentration in the testis is essential for spermatogenesis, the minimum necessary concentration is unknown (O'Donnell et al. 1994, Sharpe 1994, Henriksen et al. 1995, Griswold 1998, Woolveridge et al. 1999, Griffin 2004, Kerr et al. 2006, O'Donnell et al. 2006, Stocco & McPhaul 2006, McCabe et al. 2010). Although a relatively lower than normal testosterone level can maintain spermatogenesis, the quantity of sperm production is estimated to decline by 20% (Sharpe 1994, O'Donnell et al. 2006). However, it is generally accepted that an undetectable level of testosterone increases germ cell loss, mainly by apoptosis, which can then lead to sterility (O'Donnell et al. 1994, Sharpe 1994, Henriksen et al. 1995, Griswold 1998, Woolveridge et al. 1999, Griffin 2004, Kerr et al. 2006, O'Donnell et al. 2006, Stocco & McPhaul 2006, McCabe et al. 2010).

Apoptosis involves an orchestrated series of biochemical events leading to characteristic cell morphological changes and ordered cell death. To eliminate the defective cells from various physiological systems and reduce the chances of local inflammation, the apoptotic process is executed in such a way that the cellular fragments and damaging proteins can be safely disposed (Schwartzman & Cidlowski 1993). The earliest morphological changes observed during apoptosis include the loss of cell junctions and other specialized plasma membrane structures followed by condensation of cytoplasm, coalition of nuclear chromatin into large masses, and fragmentation of the nucleus. Consequently, the cytoplasmic volume decreases markedly with the apparent loss of intracellular fluid and ions (Schwartzman & Cidlowski 1993). Loss of intracellular fluid is the result of the dilation of the endoplasmic reticulum that forms

10

vesicles, which fuse with the plasma membrane to empty their contents outside the cell membrane (Schwartzman & Cidlowski 1993). The cell then transiently adopts a deeply convoluted outline and eventually breaks up into several membrane-bound, smooth-surfaced apoptotic bodies containing a variety of intact cytoplasmic organelles and some nuclear fragments. Apoptotic bodies are typically phagocytosed, mainly by the nearby mononuclear phagocytes, and sometimes by normal epithelial cells, vascular endothelium, or tumor cells (Schwartzman & Cidlowski 1993). In the testis, such phagocytosis activity is also observed in Sertoli cells (Mruk & Cheng 2004).

The process of apoptosis is controlled by a diverse range of cellular signals which may be either extracellular (extrinsic inducers) or intracellular (intrinsic inducers). Extracellular signals may include hormones, growth factors and cytokines, and the intracellular apoptotic signaling response may occur as a result of various stressors such as viral infections (Schwartzman & Cidlowski 1993). Intrinsic pathway-induced apoptosis is mainly due to cellular stress signals like DNA damage. The extrinsic pathway is commonly observed during growth and development of an organism or tissue where unwanted cells are eliminated by apoptosis (Schwartzman & Cidlowski 1993). During the intrinsic pathway, the *B-cell lymphoma-2* (*Bcl-2*) family of genes, such as *Bad, Bok, Bcl-W, Bcl-XL* and *Bcl-2* are involved (Sasi *et al.* 2009); the extrinsic pathway involves mainly the *tumor necrosis factor* (*Tnf*) family of genes, such as *Fas, FasL* and *Tnfα* (Wallach *et al.* 2008). The extrinsic pathway can also be initiated through cytotoxic CD8^{+} T lymphocytes (CTLs), through secreted cytotoxic granules. These cytotoxic granules contain proteolytic enzymes, such as perforin (PRF), that create pores on the

11

membrane of the target cells, and granzymes (GZM), that enter through those pores to induce apoptosis (Andersen *et al.* 2006). Both extrinsic and intrinsic pathways may merge to activate effector caspases for execution of apoptosis (Marsden & Strasser 2003). Induction of apoptosis may also take place by interaction between different pathways. For example, TNF members are sometimes required to activate CTLs for release of PRF and GZM into the target cells (Andersen *et al.* 2006), and GZMs can activate the pro-apoptotic BCL-2 member, BID, thereby inducing the intrinsic pathway for apoptosis (Froelich *et al.* 2004). Among the regulators of intrinsic and extrinsic pathways, the role of GZM and PRF in testes remains elusive and is of particular interest.

Granzymes and perforin are expressed inside activated CTLs, which are activated when they come in contact with an antigen-class I major histocompatibility complex (MHC) on the surface of a target cell (Goldsby *et al.* 2000). Upon activation, CTLs, they proliferate and differentiate into effector cells called cytotoxic T lymphocytes (CTLs). These CTLs express CD8 glycoprotein on their cell membrane (Goldsby *et al.* 2000) and thus are called CD8^{+} T cells. These CD8^{+} T cells contain two types of storage granules, PRF and GZM. Perforin is a 65 kDa pore-forming protease, and granzymes are serine proteases (Goldsby *et al.* 2000). Upon receptor mediated interaction with the target cell, CD8^{+} T cells concentrate storage granules and conjugate with the target cell through ligand-receptor interaction (Chavez-Galan *et al.* 2009). After conjugation, the storage granules reorient themselves and release their contents through exocytosis into the junctional space of the two cells. Perforin monomers released from the granules polymerize in the presence of Ca^{2+} and form cylindrical pores on the cell membrane of

12

the target cell. Through these pores, granzymes enter into the target cell and induce apoptosis (Chavez-Galan *et al.* 2009). However, granzymes are proteases and cannot induce fragmentation of DNA, which is an absolute necessity for cells to undergo apoptosis. Instead, granzymes activate effector caspases by protelytically cleaving pro-caspaeses, which can subsequently induce DNA fragmentation and lead the cell toward apoptosis (Goldsby *et al.* 2000).

Numerous macrophages, dendritic cells, mast cells, natural killer cells and lymphocytes reside in the testicular interstitium (Hedger & Hales 2006). The lymphocyte population in the rat testis is assumed to be approximately 10 to 20% of the total leukocyte population in the rat testis (Wang *et al.* 1994). Although CTLs proliferate significantly in the rat testis after testosterone depletion (Wang *et al.* 1994), they were not reported to migrate through the BTB into the seminiferous tubule. However, GZMB (Hirst *et al.* 2001) and GZMN (Takano *et al.* 2004) are expressed inside the seminiferous tubules of human and mice testes. The BTB is not a rigid impermeable barrier and it remains in a constant state of flux to allow developing germ cells to move towards the lumen of the seminiferous tubule during development of germ cells (Hedger 2002). In fact, the BTB is completely broken down periodically in seasonal breeders (Pelletier 1986). Moreover, functionality and intactness of the BTB is testosterone-dependent (Russell 1993, O'Donnell *et al.* 1996, Mruk & Cheng 2004, McCabe *et al.* 2010). Therefore, it is hypothesized that CTLs can potentially enter into the seminiferous tubule (Dym & Romrell 1975) and may induce inflammation and apoptosis of germ cells following testosterone depletion. In fact, many inflammatory and immune regulatory

13

cytokines [interlukin-1 (IL-1), interlukin-6 (IL-6), tumor necrosis factor-α (TNF-α) and transforming growth factor-β (TGF-β)] that may facilitate proliferation of CTLs, are expressed in Sertoli cells under the influence of FSH (Hedger & Hales 2006). In spermatozoa, class I and class II MHCs are also expressed, presumably to protect sperm from immune cells and infections in the reproductive tract (Hedger & Hales 2006). However, very little is known about the relationship between CTLs and testosterone in testes.

In the current study, the localization of CTLs and the expression and co-localization of granzymes and perforin in the rat testis following testosterone withdrawal is investigated. Testosterone is depleted by selective elimination of adult Leydig cells from rat testes using ethylene dimethane sulfonate (EDS). Ethane dimethane sulfonate is a non-volatile methanesulfonic di-ester of ethylene glycol (Jackson & Jackson 1984). Like other glycol di-esters [$CH_3SO_2O(CH_2)_nOSO_2CH_3$] that are used in chemotherapy (busulfan), EDS also possesses mild alkylating properties and is cytotoxic (O'Shaughnessy $et\ al.$ 2008). However, unlike busulfan, EDS has low toxicity on primary cells of bone marrow and germ cells, but, in rats, causes depletion of testosterone by selectively killing the adult Leydig cells (Taylor $et\ al.$ 1998). A single dose of EDS (75 mg/kg of body weight) in rats initiates temporary loss of Leydig cells and completely eliminates them by 24 hours (Henriksen $et\ al.$ 1995). The elimination of the Leydig cells is a temporary event because, after 21 days of treatment, Leydig cells start to reappear through differentiation of mesenchymal cells and completely re-populate the interstitium of the testis by 60 days post-EDS treatment (Ariyaratne $et\ al.$ 2003). Although the

14

Leydig cells are eliminated from testes within 24 hours post-EDS treatment, the effect of testosterone-withdrawal cannot be seen on germ cells until after 3 days due to the presence of local residual testosterone (Henriksen *et al*. 1995). After 3 days of EDS treatment, however, when testosterone has been cleared from the testes, germ cell apoptosis begins. By the 7th day, the rate of germ cell apoptosis becomes high and, by the 14th day, the seminiferous tubules are almost completely devoid of germ cells (Henriksen *et al*. 1995). This results in the progressive reduction of testicular weight and size, mainly due to the loss of different germ cell populations (Ariyaratne *et al*. 2003). By day 21, the concentration of testosterone in the testis starts to elevate, peaks after 28 days, and attains the normal (control) concentration level around 60 days post-EDS treatment. At this point, normal spermatogenesis is fully restored (Ariyaratne *et al*. 2003). Hence, this is a good model to study gene expression in the testis and determine testosterone-dependent or responsive genes. With this model we investigated the expression patterns of granzyme variants and perforin in rat testes.

Although different GZM variants are present in testes (Takano *et al*. 2004), their relative abundance, testosterone-responsiveness and localization are unknown. Moreover, presence of PRF, the protein that help GZM to enter into target cells was never reported in testes. In rats, there are seven known *Gzm* variants – *GzmA, GzmB, GzmC, GzmF, GzmK, GzmM* and *GzmN* (Grossman *et al*. 2003). It is hypothesized that loss of testosterone would result in increased expression of *Prf* and at least one, if not all, *Gzm* variants in EDS-treated rat testes. It is also hypothesized that exogenous testosterone replacement after EDS treatment would restore (maybe partially) the normal

15

expression levels of *Prf* and *Gzm* in rat testes. Since *Gzm* and *Prf* are expressed in CTLs (Andersen *et al*. 2006), abundance of granzyme and perforin containing cells (CD8^{+} T cells) is expected to follow a pattern similar to that of *Gzm* and *Prf*. Moreover, since testosterone depletion results in germ cell apoptosis (Nandi *et al*. 1999, Taylor *et al*. 1999, Woolveridge *et al*. 1999, Woolveridge *et al*. 2001), it is expected that CTLs could mediate germ cell apoptosis through GZM and PRF by migrating inside the seminiferous tubule. Hence, in the testosterone-depleted rat testis, CD8^{+} T cells along with GZM and PRF are expected to be localized inside the seminiferous tubule. However, CD8^{+} T cells may not migrate at all inside the seminiferous tubule and *Gzm* and *Prf* may not show any difference after testosterone depletion. Since GZMs are known to have non-apoptotic roles in some systems (Buzza & Bird 2006), it is possible that, in the testis, they may regulate some non-apoptotic proteolytic function such as remodeling of BTB and other extracellular matrices during germ cell development.

Therefore, the specific aims for this project are to determine: (1) whether *Prf* and *Gzm* expression are associated with germ cell apoptosis in rat testes following EDS-induced testosterone depletion; and, (2) whether *Prf* and *Gzm* expressions are regulated by testosterone in rat testes.

CHAPTER II

MATERIALS AND METHODS

Drugs

Ethylene dimethane sulfonate (EDS) is not commercially available. Hence, EDS was synthesized in our laboratory using a previously described method (Jackson & Jackson 1984) and was dissolved in 25% dimethylsulfoxide (DMSO). Testosterone propionate (TP) (Sigma) was dissolved in sesame seed oil (SSO) (20 mg/ml).

Animals

Adult male Sprague-Dawley rats weighing approximately 250 – 300 gm and 90 days of age were purchased from Charles River Laboratories and acclimated to the University vivarium for at least 10 days with water and food provided *ad libitum*. Rats were treated for 5 and 7 days before tissue collection. Sixty rats were randomly assigned to ten treatment groups with an n = 6/group, five groups for each tissue collection time point. The groups were: [1] No treatment (NT); [2] Vehicle (VEH) (DMSO + SSO); [3] Testosterone-supplemented (TES); [4] EDS; and [5] EDS + TES (testosterone-replaced).

Treatment

Ethylene dimethane sulfonate was injected intraperitoneally (ip) as a single dose of 75 mg/kg of body weight to the EDS and EDS + TES groups. For testosterone supplementation and replacement, TP at 10 mg/kg of body weight was injected

subcutaneously (sc) into TES and EDS + TES groups. On day 0, rats in every group (except NT) received either DMSO or EDS and either SSO or TP (Table 1). For maintenance of testosterone in the circulation in groups TES and EDS + TES, rats in these groups received TP on the initial day of treatment (day 0) and then on 2nd, 4th and 6th day. Rats were sacrificed on the 5th day (for 5 day study) and on the 7th day (for 7 day study). All protocols for animal care and usage were followed in accordance with the NIH guidelines and were approved by Texas Woman's University's Institutional Animal Care and Use Committee (IACUC) (Protocol # 2007-05).

Table 1: Treatment regimen for 5 day and 7 day post-EDS treatment study

	DMSO[1]	EDS[2]
SSO[3]	DMSO & SSO (VEH)	EDS & SSO (EDS)
TP[4]	DMSO & TP (TES)	EDS & TP (EDS + TES)

Hormone Measurements

Trunk blood collected after decapitation of the rats was allowed to coagulate for 30 min on ice followed by centrifugation at 8300 x g for 10 min at 4 °C to collect serum for measurement of circulating testosterone concentrations. For measurement of intratesticular testosterone (ITT), approximately 200 mg of testes after decapsulation

[1] Dimethylsulfoxide

[2] Ethylene dimethane sulfonate

[3] Sesame seed oil

[4] Testosterone Propionate

(removal of tunica albuginea) were homogenized in 5 ml of 20 mM $NaC_2H_3O_2$ (sodium acetate), pH 5.0, for one minute. A pH of 5.0 releases testosterone from androgen binding proteins and allows more accurate measurement of total testosterone in samples (O'Donnell *et al*. 1994). Homogenates were centrifuged at 8000 x g for 10 min at 4 °C and supernatants were collected for measurement of ITT. Serum testosterone and ITT were both measured with a radioimmunoassay (RIA) kit having a detection limit of 0.05 ng/ml (Testosterone RIA DSL– 4100, Webster, TX). Radioimmunoassay is a competitive inhibition binding assay where a constant amount of anti-testosterone antibody (known) is coated in the tube provided in the kit. A small amount of radiolabeled testosterone (I^{125}) plus increasing amounts of unlabelled reference standard or sample are added to the tubes. After 1 hr of incubation, the antibody-bound (labeled & unlabelled) testosterone is separated from the free or unbound testosterone. Because a fixed amount of antibody and labeled testosterone is present in each assay tube, the amount of labeled testosterone bound to antibody (the measured radioactivity by Beckman's Gamma 5500) depends on the concentration of unlabeled testosterone in either the standard or samples. The higher the concentration of unlabeled testosterone, the more labeled testosterone is displaced from the antibody and thus lower radioactivity is bound to the fixed amount of antibody in the tube. A standard curve is generated by plotting the ratio of the amount of labeled testosterone bound in the presence of the standard to the amount bound in the absence of any unlabeled testosterone as a function of amount of standard. Quantification of the amount of testosterone present in the serum and testicular samples is done by interpolation of the standard curve.

19

RNA Extraction

Total RNA was extracted using TRIzol (Invitrogen) according to the manufacturer's protocol. For extraction of total RNA, approximately 200 mg of testis from each rat was homogenized in 2.0 ml TRIzol with an Ultra-Turrax homogenizer for 1 min by a small generator probe at 2300 rotations/min in a 15 ml polypropylene tube. The homogenate was incubated for 15 min in a 30 °C water bath. Following incubation at 30 °C, 0.20 ml of chloroform/ml of TRIzol was added to the homogenates and vortexed vigorously. The chloroform containing homogenate was incubated at room temperature for 15 min followed by centrifugation at 9000 x g for 15 min at 4 °C. Centrifugation resulted in the separation of the homogenate into two distinct phases, a clear (aqueous) phase on top of a red layer (organic phase). The aqueous phase (containing RNA) was transferred to a new tube and an equal volume of 100% isopropanol was added. The tubes were vortexed and incubated at –20 °C for 30 min to facilitate the precipitation of total RNA. The organic phase was discarded in chemical waste. Tubes were centrifuged at 9000 x g for 20 min at 4 °C to collect total RNA and the alcohol supernate was decanted leaving a white pellet at the bottom of each tube. One milliliter of 75% ethanol for each milliliter of TRIzol was added to the RNA pellets and vortexed thoroughly to wash any phenol residue from the RNA pellets. The RNAs were centrifuged again at 9000 x g for 20 min at 4 °C. The supernate of ethanol was decanted and the pellets air dried for 20 min at room temperature. The RNA pellets were dissolved in 500 µl Tris-EDTA (1.0 mM Tris and 0.10 mM EDTA) and stored at – 20 °C for further analysis.

Quantification of Total RNA

The extracted total RNAs were diluted 100-fold in Tris-EDTA and subjected to spectrophotometrical analysis to assess purity and intactness. The purity was assessed by the A_{260nm}/A_{280nm} ratio with ratios of $1.8 - 2.1$ considered to be free of any protein contamination. The extinction coefficient of 25 A_{260nm}/mg of RNA was used to determine total RNA concentration in each extract. From each extract, 3.0 μg of RNA was subjected to 1.5% agarose gel electrophoresis in Tris-Acetate-EDTA (TAE) buffer and stained for an hour with 0.5 μg/ml of ethidium bromide. The quality and intactness of RNA was analyzed from the gel by calculating the ratio of 28S/18S bands with the help of Alpha Innotech's FluorChem HD2 gel imaging software. Ratio of $1.2 - 1.5$ was considered to be of sufficient purity for further analysis.

Reverse Transcription Polymerase Chain Reaction (RT-PCR)

Representative samples of total RNAs (2.0 μg) from each testis were used to make complementary DNA (cDNA) using the Invitrogen SuperScript III® First-Strand Synthesis kit for reverse transcription in a thermal cycler (PTC-100 from MJ Research). To synthesize cDNA, 2.0 μg of total RNA was mixed with 1.0 μl of 50 μM oligo $(dT)_{20}$ (to target the polyA tail of mRNAs) and 1.0 μl of dNTP set containing 20 mM of each dNTP. The reaction mix was heated to 65 °C for 5 min to denature the secondary structures of the RNA. To that RNA mix, 10.0 μl of cDNA synthesis mix [2.0 μl of 10X RT buffer, 1.6 μl of 25 mM $MgCl_2$, 2.0 μL of 0.10 M DTT, 1.0 μl of RNaseOUT (40 U/μl), and 1.0 μl of SuperScript III® Reverse Transcriptase (200 U/μl) + 2.40 μl of deionized H_2O] were added and incubated for 50 min at 48 °C to synthesize cDNA. The

cDNA synthesis reaction was terminated by denaturing the reverse transcriptase at 85 °C for 5 min. From the resultant RNA/DNA hybrid, RNA was digested with 1.0 µl of RNase H at 37 °C for 40 min. From the resultant 21.0 µl of final reaction volume of cDNA, an aliquot was diluted 25-fold with 25 µg/ml acetylated-BSA (Invitrogen) for quantitative real-time PCR (qPCR).

Primer Design and Function

Since DNA polymerase requires an open 3' –OH group for strand extension, primers are required to initiate DNA synthesis. The selected genes for this study were targeted by designing gene-specific primers of 20 to 27 nucleotides for both forward (+) and reverse (–) strands of the DNA encoding those genes. To keep the cycle time short and to obtain better completion of the dsDNA fragments, the primers were designed to produce short dsDNA products with 3' specific primer sets. Each primer had a T_m of 64 – 66 °C and 40 – 60% GC content. The product lengths of the amplified cDNAs were kept to approximately 210 to 300 bp to have comparable cycle numbers for the products. The primer sets for the targeted region of the genes were picked from two different exons to ensure that the amplified cDNAs were only from the original cDNAs and not from any genomic DNA that might be present as a contaminant from the RNA extraction process. If the genomic DNA is amplified, the product lengths will be longer (product comprised of lengths of exons and introns) than the fragments obtained from the amplification of cDNAs. All primers were designed using Invitrogen's Vector NTI® Advance 11 software. Primer sequences of the genes for this study are listed in Table 2.

Table 2: Primer sequences of genes of interest

Gene	GenBank® Accession Number	Primer Sequences	Product Length
Lhr	NM_012978	**Fwd:** TGCGGTGCAGCTGGCTTCTTTACTG **Rev:** ATGGGGAGGCAGATGCTGACCTTC	237 bp
Inls3	NM_053680	**Fwd:** TGCAGTGGCTGGAGCAACGACATC **Rev:** TTCATTGGCACAGCTGTNAGGTGGG	265 bp
Prf	NM_017330	**Fwd:** ATTCATGCCAGTGTGTGTGCCAGG **Rev:** AGCCATTGTCAGCATCCCAGACCTG	295 bp
GzmA	NM_153468	**Fwd:** GAAATCTGAGGTCATTCTTGGGGCTCA **Rev:** TGGTTCCTGGTTTCACATCATCCCC	215 bp
GzmB	NM_138517	**Fwd:** AGTGATCAACCCTGTCCTTGGCAGATG **Rev:** CAAAGAGCACACCAGTGACTTGGGTC	235 bp
GzmK	NM_017119	**Fwd:** AAGCTTCGCACGGCTGCAGAACTG **Rev:** GCGATCCCCTGCACAGATCATGTC	250 bp
GzmN	NM_001191116	**Fwd:** CGCAAAGACCACGTAAATCCAGGG **Rev:** CGAGTCACCCTTGGAAGGAGCCTC	222 bp
Cd4	NM_012705	**Fwd:** AGTTCCAGCTGTCCGAAACGCTCC **Rev:** AAGTTCCAGCTGTCCGAAACGCTCC	237 bp
Cd8	NM_031539	**Fwd:** GCCTGAACTGCTGCAAGTCCTGTG **Rev:** GACGCCAAAAAGCCAGTCATGCTG	231 bp
Gapdh	NM_017008	**Fwd:** TGAACGGGAAGCTCACTGGCATGG **Rev:** CAATGCCAGCCCCAGCATCAAAG	234 bp

Quantitative Real-time Polymerase Chain Reaction (qPCR)

Quantitative real-time PCR (qPCR) was conducted using Roche's FastStart SYBR Green Master Mix kit in Opticon Monitor 3 real-time PCR system (Bio-Rad) for quantification of mRNA abundance. A 25.0 µl reaction mixture was made by adding 13.0 µl of the Roche's FastStart SYBR Green Master Mix, 1.5 µl of 10 µM forward primer, 1.5 µl of 10 µM reverse primer, 6.0 µl of the diluted cDNA (1:25) sample from the RT reaction and 3.0 µl of deionized H_2O. Thermal cycling was set at 95 °C for 10 min for the activation of the Taq polymerase. Then 40 cycles of template denaturation at 94 °C for 30 sec, primer annealing at 60 °C for 25 sec, extension for 25 sec at 72 °C and fluorescence reading at 78 °C were performed. After 40 cycles, the temperature was ramped slowly to obtain the melting curve of the amplified dsDNA product to establish the quality and accuracy of the dsDNA synthesis. The qPCR products were also assessed by agarose gel (1.5%) electrophoresis. For each gene, one band is expected in each lane of their respective product sizes. Reactions with no template were run concurrently as negative controls and glyceraldehyde 3-phosphate dehydrogenase (*Gapgh*) was used as the housekeeping gene. The difference in quantity of the mRNAs expressed were performed by the $2^{-\Delta\Delta C(t)}$ method (Kubista *et al.* 2006) (Fig. 4).
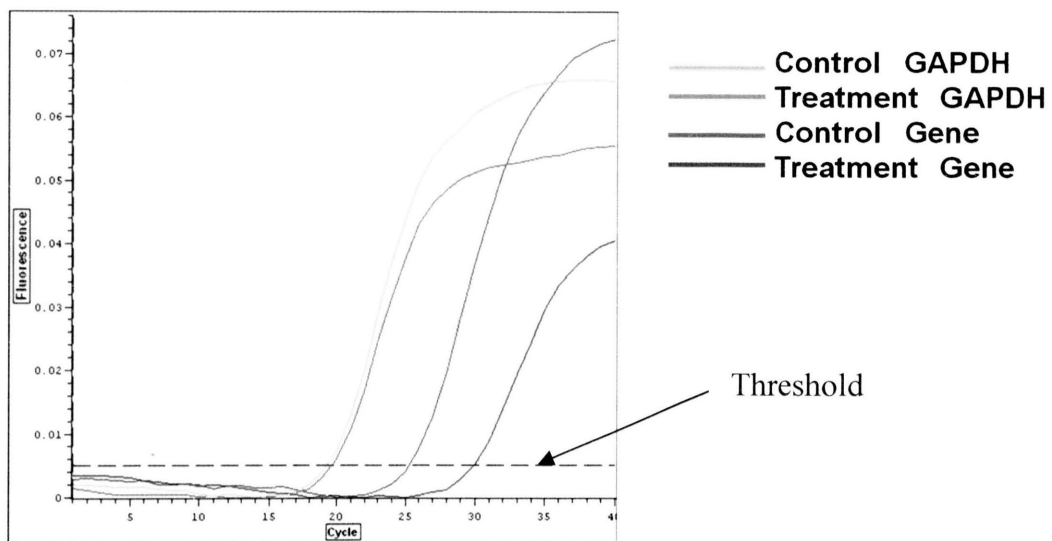
Control

$$\text{Gene} - \text{GAPDH} = \Delta C_{(t)}$$

$$\text{Control} \, \Delta C_{(t)} - \text{Treatment} \, \Delta C_{(t)} = \Delta\Delta C_{(t)}$$

Treatment

$$\text{Gene} - \text{GAPDH} = \Delta C_{(t)}$$

$$(2)^{-\Delta\Delta C(t)} = \textbf{Fold Change}$$

Figure 4:   Calculation of relative abundance of mRNA by quantitative real-time PCR. At a specific threshold, which is set above the background of fluorescence and on the exponential region of the amplification curve, the $C_{(t)}$ values are selected for each gene. The $C_{(t)}$ value of the gene to be analyzed is subtracted from the $C_{(t)}$ value of the housekeeping gene (*Gapdh*) for the control sample, which gives $\Delta C_{(t)}$ for control. Similarly, $C_{(t)}$ value of the gene to be analyzed is subtracted from the $C_{(t)}$ value of the housekeeping gene (*Gapdh*) for the treatment sample, which gives $\Delta C_{(t)}$ for treatment. The control $\Delta C_{(t)}$ value is subtracted from the treatment $\Delta C_{(t)}$, which gives $\Delta\Delta C_{(t)}$ for the gene being analyzed. Since, cDNA is single-stranded, and with PCR they are being amplified to double-stranded, the difference in number of copies of mRNA is determined by $(2)^{-\Delta\Delta C(t)}$.

Preparation of the Fixative

For preparation of modified Davidson's fixative (mDF), 30 ml of 37% formalin (11% formaldehyde), 15 ml of absolute ethanol (15%) and 5 ml glacial acetic acid (0.9 M) were added to 50 ml of deionized water and mixed (Tornusciolo *et al.* 1995, Stahelin *et al.* 1998, Lanning *et al.* 2002, Latendresse *et al.* 2002, Garrity *et al.* 2003). Modified Davidson's fixative (mDF) had a pH of 3.40. Since methylene hydrate, the reactive form of formaldehyde in water is slow to form at lower pH (Kiernan. 1990), mDF was prepared several days in advance of usage.

Preparation of Slides

Sectioned testicular tissues are difficult to maintain on glass slides for extended procedures and proteinase K digestions; therefore, slides were routinely cleaned and coated (subbed) (Shuttlesworth &Mills 1995). Glass slides (Fisher) were cleaned by soaking in a solution of 0.2 N HCl and 95% ethanol for 20 minutes, followed by rinsing with tap water and distilled water, sequentially. Slides were air dried after cleaning. To prepare the chromate-collagen mixture for subbing, 0.5 gm of bovine gelatin (EM Science, Gibbstown, NJ, USA) was dissolved in 80 ml of warmed deionized water. To that solution, 0.50 ml of Hipure liquid gelatin (cod fish skin, Norland Products, North Brunswick, NJ, USA) was added. After cooling, 20 ml of deionized water containing 0.10 gm of dissolved chrome alum or chromium potassium disulfate dodecahydrate $[(CrK(SO_4)_2 \cdot 12H_2O]$ (EM Science) was added to the gelatin mixture (Shuttlesworth &Mills. 1995). Slides were subbed with the chromate-gelatin only on the frosted side with a cotton swab. Subbed slides were air dried overnight at room temperature and

26

stored in slide boxes at refrigerated temperatures until use. Subbed slides in boxes were set at room temperature before use to prevent moisture accumulation between the sections and subbed surface of the slides.

Fixation and Paraffin Wax Embedding

After dissection, intact testes were immersed into mDF with tissue to fixative ratio of 1:10 (weight:volume) and were refrigerated. Prior to fixation, testes were pierced superficially at 5 – 6 locations on both ends with a 23–gauge needle to facilitate fixative permeation (Latendresse *et al.* 2002). After immersion for 2 to 3 hr, testes were trimmed into 3 to 5 mm pieces and fixation was continued for 24 hr in the refrigerator (4 °C). After fixation, testes were dehydrated in the refrigerator with ascending concentrations of 70%, 90% and 100% ethanol for 2 hr each. At room temperature, testes were cleared by immersion in a 50:50 mix of xylene-ethanol for 2 hr followed by two changes of xylene for 2 hr each. For paraffin embedding, testes were first transferred to a mix of 50:50 molten paraffin wax-xylene and incubated at 60 °C for 1 hr followed by three changes of pure molten paraffin wax for 1 hr each at 60 °C. Each piece of testis was transferred to warmed stainless steel tissue molds for paraffin wax embedding. From each tissue block, 7 μm thick sections were cut with a rotator microtome and the ribbons floated in a 37 °C water bath to permit section spreading. The sections were collected onto the subbed slides and allowed to dry and attach to the subbed slides by warming the slides at 40 °C for 15 – 20 min on a slide warmer. The slides were refrigerated in a slide box until use.

Hematoxylin and Eosin (H&E) Staining

For H&E staining, the sections were first dewaxed with xylene followed by rehydration in descending concentration of ethanol (100%, 90% and 70%) for 15 min each at room temperature. Rehydrated sections were stained with Modified Mayer's hematoxylin (American MasterTech) (diluted 1:1 with distilled water) for 3 min at room temperature. Sections were counterstained with eosin (0.10% Eosin Y; 0.50% glacial acetic acid v/v dissolved in 1.0 L of 70% ethanol) for 3 min at room temperature. After dehydration of stained sections in increasing concentrations of ethanol (70%, 90% and 100%) for 3 min each followed by 5 min in xylene, sections were covered with Permount and mounted with cover-slips.

Terminal Deoxynucleotidyl Transferase dUTP Nick End-labeling (TUNEL) Assay

The TUNEL assay was performed using the ApopTag® Plus Peroxidase *In Situ* Apoptosis Kit (Millipore) following the manufacturer's instructions with minor modifications. The sections were dewaxed in xylene and rehydrated in descending concentration of ethanol (100%, 90% and 70%) for 15 min each at room temperature. Following rehydration, sections were washed in PBS for 5 min. Sections were then treated with proteinase K (3.0 µg/ml) (Amresco) for 3 min at room temperature to digest the proteins around the cells and nuclei for better accessibility of the 3'–OH ends of the fragmented DNA in the apoptotic nuclei. The concentration of proteinase K was kept very low (3.0 µg/ml) compared to the manufacturer's recommendation (20 µg/ml) and the duration of tissue section incubation in proteinase K was also reduced from the recommended duration of 15 min to 3 min. It has been reported that higher concentration

of proteinase K (> 5.0 µg/ml) and longer duration of incubation of tissue sections increase non-specific TUNEL staining, destruction of tissue architecture, and loss of some antigenic sites (Tornusciolo *et al*. 1995, Stahelin *et al*. 1998, Garrity *et al*. 2003). Following proteinase K digestion, endogenous peroxidase was quenched from the sections by treating the sections with 3% H_2O_2 for 10 min at room temperature. The sections were stained for broken DNA fragments by TUNEL assay. For TUNEL assay, free 3' –OH DNA termini generated due to random fragmentation during apoptosis were enzymatically labeled with digoxigenin-conjugated and unconjugated nucleotides to the fragmented DNA by terminal deoxynucleotidyl transferase (TdT). The reaction was carried out in a 37 °C humidified chamber for 1 hr. Addition of nucleotide triphosphates (NTPs) to the 3' –OH ends of double-stranded or single-stranded DNA by TdT is a template-independent process. The incorporated nucleotides form an oligomer composed of digoxigenin-conjugated nucleotide and unlabeled nucleotide randomly. The TdT enzyme reaction was terminated after 1 hr by treating the sections with the Stop buffer provided in the kit. Digoxigenin nucleotide-labeled DNA fragments were allowed to bind peroxidase-conjugated anti-digoxigenin antibody by incubation in a humidified chamber for 30 min at room temperature. The apoptotic cells in sections with bound peroxidase-conjugated antibody generated a permanent, intense, localized brown perceptible stain after treatment with the peroxidase chromogenic substrate 3,3'-diaminobenzidine (DAB). Counterstaining of the normal nuclei was performed with Immunomaster's Hematoxylin (American MasterTech) (diluted to 1:10 with distilled water) by incubating the sections at room temperature for 10 min. As negative controls,

29

sections containing no recombinant terminal deoxynucleotidyl transferase (TdT) enzyme were processed in parallel.

Image Capture and Cell Counting

All images were captured using the Nikon's eclipse 90i digital microscope at a voltage of 9.2 and exposure time of 4 mSec. Areas of seminiferous tubules were measured with Nikon's NIS-Elements Basic Research version 3.1 software's annotation and measurement tool. Cell counting was performed with the same software's object count tool. For counting of TUNEL-positive cells, in each field, at least one TUNEL positive cell was selected to specify the intensity of the objects to be counted with the 6 point circle tool of the software. The 6 point circle tool picks the threshold of the color intensity of the selected TUNEL-positive nucleus from the circle radius defined by 6 pixels. The threshold limits were from 30 – 40 (lower limit) and 120 – 140 (upper limit). The binary image was cleaned by performing 6 iterations to remove any non-specific object(s) and the binary image contours were smoothened by performing 16 iterations. Adobe photoshop 7.0 was used to adjust the brightness and contrast of the images for visual presentation.

Immunohistochemistry (IHC)

For IHC, sections were deparaffinized, rehydrated and boiled in 1.0 L of 1.0 mM EDTA (pH 7.5) for 15 min in an 800 Watt microwave for antigen retrieval (McCabe et al. 2010). To block non-specific antigenic sites, sections were preincubated in 10% normal donkey serum (Jackson Immunoresearch) in PBS for 1 hr in a 37 °C humidified chamber. Primary antibodies [goat anti-GZMK (sc-49021; Santa Cruz Biotechnology),

rabbit anti-CD8b (sc-9147; Santa Cruz Biotechnology), goat anti-CD4 (sc-1140; Santa Cruz Biotechnology), mouse anti-PRF (sc-136994; Santa Cruz Biotechnology)], diluted 50-fold with 10% normal donkey serum in PBS were applied to the sections and incubated in a humidified chamber at room temperature (23 °C) for 18 hr. Isotope matched non-specific mouse immunoglobulin 1 (IgG1) or 10% normal donkey serum was used instead of primary antibody for negative controls. Detection of primary antibodies was with either donkey anti-rabbit DyLight 649 (711-495-152; Jackson Immunoresearch), donkey anti-goat DyLight 594 (705-515-147; Jackson Immunoresearch), donkey anti-goat DyLight 649 (705-496-147; Jackson Immunoresearch) or donkey anti-mouse DyLight 594 (715-515-150; Jackson Immunoresearch) dilution of 1:500 with 10% normal donkey serum in PBS. Sections were mounted in Vectashield mounting medium with 4',6-diamidino-2-phenylindole (DAPI) (Vector Laboratories) and photographs were captured with Nikon's Eclipse Ti confocal microscope.

Statistical Analysis

Data for mRNA levels for genes from all treatment groups were normalized to the untreated (NT) group and were compared by 3-way analysis of variance (ANOVA) with SPSS version 15 software. Comparisons were between EDS treatment (EDS), testosterone supplementation (TES) and testosterone replacement (EDS + TES), and effect of days (5 and 7). Comparison between untreated (NT) and vehicle (VEH) groups were performed by Student's t-test. To compare concentrations of serum testosterone, 2-way ANOVA, and to compare ITT concentrations, 1-way ANOVA was performed. Post-

hoc comparisons were performed with Newman-Keuls test and p-value ≤ 0.05 was considered significant (Zar 1999). All data are reported as mean $\pm$ standard error of mean (SEM), and graphs were generated by DeltaGraph version 5 software.

CHAPTER III

RESULTS

The present study was designed to investigate the role of testosterone on germ cell viability and pathways that lead to germ cell apoptosis following testosterone withdrawal. Histological evaluation and gross morphology may be good to evaluate the effects of testosterone depletion; however, techniques for gene expression analysis, radioimmunoassay and immunohistochemistry for localization of proteins are essential to decipher the effects of testosterone ablation in testes. Therefore, using the above mentioned techniques in this study, the following aims were examined: whether perforin (PRF) and granzymes (GZM) are associated with germ cell apoptosis in rat testes following EDS-induced testosterone depletion and whether mRNAs for *Prf* and *Gzm* are regulated by testosterone in testes.

Testicular Weight

Although gross morphological appearance of testes was not different between EDS-treated rats after 5 days or 7 days and controls (Fig. 5), there was a significant reduction in total testes weight among both 5 day and 7 day EDS-treated rats compared to the controls. The average loss of testes weight was 13% and 18% after 5 days and 7 days, respectively. Since, in the adult rat testis, Leydig cells constitute only 2.7% of the total testicular volume (Mori & Christensen 1980), loss of 13% and 18% weight can be

33

due to the loss of germ cells as well. In rats receiving testosterone (TES) replacement after EDS treatment, the testes weights remained at the control levels (Fig. 6).
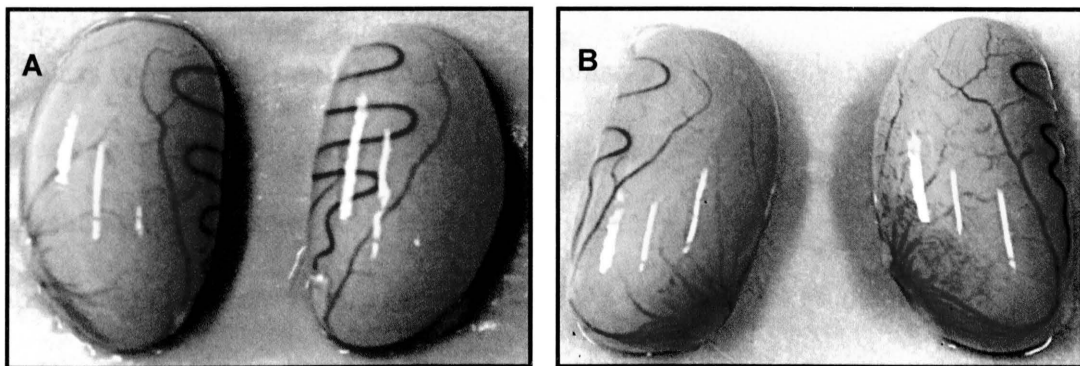

Figure 5: Gross morphological appearance of rat testes after 7 days of treatment. **(A)** Untreated (NT); **(B)** EDS-treated.

Testosterone Concentrations in Serum and Testes

Since EDS is known to eliminate mature Leydig cells, the source of testosterone production, the effect of EDS treatment was evaluated by measuring testosterone concentrations in serum and testes. Serum testosterone in EDS-treated rats after 5 and 7 days was below the detection limit of the assay (Fig. 7). Testosterone levels in testosterone-supplemented (TES) and testosterone-replaced (EDS + TES) rats in both 5 and 7 days were considerably higher than the untreated (NT) and vehicle (VEH)-treated rats because in those rats testosterone propionate (TP) was injected on alternate days. Intratesticular testosterone (ITT) levels were checked for 7 day rats only because 5 day samples were lost. Like serum, ITT in 7 day EDS-treated rats was also below the detection level (Fig. 8 and 9). In testosterone-supplemented (TES) rats, the concentration of testosterone (10 ng/gm) was very low compared to the untreated (NT) and vehicle (VEH)-treated rats (68 ng/gm and 85 ng/gm, respectively). Normally ITT concentration is (65 – 85 ng/gm) higher than serum testosterone concentration (5 – 7 ng/gm). In TES rats, because of the negative feedback on pituitary by the excess serum testosterone, ITT level was below normal. Although complete restoration of ITT in EDS + TES rats was not observed after testosterone replacement, the level was comparable to the testosterone-supplemented (TES) rats (10 ng/gm) and was enough to maintain testicular weight after EDS treatment (see Fig. 6).
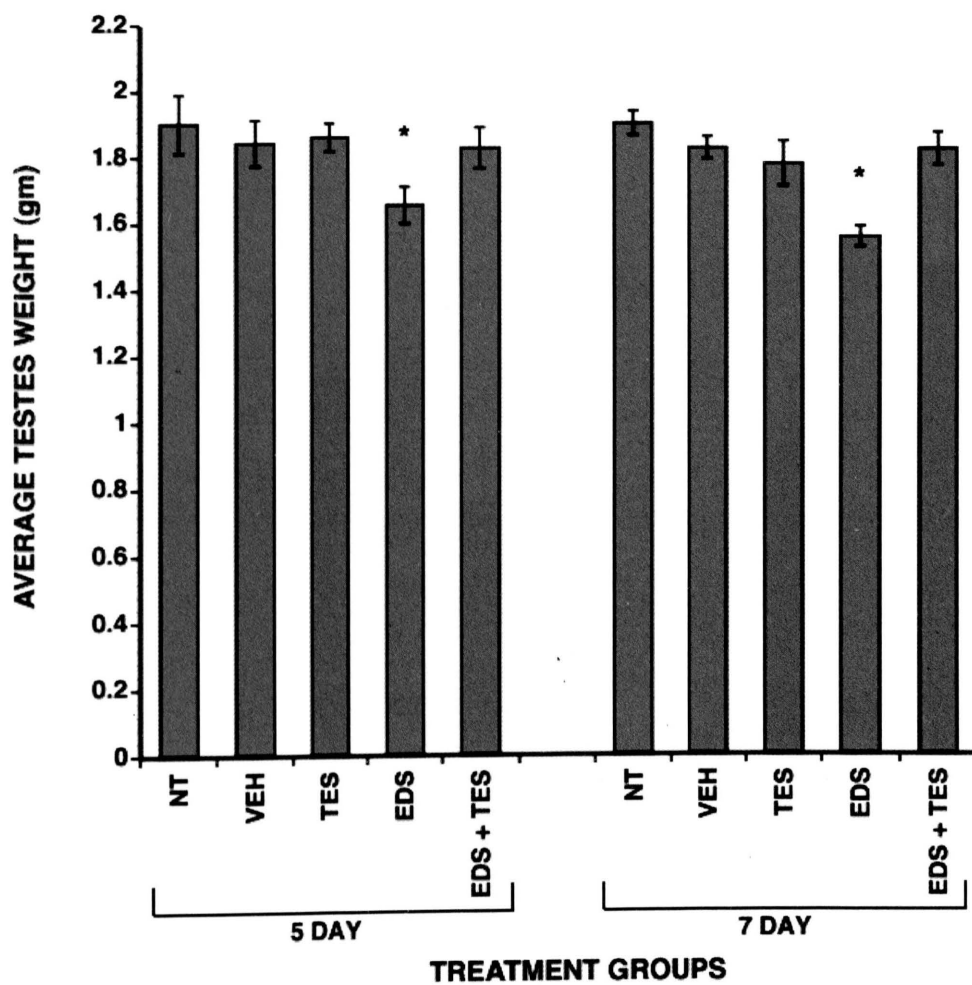
Figure 6: Average testes weights. Error bars represent SEM with n = 6. Asterisk (*) indicates significant difference from all other treatment groups within the same day.
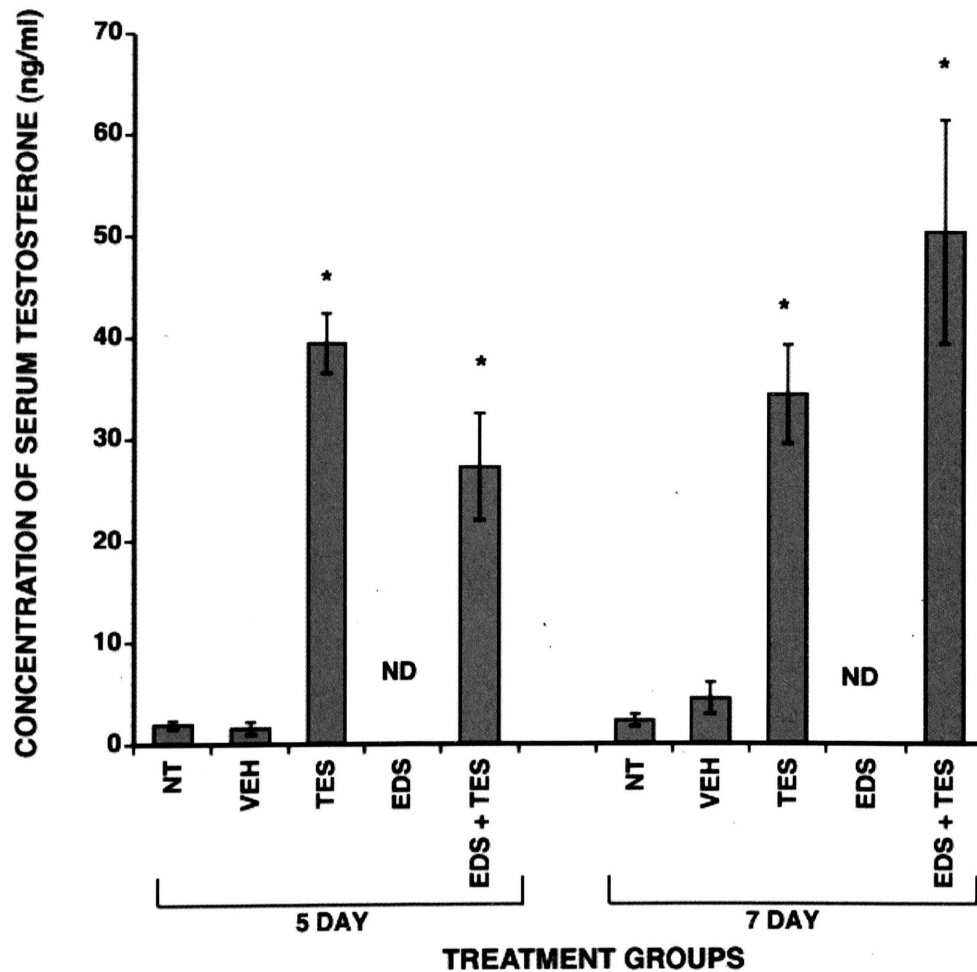
Figure 7: Mean serum testosterone levels. Error bars represent SEM with n = 6. Asterisk (*) indicates significant difference from NT and VEH within the same day. In EDS-treated rats, serum testosterone was below the detection level (0.05 ng/ml) of the assay (ND).

Figure 8: Mean intratesticular testosterone (ITT) concentration. Error bars represent SEM with n = 6. Asterisk (*) indicates significant difference from NT and VEH. In EDS-treated rats ITT was below the detection level (0.05 ng/ml) of the assay (ND).

Figure 9: Mean serum and intratesticular testosterone (ITT) concentrations. Error bars represent SEM with n = 6. Asterisk (*) indicates s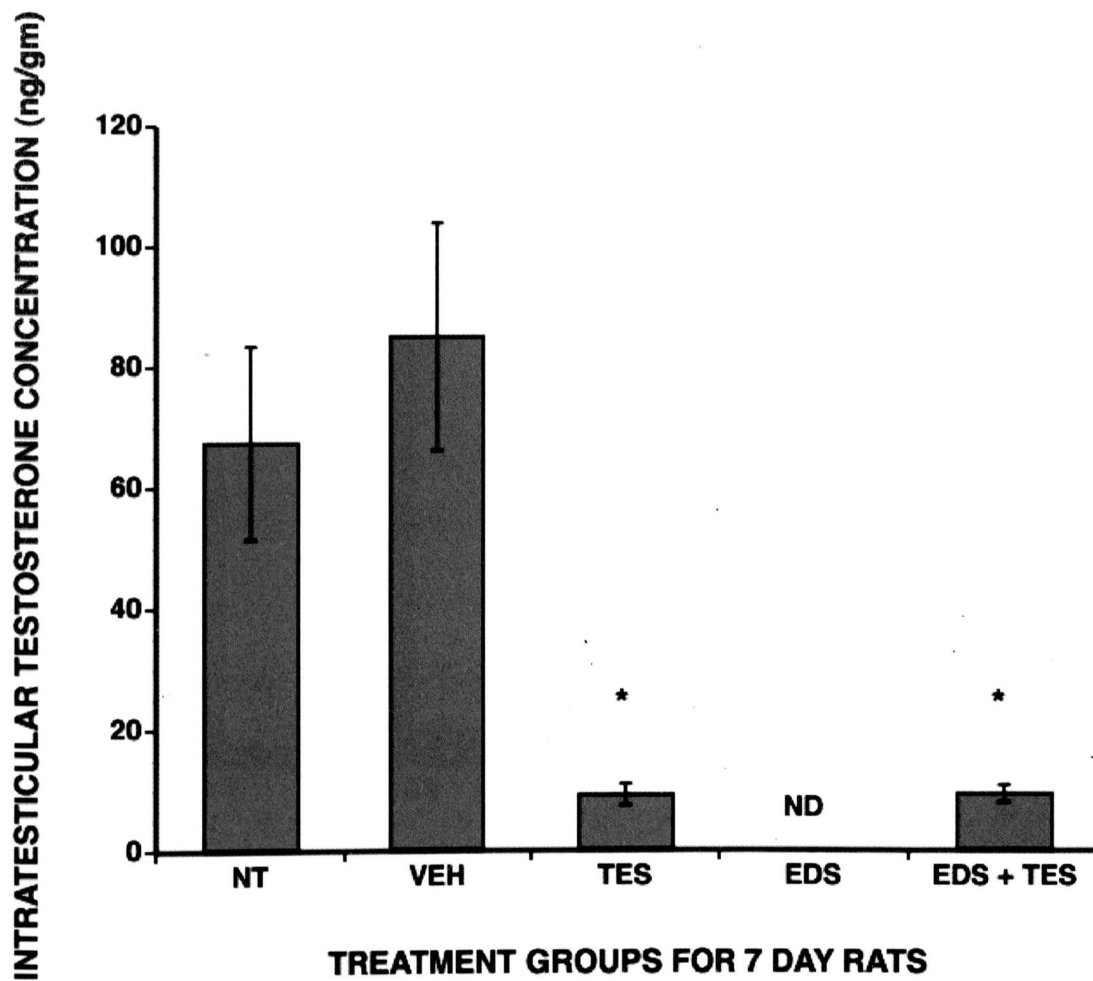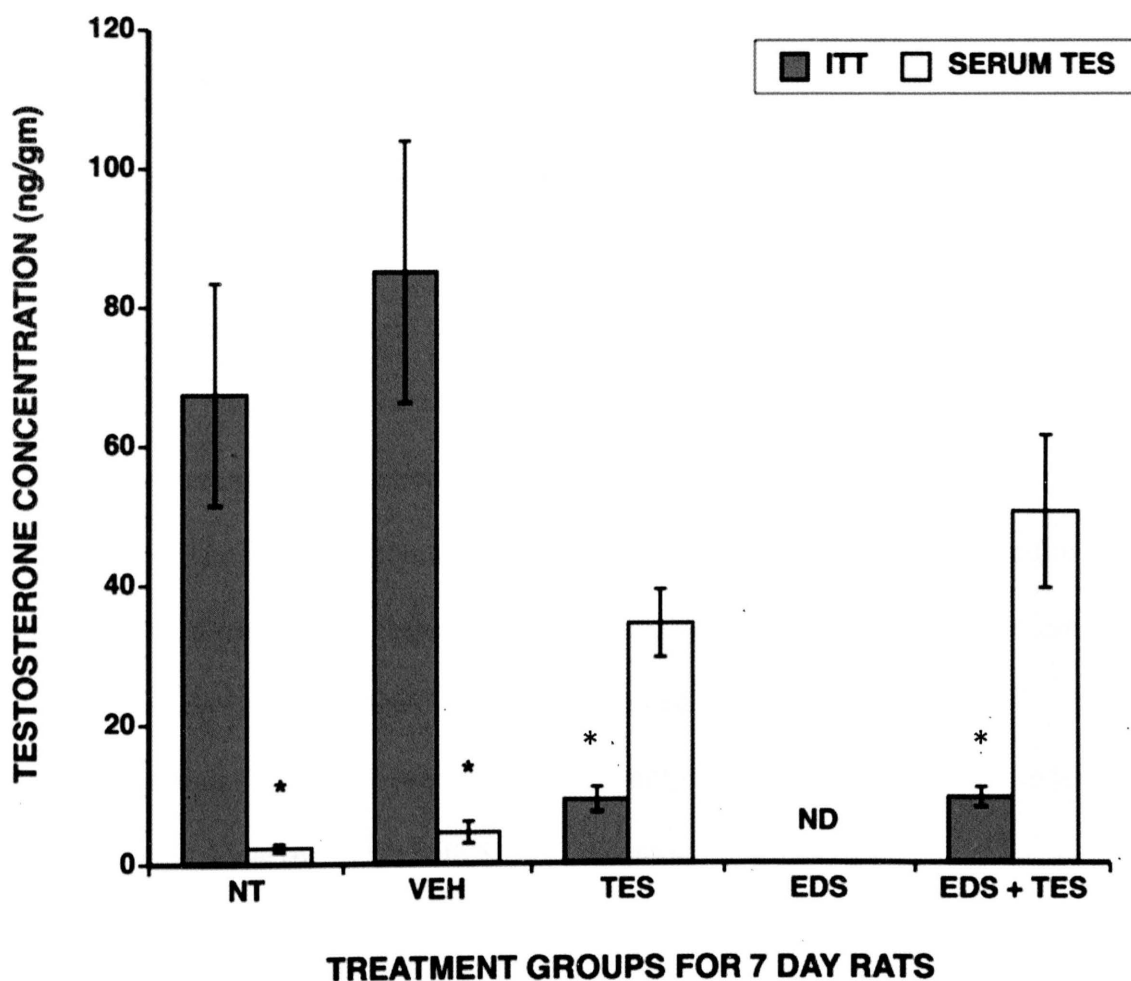ignificant difference within the same treatment group. In EDS-treated rats, serum testosterone and ITT were below the detection level (0.05 ng/ml) of the assay (ND).

Relative Abundance of mRNAs for Luteinizing Hormone Receptor (*Lhr*) and Insulin-like Peptide 3 (*Insl3*)

Although undetectable testosterone in both serum and testes assayed by RIA may suggest elimination of Leydig cells, complete elimination cannot be confirmed due to the limitation of the RIA technique (concentrations below 0.05 ng/ml cannot be detected). Therefore, the levels of two Leydig cell-specific mRNAs (*Lhr* and *Insl3*) were quantified by qPCR to determine the degree of Leydig cell loss (Ferlin *et al.* 2006, O'Shaughnessy *et al.* 2008). The relative amount of mRNA for *Lhr* was 82% and 92% reduced in 5 day and 7 day EDS-treated rats, respectively (Fig. 10). After testosterone replacement (EDS + TES), the level of *Lhr* mRNA was further reduced by 5%. Testosterone supplementation (TES) also resulted in significantly lower *Lhr* mRNA levels in testes compared to vehicle (VEH) in both 5 and 7 day rats.

The mRNA for *Insl3* was reduced by 99% in the testis of 5 day and 7 day rats in both EDS and EDS + TES treatment groups (Fig. 11). Testosterone supplementation (TES) showed time-dependent reduction in the relative mRNA level of *Insl3* in the testis. After 5 days and 7 days, the relative amount of *Insl3* mRNA was 30- and 70-fold, respectively, less than vehicle (VEH)-treated rats. The disparity between *Lhr* and *Insl3* mRNA expression profile may be due to the report that LHR is present in interstitial macrophages as well as Leydig cells (Hedger &Hales. 2006), whereas, INSL3 is exclusive to the mature Leydig cells and *Insl3* mRNA expression is directly regulated by LH (Ferlin *et al.* 2006). Therefore, from the data of Insl3 mRNA expression pattern it can be concluded that 99% of the mature Leydig cells were eliminated from both 5 and 7

day rats. Although testosterone had no protective effect on EDS-induced Leydig cells death, testosterone supplementation resulted in a down regulation of *Lhr* and *Insl3* mRNA levels, possibly via negative feedback regulation of the hypothalamus-pituitary-gonad axis (see Fig. 2).

Figure 10: *Lhr* mRNA levels with *Gpdh* as the reference gene. Error bars represent SEM with n = 6. Horizontal bar represents the normalized value for the untreated (NT) group. Single * indicates significant difference from VEH within the same day. Double * indicates significant difference from TES within the same day.
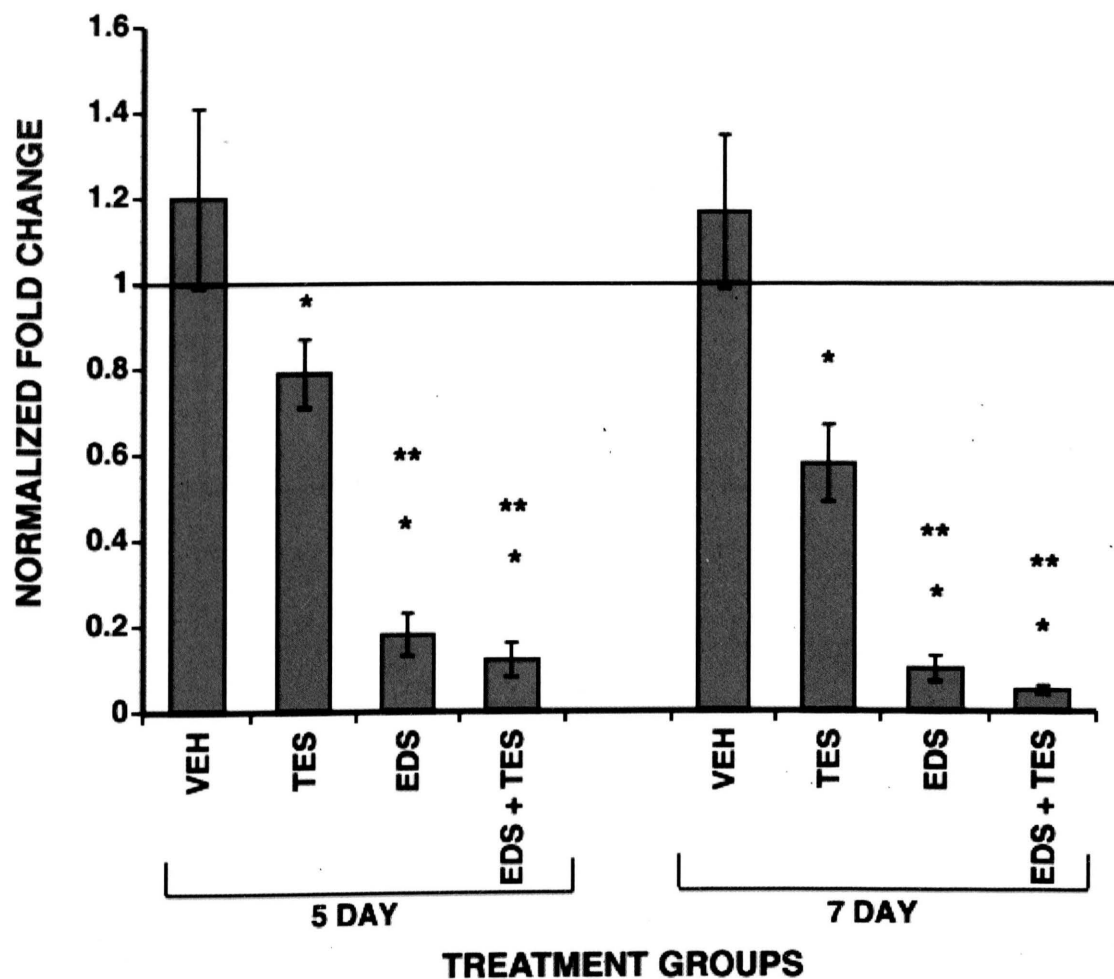
Figure 11: *Insl3* mRNA levels with *Gapdh* as the reference gene. Error bars represent SEM with n = 6. Horizontal bar represents the normalized value for the untreated (NT) group. Single * indicates significant difference from VEH within the same day. Double * indicates significant diff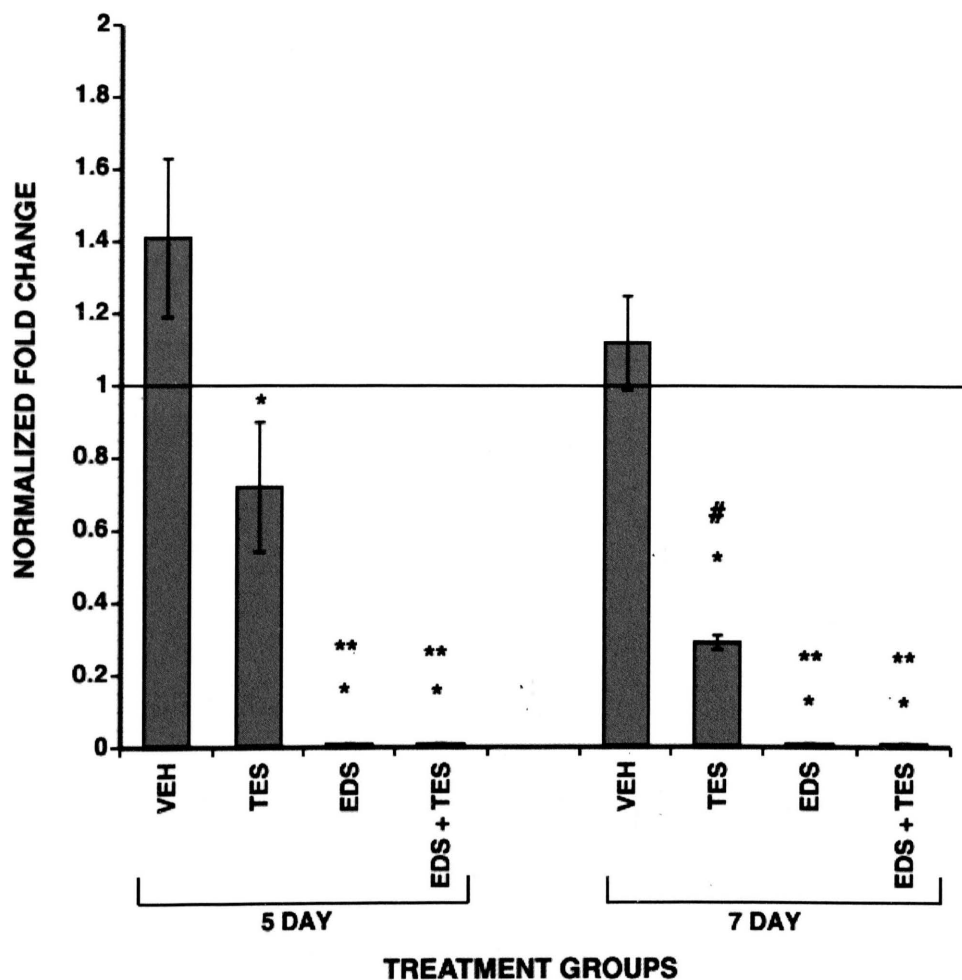erence from TES within the same day. # indicates significant difference between 5 day and 7 day within the same treatment group.

Histological Evaluation of Testicular Cross-sections

Leydig cells reside in the interstitium of rat testes (Kerr *et al.* 2006). With hematoxylin and eosin stain, no Leydig cells were detected in EDS and EDS + TES testicular cross-sections (Fig. 12 – 15). This is consistent with the hormonal measurement and mRNA quantification results. Normal Leydig cells were observed in cross-sections of vehicle (VEH) and testosterone-supplemented (TES) rat testis.
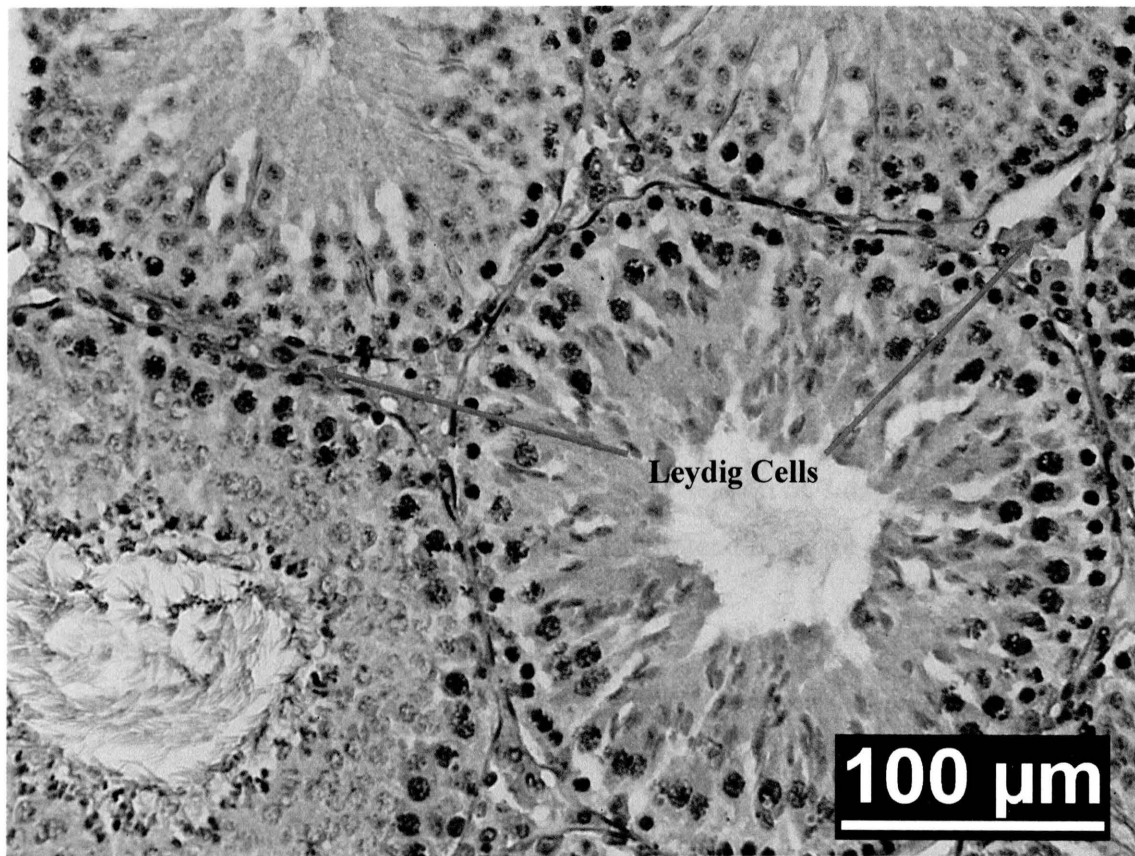
Figure 12: Hematoxylin and eosin stained cross-section of 7 day VEH-treated rat testis. Leydig cells in the interstitium are shown by red arrows.
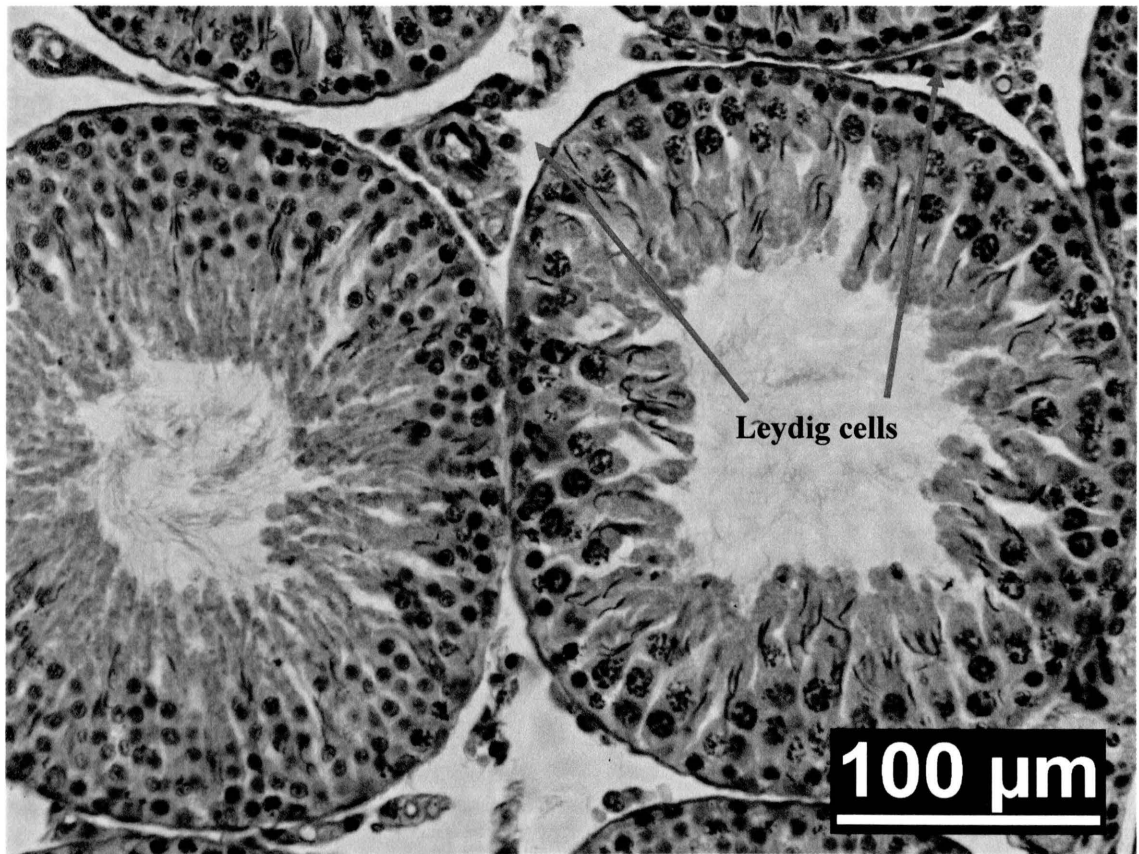
Figure 13: Hematoxylin and eosin stained cross-section of 7 day testosterone-supplemented (TES) rat testis. Leydig cells in the interstitium are shown by red arrows.

Figure 14: Hematoxylin and eosin stained cross-section of 7 day EDS-treated rat testis. The interstitium is devoid of any Leydig cell (marked by red arrows).
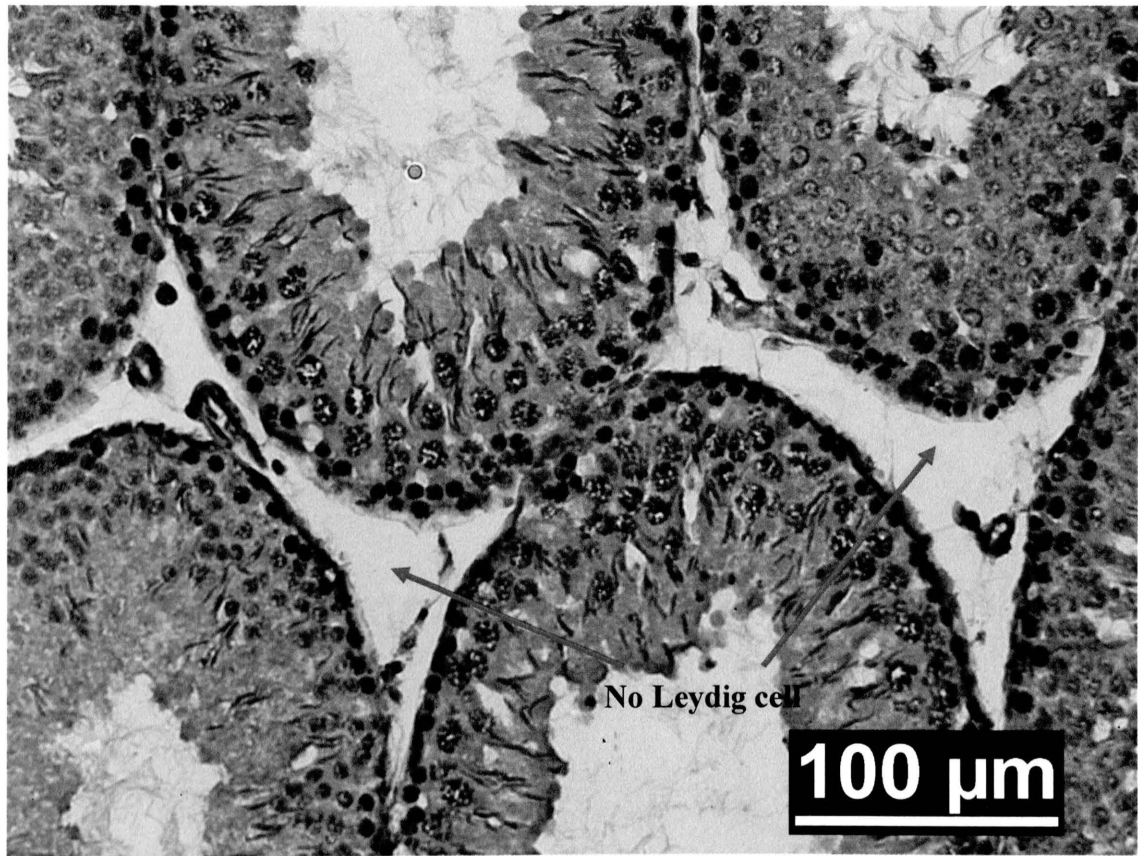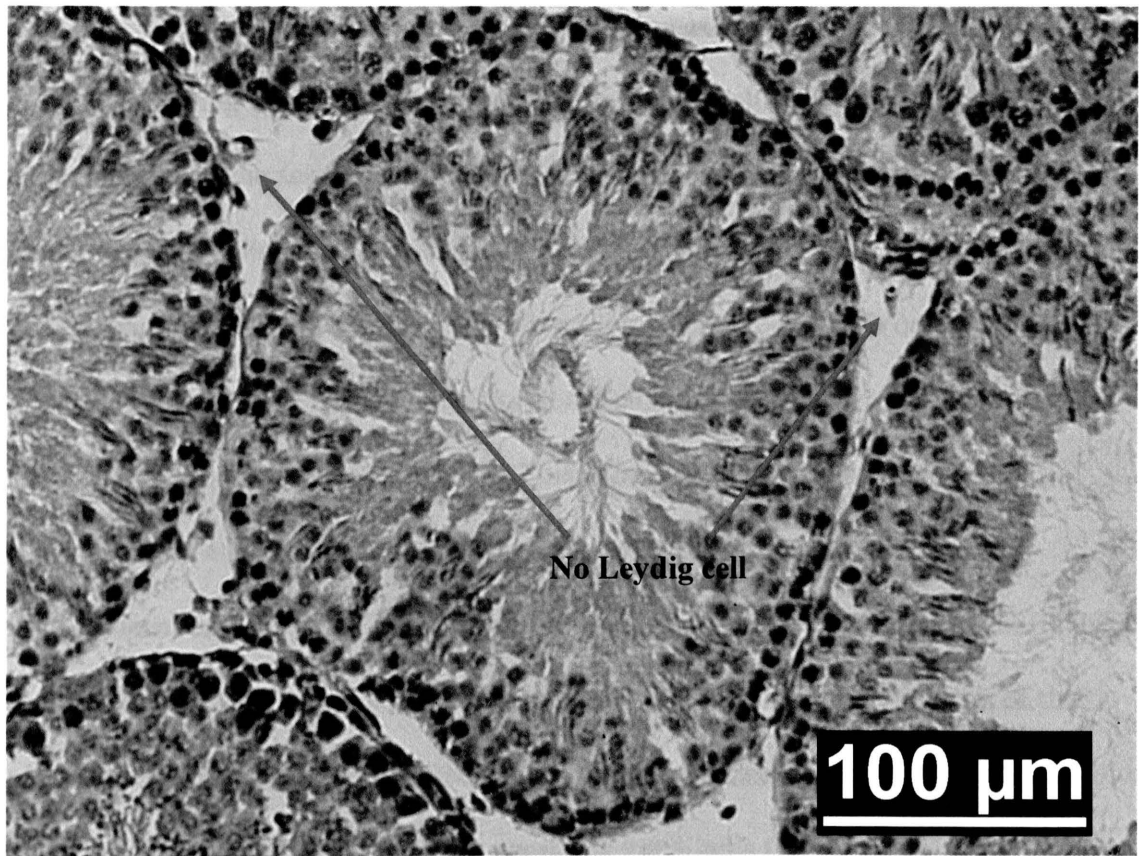
No Leydig cell

Figure 15: Hematoxylin and eosin stained cross-section of 7 day testosterone-replaced rat testis. The interstitium is devoid of any Leydig cell (marked by red arrows).

Testosterone Depletion Induces Significant Increase in Germ Cell Apoptosis

Following depletion of testosterone, there was a time-dependent increase in germ cell apoptosis in the seminiferous epithelium (Fig. 16). In normal testes, potentially defective germ cells are eliminated by apoptosis (Kerr *et al.* 2006). However, the cells undergoing apoptosis in normal testes are mainly spermatogonia (Woolveridge *et al.* 1999) and testosterone depletion results in apoptosis of pachytene spermatocytes and spermatids (Woolveridge *et al.* 1999). This means testosterone is essential for spermatocytes and spermatids to differentiate into sperm.

Germ cell apoptosis in the testicular cross-sections was detected by the TUNEL assay. The TUNEL-positive nuclei appeared brown due to the precipitation of the peroxidase substrate *3,3'*-diaminobenzidine (DAB) and normal nuclei stained blue with hematoxylin. There were only a few apoptotic germ cells (1 – 4), mainly spermatogonia, in 5 day and 7 day untreated (NT) and vehicle (VEH)-treated rat testicular cross-sections (Fig. 17 & 18). Testosterone supplementation (TES) had no discernable apoptotic effect on germ cells and appeared to be similar to VEH and NT rats (Fig. 19). There was a significant increase in germ cell apoptosis 5 days post-EDS treatment (30 – 35) which increased even further after 7 days (120 – 140) (Fig. 20 & 21). The predominant TUNEL-positive cells that were in EDS-treated testicular cross-sections were spermatocytes and round spermatids (Fig. 20 & 21). However, the number of apoptotic germ cells decreased significantly because of testosterone replacement after EDS treatment (EDS + TES) in both 5 and 7 day rats (Fig. 22).
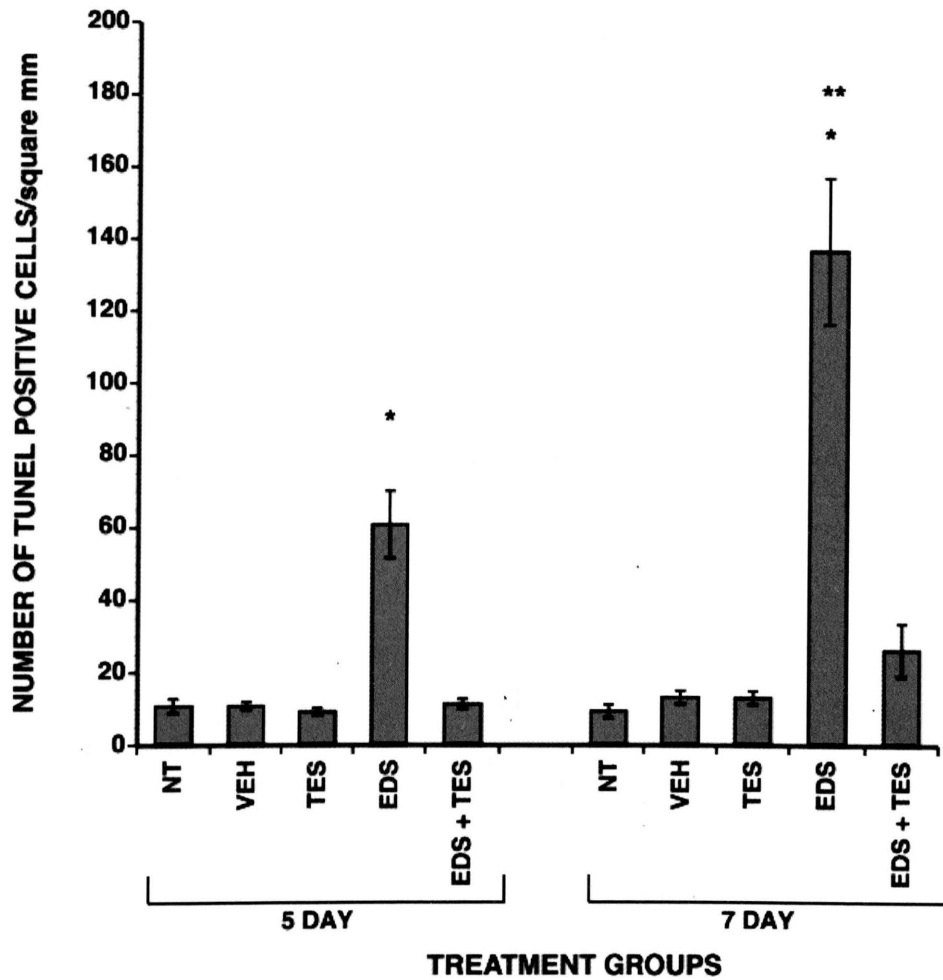
Figure 16: Average number of TUNEL-positive cells. Error bars represent SEM with n = 6. Single * indicates significant difference from all other treatment groups within the same day. Double * indicates significant difference between 5 day and 7 day within treatment.

Figure 17: Apoptotic cells in the seminiferous tubule of 7 day untreated (NT) rat testis cross-section detected by the TUNEL assay. Normal nuclei were counter-stained by hematoxylin. A TUNEL-positive apoptotic spermatogonium (brown stain) is indicated by an arrow.
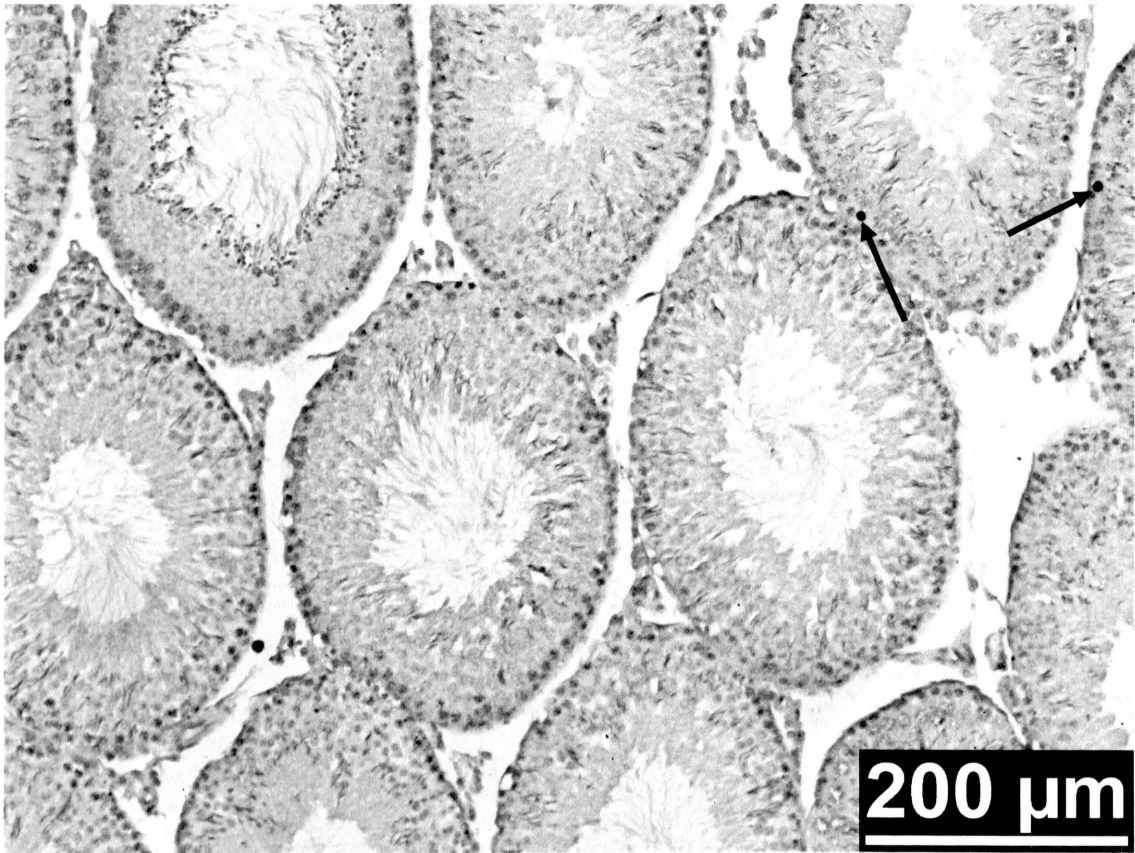
Figure 18: Apoptotic cells in the seminiferous tubule of 7 day VEH-treated rat testis cross-section detected by the TUNEL assay. Normal nuclei were counter-stained by hematoxylin. TUNEL-positive apoptotic spermatogonia (brown stain) are indicated by arrows.
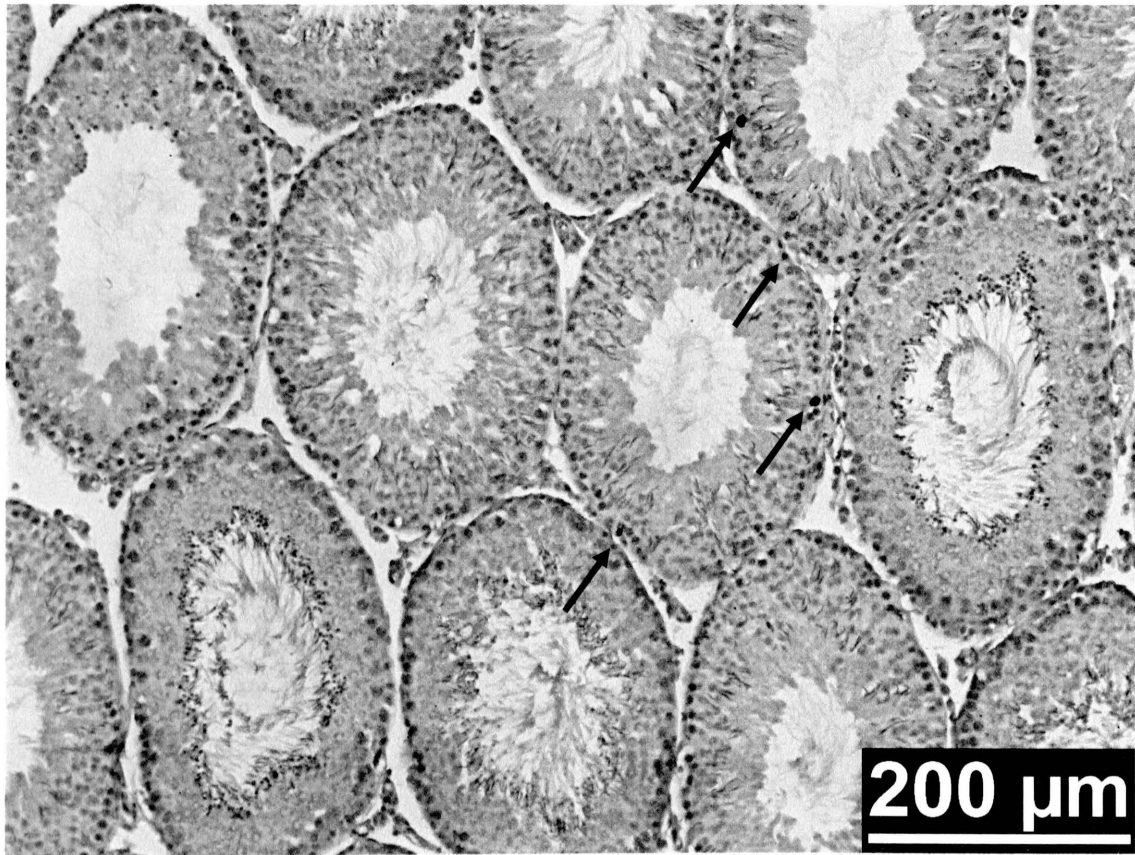
Figure 19: Apoptotic cells in the seminiferous tubule of 7 day testosterone-supplemented rat testis cross-section detected by the TUNEL assay. Normal nuclei were counter-stained by hematoxylin. TUNEL-positive apoptotic spermatogonia (brown stain) are indicated by arrows.
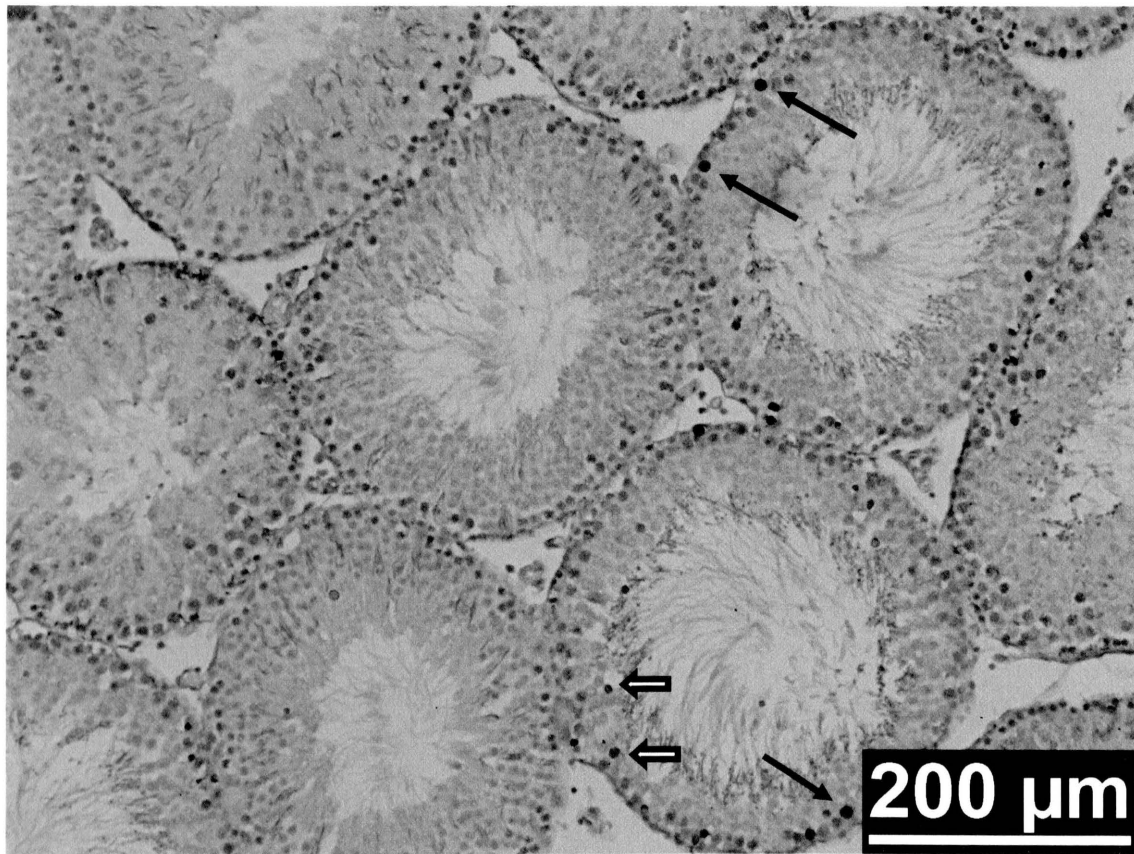
Figure 20: Apoptotic cells in the seminiferous tubule of 5 day EDS-treated rat testis cross-section detected by the TUNEL assay. Normal nuclei were counter-stained by hematoxylin. ➜ Represent TUNEL-positive apoptotic primary spematocyte and ⇨ represent apoptotic secondary spermatocyte.
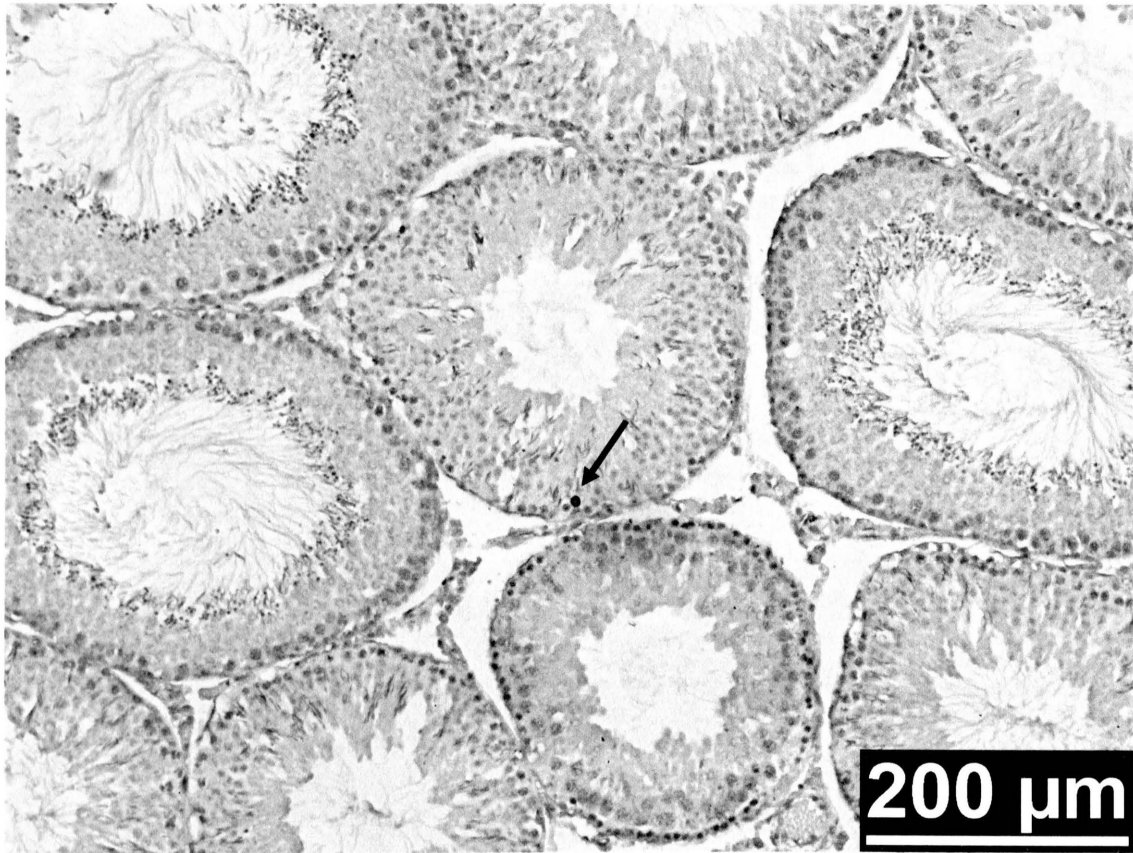
Figure 21: Apoptotic cells in the seminiferous tubule of 7 day EDS-treated rat testis cross-section detected by the TUNEL assay. Normal nuclei were counter-stained by hematoxylin. → Represent TUNEL-positive apoptotic primary spematocyte; ⇒ represent apoptotic secondary spermatocyte and; ▭▷ apoptotic elongated spermatid.
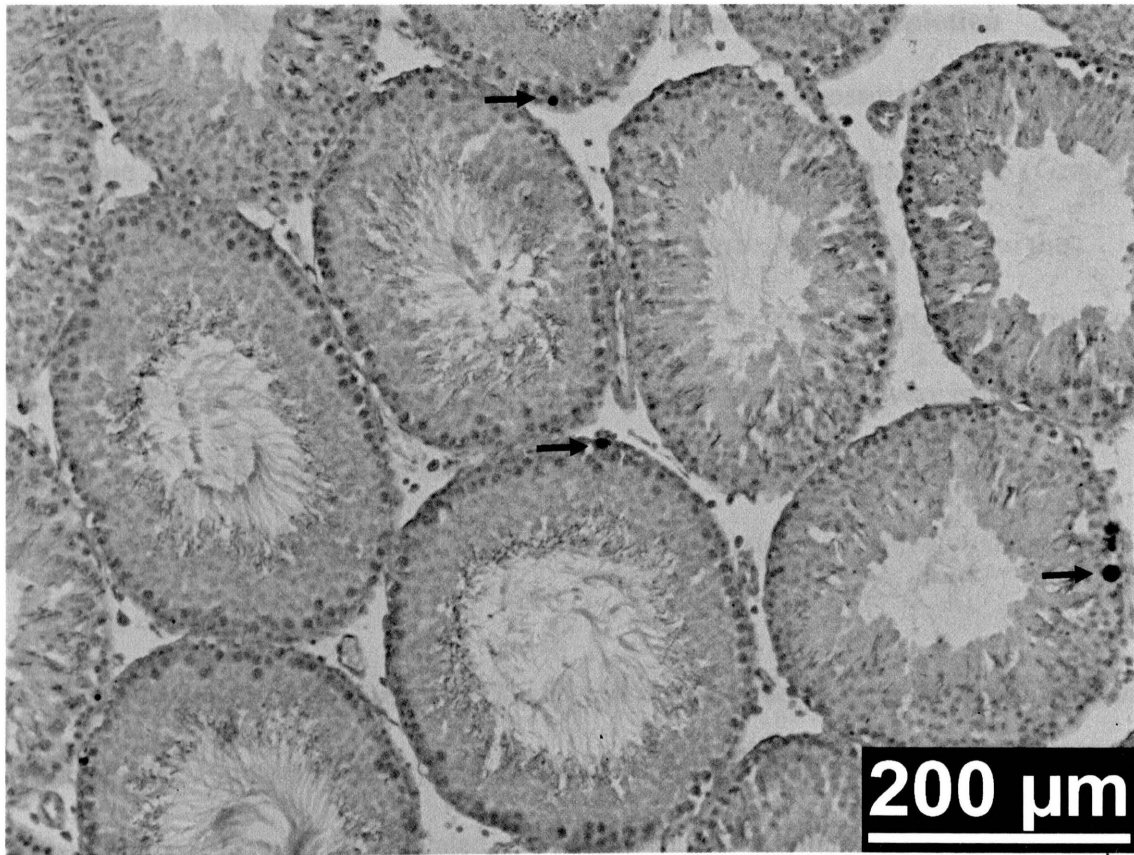
Figure 22:   Apoptotic cells in the seminiferous tubule of 7 day testosterone-replaced rat testis cross-section detected by the TUNEL assay. Normal nuclei were counter-stained by hematoxylin. TUNEL-positive apoptotic spermatogonia (brown stain) are indicated by arrows.
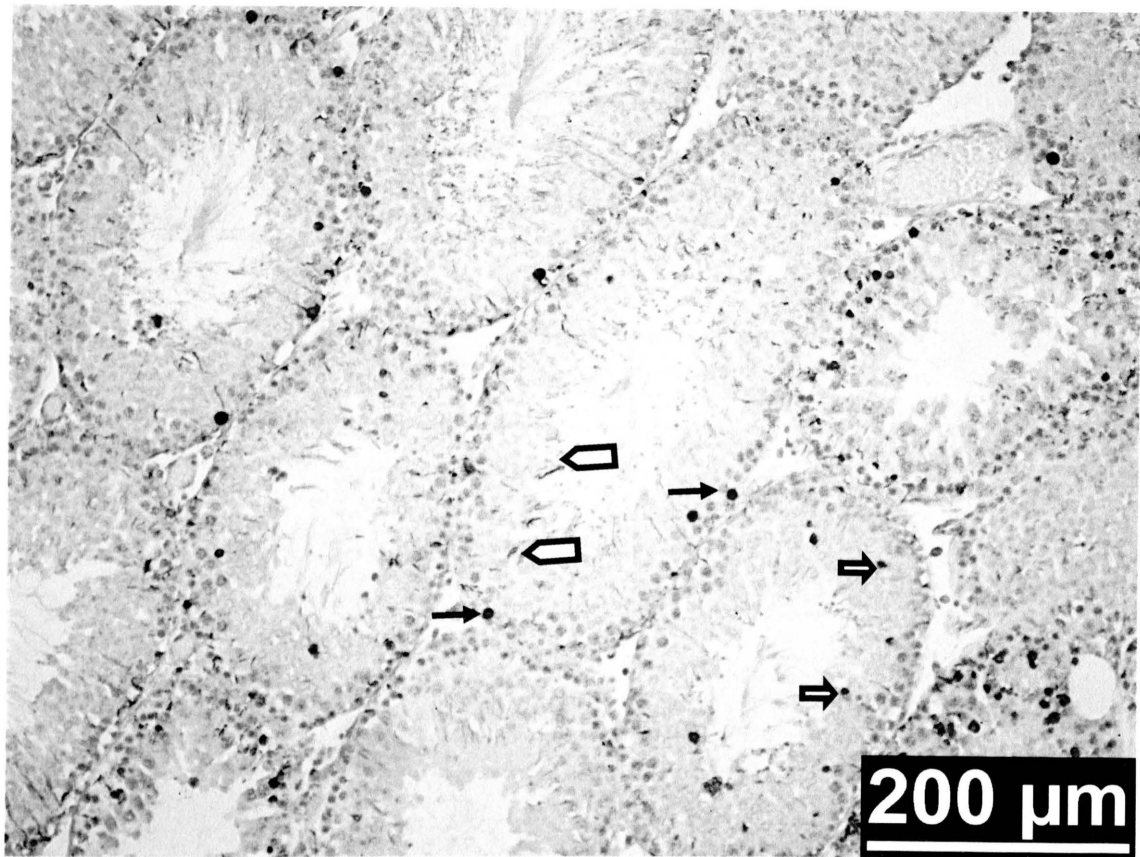
Expression Profiles of Granzyme Variants After Testosterone Depletion

In rats, seven *granzyme* variants have been reported (Grossman *et al.* 2003), granzyme A (*GzmA*), granzyme B (*GzmB*), granzyme C (*GzmC*), granzyme F (*GzmF*), granzyme K (*GzmK*), granzyme M (*GzmM*) and granzyme N (*GzmN*). Due to the absence of any unique region on the mRNA, primers could not be designed for three of these variants, *GzmC*, *GzmF* and *GzmM*. Hence, these three genes were excluded from this project. For the remaining four *Gzm* variants (*GzmA*, *GzmB*, *GzmK* and *GzmN*), mRNA expression patterns, relative abundance and testosterone responsiveness were analyzed.

The mRNAs for *GzmA* and *GzmB* were not affected by testosterone withdrawal, replacement or supplementation (Fig. 23 and 24). In contrast, *GzmN* mRNA expression had an increase in 5 day EDS-treated rats (statistically insignificant) but had a significant increase after 7 days of EDS treatment (Fig. 25) compared to VEH, TES or EDS + TES rats. After testosterone replacement (EDS + TES), however, *GzmN* mRNA level was reversed to the levels of VEH and TES rats. Therefore, testosterone depletion may have a delayed effect on *GzmN* mRNA expression. The mRNA for *GzmK* increased significantly in both 5 day and 7 day EDS-treated rats and was restored to the levels of VEH- and TES-treated rats after testosterone replacement (EDS + TES) in 7 day but not in 5 day rats (Fig. 26). This may be due to the lower levels of testosterone detected in serum of 5 day testosterone-replaced (EDS + TES) rats compared to 7 day testosterone-replaced (EDS + TES) rats (see Fig. 7).

Figure 23: *GzmA* mRNA levels with *Gapdh* as the reference gene. Error bars represent SEM with n = 6. Horizontal bar represents the normalized value for the untreated (NT) group.

Figure 24: *GzmB* mRNA levels with *Gapdh* as the reference gene. Error bars represent SEM with n = 6. Horizontal bar represents the normalized value for the untreated (NT) group.

Figure 25: *GzmN* mRNA levels with *Gapdh* as the reference gene. Error bars represent SEM with n = 6. Horizontal bar represents the normalized value for the untreated (NT) group. Asterisk (*) indicates significant difference from all other treatment groups within the same day.

Figure 26: *GzmK* mRNA levels with *Gapdh* as the reference gene. Error bars represent SEM with n = 6. Horizontal bar represents the normalized value for the untreated (NT) group. Asterisk (*) indicates significant difference from all other treatment groups within the same day.

59

Comparative Expression Profile of Granzyme Variants in Normal Rat Testes

Among known granzyme variants, *GzmA* and *GzmB* are highest in most mammalian tissues (Chowdhury & Lieberman 2008). However, *GzmN* is the most abundant *Gzm* variant in mouse testes (Takano *et al.* 2004). In rat testes, *GzmK* was the least abundant and *GzmN* was the most abundant *Gzm* variants (Fig. 27). The average $C_{(t)}$ values of *GzmK*, *GzmA*, *GzmB* and *GzmN* were 28.5, 27.5, 26.5 and 21, respectively and compared to *GzmK*, the mRNA level of *GzmN* is 140-fold higher followed by *GzmB* (2.65-fold) and *GzmA* (1.32-fold).
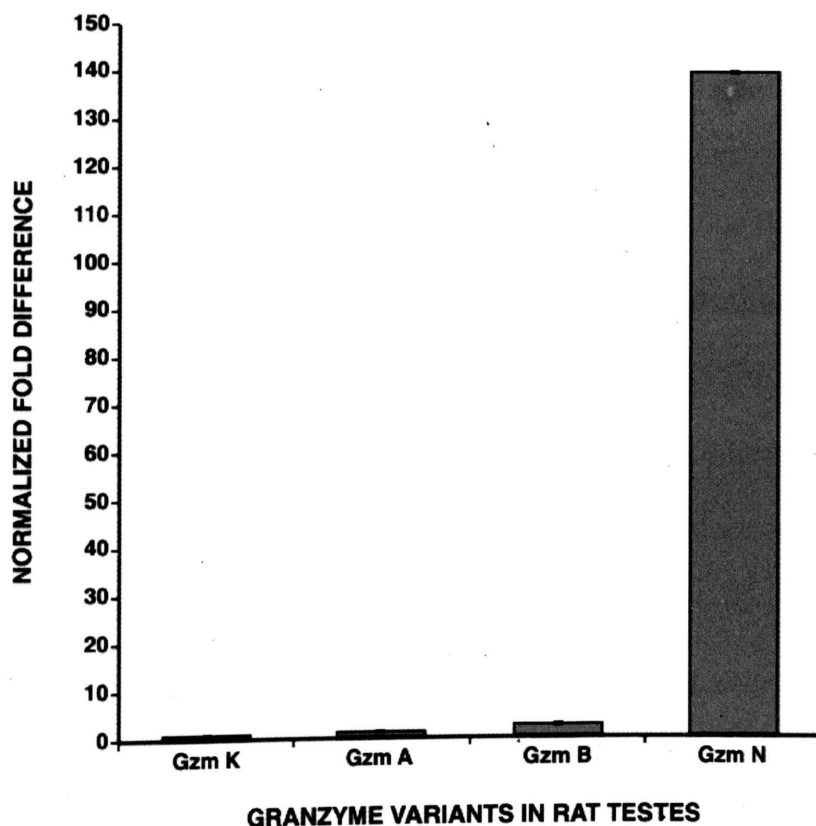
Figure 27: Relative mRNA abundance of *GzmA*, *GzmB* and *GzmN* with reference to *GzmK* in normal rat testes. Error bars represent SEM with n = 12.

Expression Profiles of Perforin and Abundance of T Cells (*Cd4*^{+} and *Cd8*^{+})

Cytotoxic T cells (CD8^{+}) release perforin and granzymes into the target cells to induce apoptosis (Andersen *et al*. 2006). Since a significant increase in apoptosis was observed in both 5 day and 7 day EDS-treated rats along with a significant increase in *GzmK* expression, it was hypothesized that germ cell apoptosis might involve cytotoxic T cells. Therefore, the mRNA expression of lymphocyte-specific markers, *Cd4* (helper T cells) and *Cd8* (cytotoxic T cells), along with perforin (*Prf*) were investigated. After EDS treatment, mRNAs for *Prf* (Fig. 28), *Cd4* (Fig. 29) and *Cd8* (Fig. 30) were all significantly higher compared to their respective controls. The mRNAs for both *Prf* and *Cd8* had very similar expression patterns to that of *GzmK* where all these three genes (*GzmK*, *Prf* and *Cd8*) were significantly higher after EDS treatment than their VEH and TES groups, and after testosterone replacement (EDS + TES), mRNAs for all three genes were significantly down-regulated. However, testosterone replacement (EDS + TES) had little effect on *Cd4* mRNA and did not reverse to the levels of VEH and TES. There was also a 2- to 3-fold increase in mRNA for *Cd8* in VEH- and TES-treated rats, consistent with previous reports (Hedger *et al*. 1998) that DMSO may induce proliferation of CD8^{+} T cells in rat testicular interstitium. The mRNA expression profile for *GzmK*, *Prf* and *Cd8* indicated that CD8^{+} T cells may be involved in regulating germ cell apoptosis in the absence of testosterone. In addition, testosterone may regulate the CD8^{+} T cell population in the testis and/or their capacity to express *GzmK* and *Prf*.
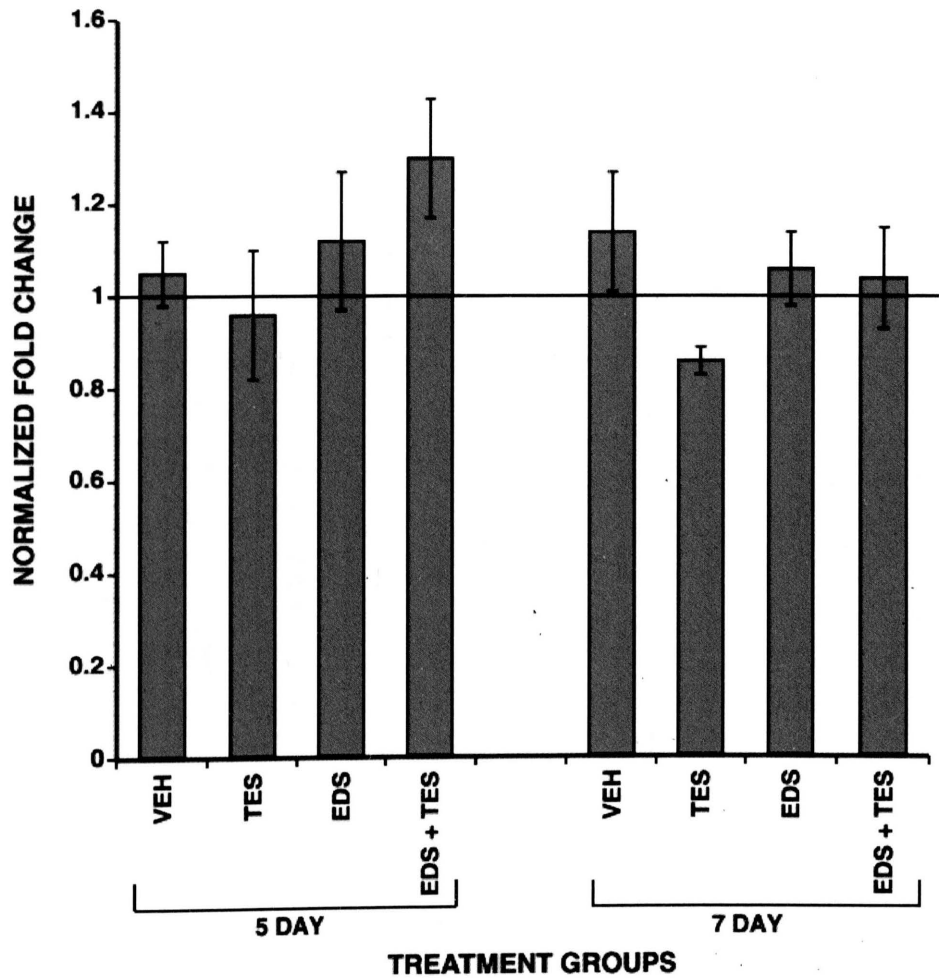
Figure 28: *Prf* mRNA levels with *Gapdh* as the reference gene. Error bars represent SEM with n = 6. Horizontal bar represents t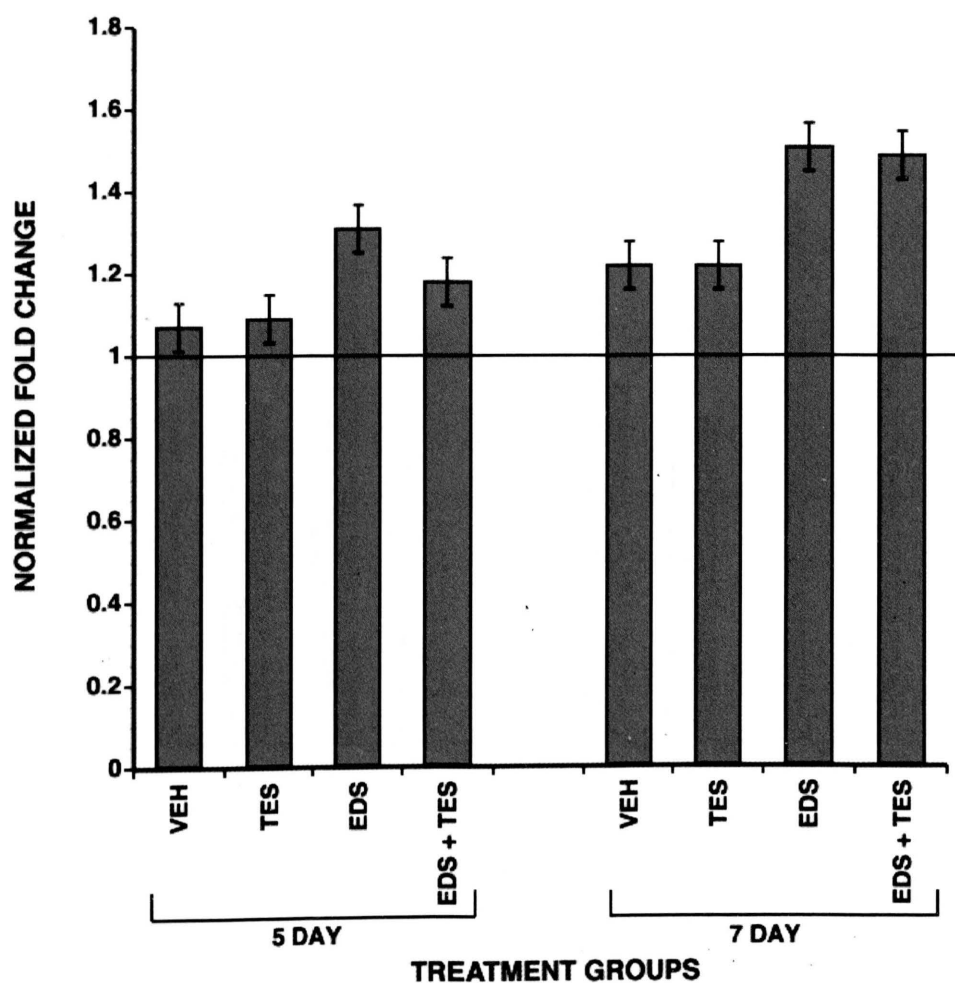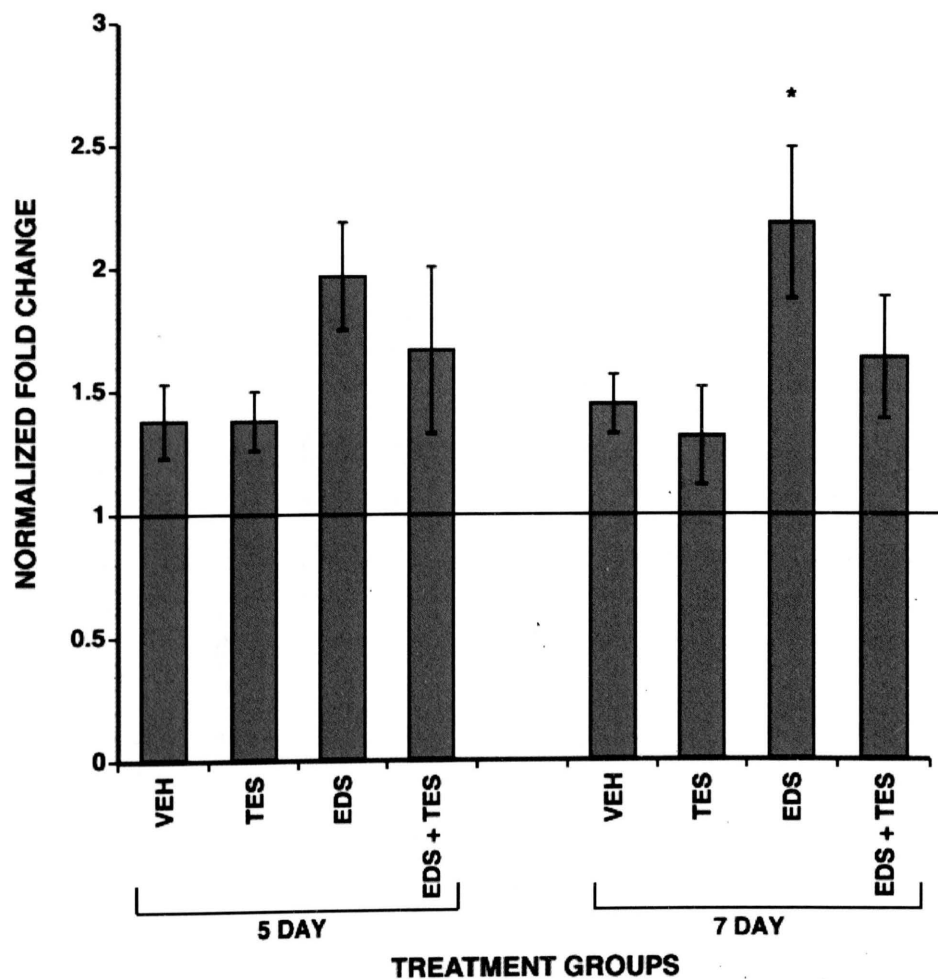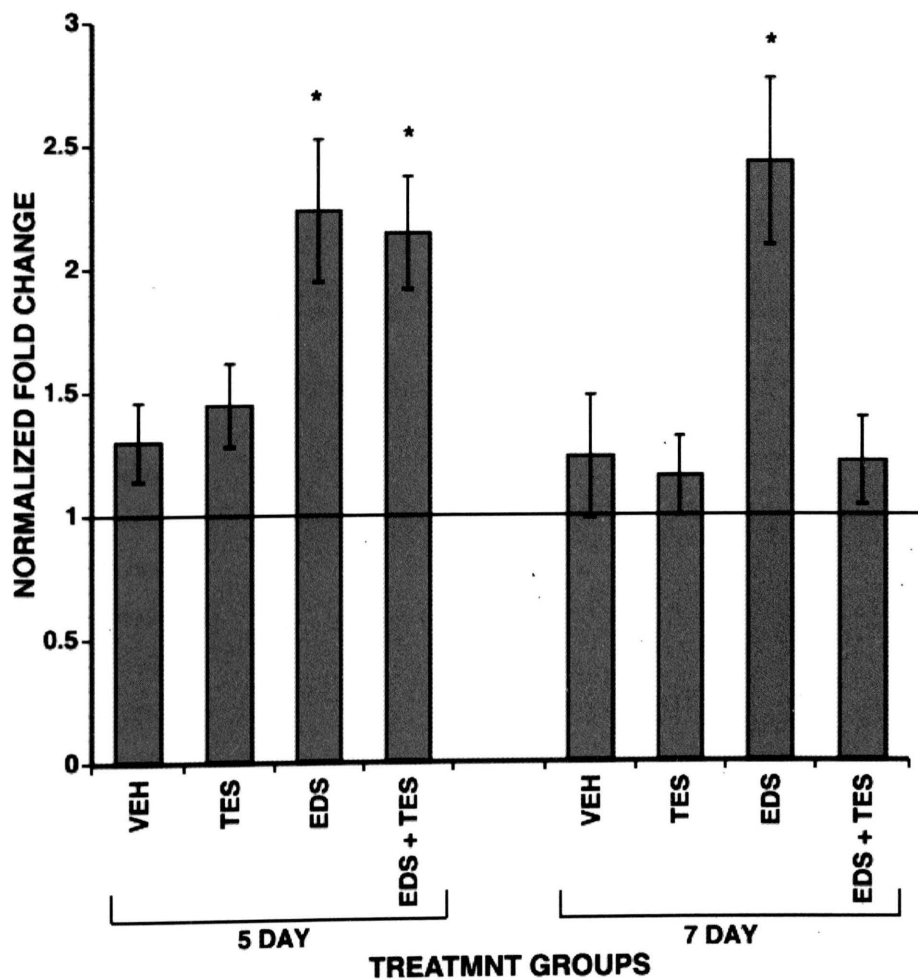he normalized value for the untreated (NT) group. Asterisk (*) indicates significant difference from VEH and TES within the same day. # indicates significant difference from VEH, TES and EDS + TES within the same day.

Figure 29: *Cd4* mRNA levels with *Gapdh* as the reference gene. Error bars represent SEM with n = 6. Horizontal bar represents the normalized value for the untreated (NT) group. Asterisk (*) indicates significant difference from VEH and TES within the same day. # indicates significant difference from VEH within the same day.

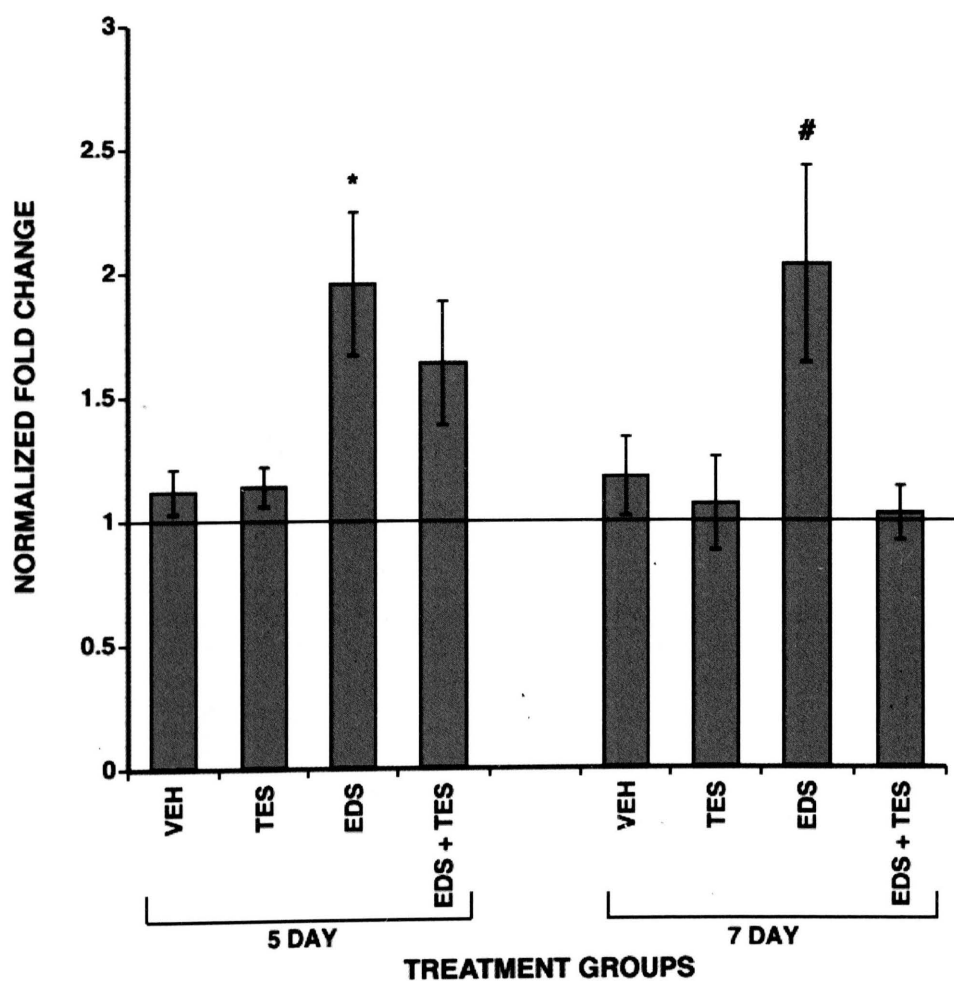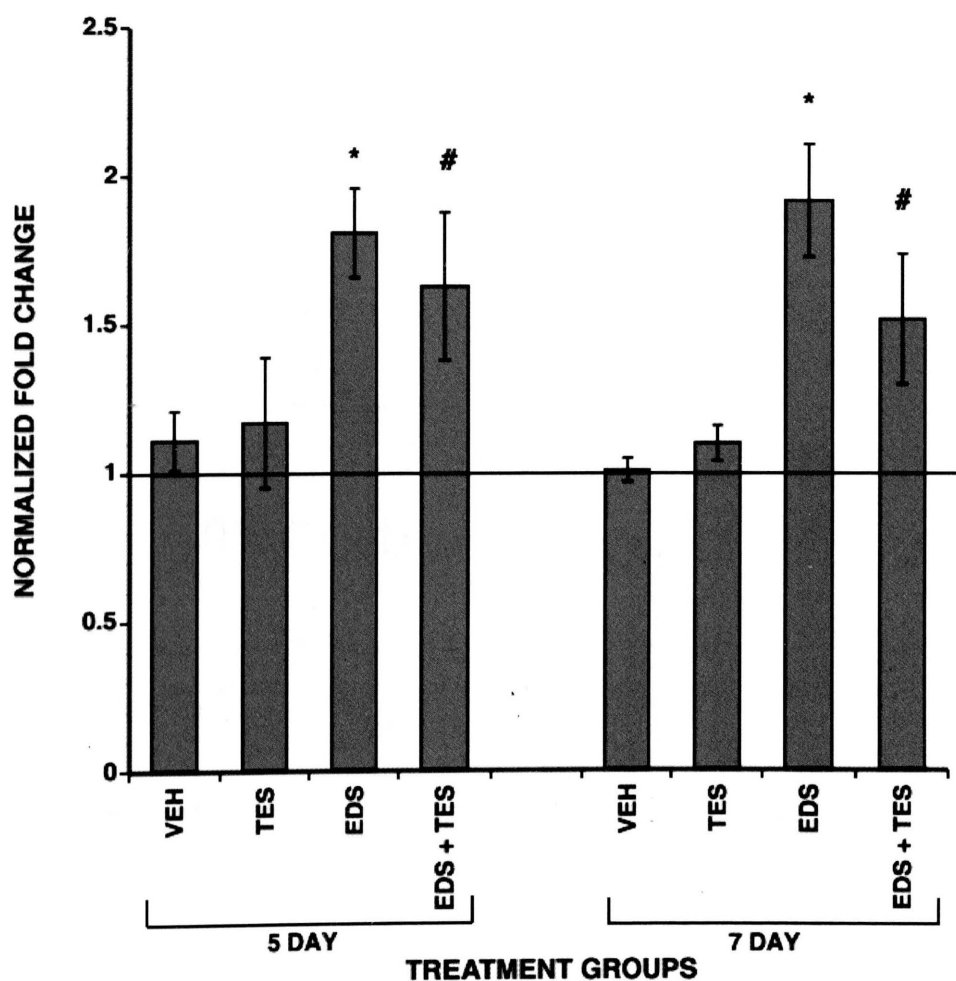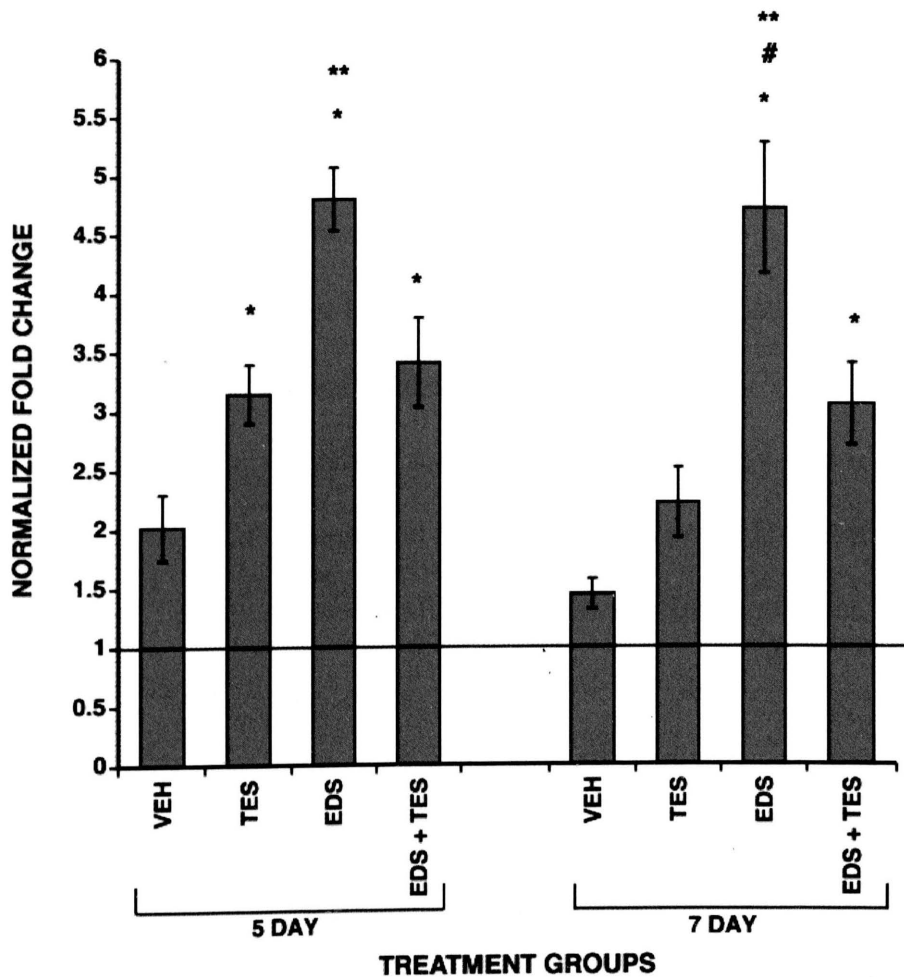**Figure 30:** *Cd8* mRNA levels with *Gapdh* as the reference gene. Error bars represent SEM with n = 6. Horizontal bar represents the normalized value for the untreated (NT) group. Single * indicates significant difference from VEH within the same day. Double * indicates significant difference from VEH, TES and EDS + TES groups within the same day. # indicates significant difference from TES within the same day.

Localization of CD4^{+}, CD8^{+} T Cells, Perforin and Granzyme K in the Rat Testis

Spermatogenesis occurs inside the secure environment of seminiferous epithelium protected from immune cells by the blood-testis barrier (BTB). However, immune cells are prevalent (Hedger & Hales 2006) in the interstitium of the testis. Besides CTLs and NK cells, macrophages and dendritic cells are also reported to be present in the interstitium, but none of these cells were ever reported to be present inside the seminiferous tubules (Hedger & Hales 2006).

In this study, an increase in apoptotic germ cells along with a significant increase in mRNAs for *Cd4*, *Cd8*, *GzmK*, and *Prf* was observed post-EDS treatment; expression of *GzmK*, *Prf* and *Cd8*^{+} was reversed after testosterone replacement. These results can be due to any of three reasons: (1) due to testosterone depletion there was disintegration of the BTB resulting in invasion of the CTLs inside the seminiferous tubules and induction of apoptosis in germ cells; (2) Sertoli cells or germ cells themselves overexpress *GzmK* and *Prf* in the absence of testosterone and induce apoptosis; or (3) germ cells overexpress *GzmK* and *Prf* in the absence of testosterone and may regulate some spermatogenic events. In order to accept or reject any of the three postulates, it was important to determine the localization of GZMK, PRF, CD4 and CD8 proteins in the testis. CD4 and CD8 staining were detected in the interstitium of the testis (Fig. 31 & 32) and are consistent with previous reports (Hedger *et al.* 1998). However, GZMK and PRF were co-localized inside the seminiferous tubule where residual bodies reside after sperm release (Fig. 33 – 36). This shows that *GzmK* and *Prf* are expressed inside the seminiferous tubules independent of CD8^{+} T cells.

65
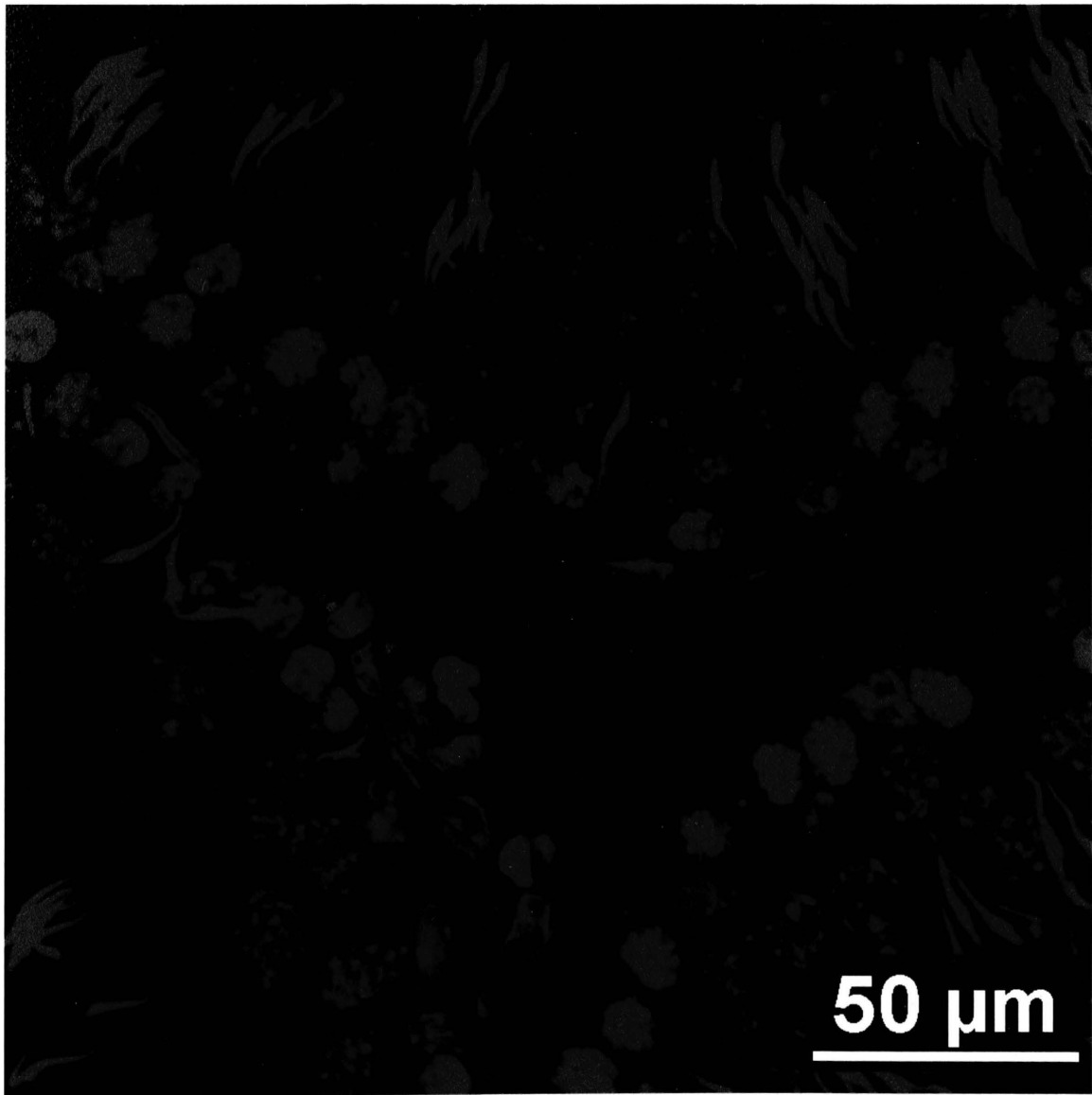
Figure 31: Confocal image of rat seminiferous tubule with localization of CD4 (red) in cross-section of 7 day EDS-treated rat testis. Anti-rat polyclonal goat anti-CD4 antibody was detected by DyLight 594-conjugated donkey anti-goat polyclonal antibody (red) and nuclei were stained by DAPI (blue).
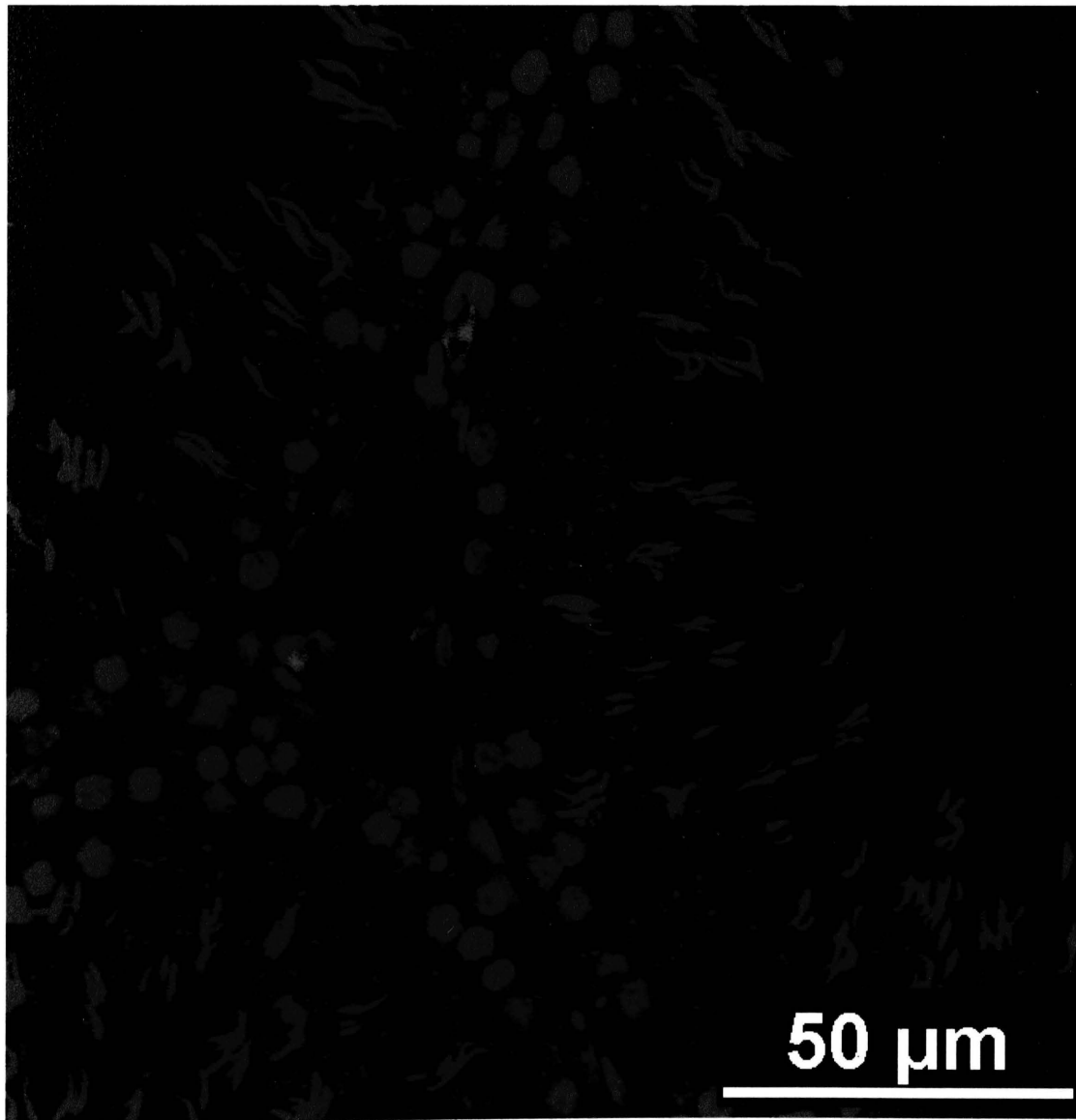
Figure 32: Confocal image of rat seminiferous tubule with localization of CD8 (red) in cross-section of 7 day EDS-treated rat testis. Anti-rat polyclonal rabbit anti-CD8b antibody was detected by DyLight 649-conjugated donkey anti-rabbit polyclonal antibody (red) and nuclei were stained by DAPI (blue).
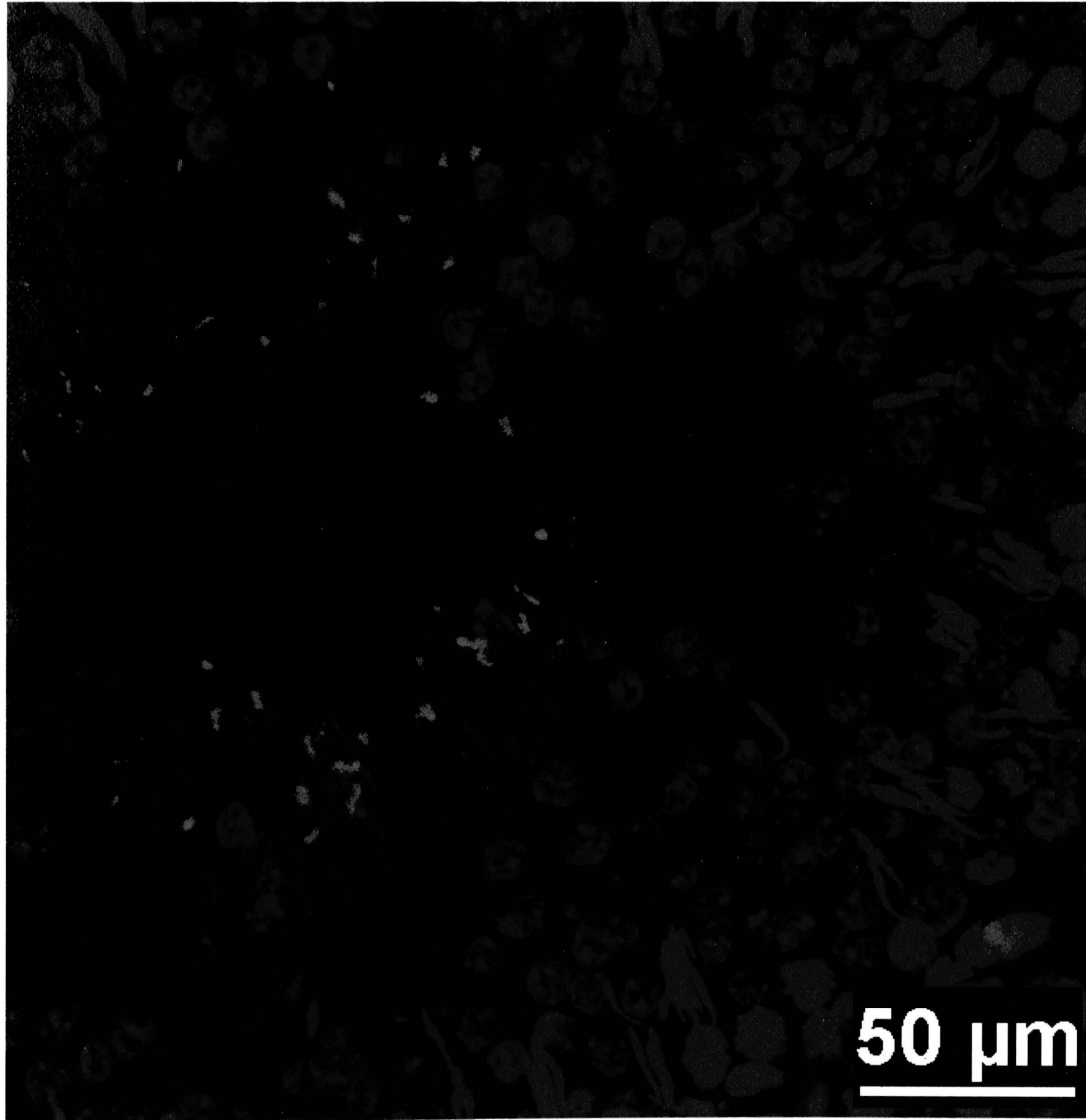
Figure 33: Confocal image of rat seminiferous tubule with localization of GZMK (green) in cross-section of 7 day EDS-treated rat testis. Anti-rat polyclonal goat anti-GZMK antibody was detected by DyLight 649-conjugated donkey anti-goat polyclonal antibody (green) and nuclei were stained by DAPI (blue).
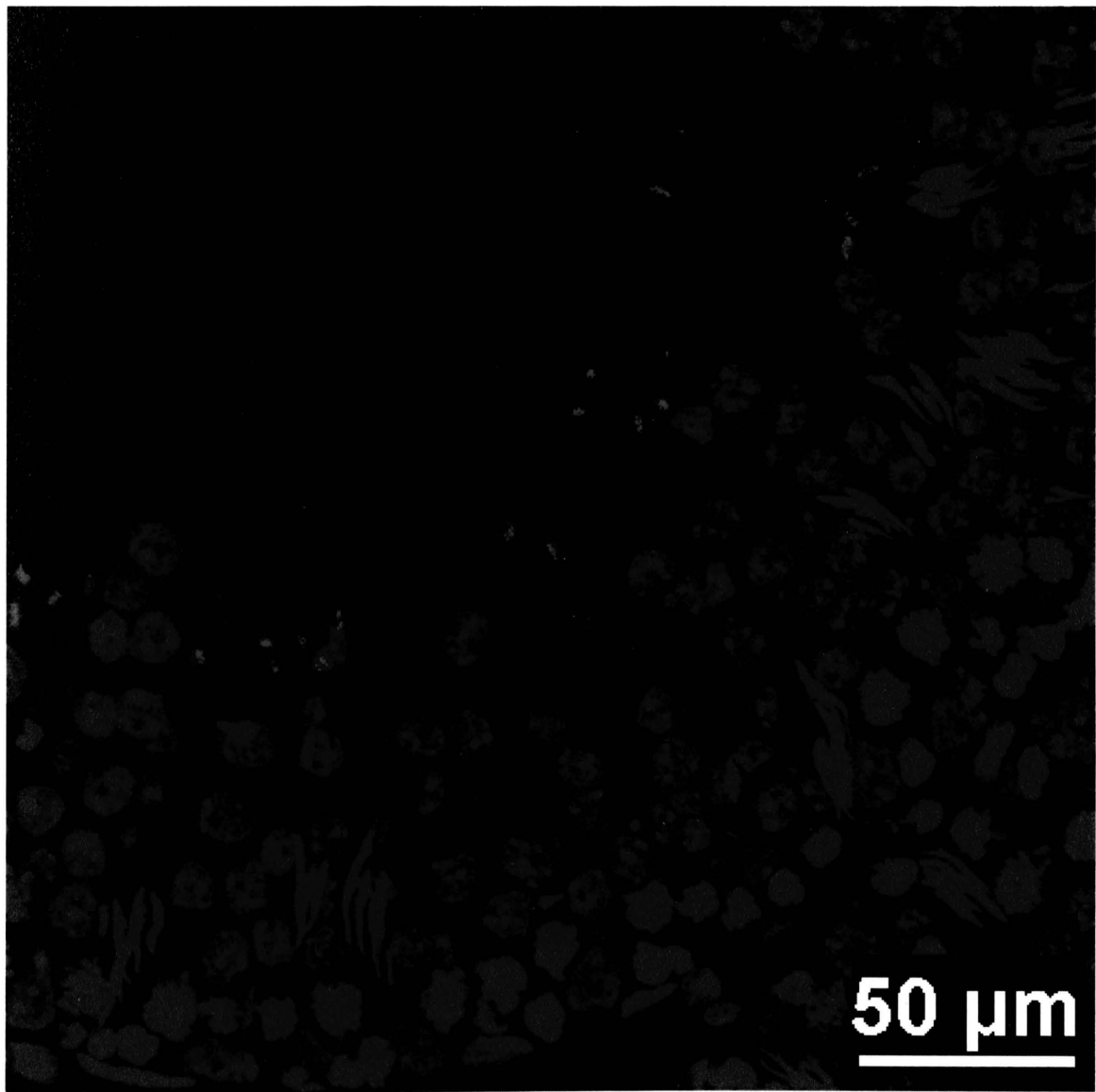
Figure 34: Confocal image of rat seminiferous tubule with localization of PRF (red) in cross-section of 7 day EDS-treated rat testis. Anti-rat polyclonal mouse anti-PRF antibody was detected by DyLight 594-conjugated donkey anti-mouse polyclonal antibody (red) and nuclei were stained by DAPI (blue).
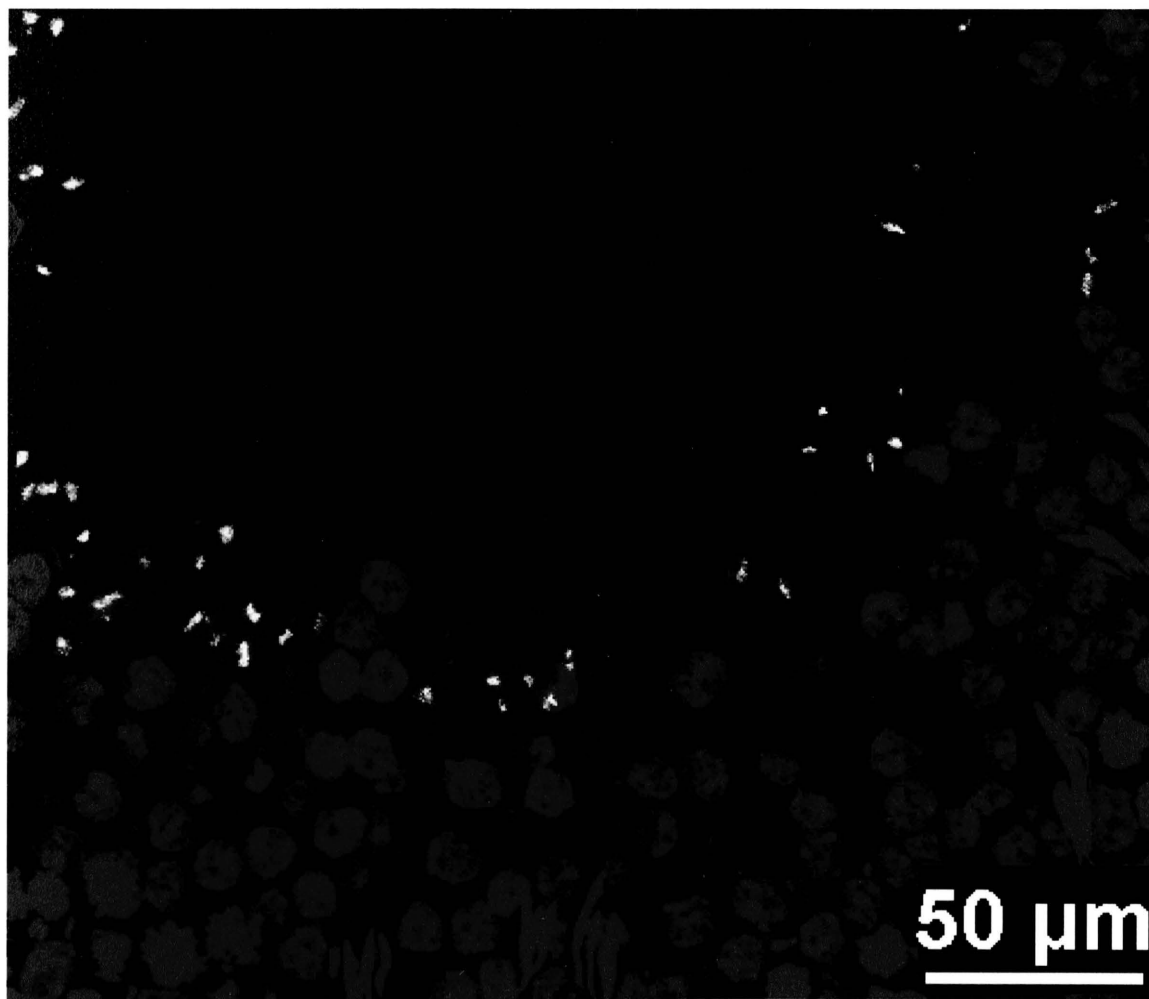
Figure 35: Confocal image of rat seminiferous tubule with co-localization of GZMK (green) and PRF (red) in cross-section of 7 day EDS-treated rat testis. Anti-rat polyclonal goat anti-GZMK antibody was detected by DyLight 649-conjugated donkey anti-goat polyclonal antibody (green) and anti-rat polyclonal mouse anti-PRF antibody was detected by DyLight 594-conjugated donkey anti-mouse polyclonal antibody (red) and nuclei were stained by DAPI (blue).
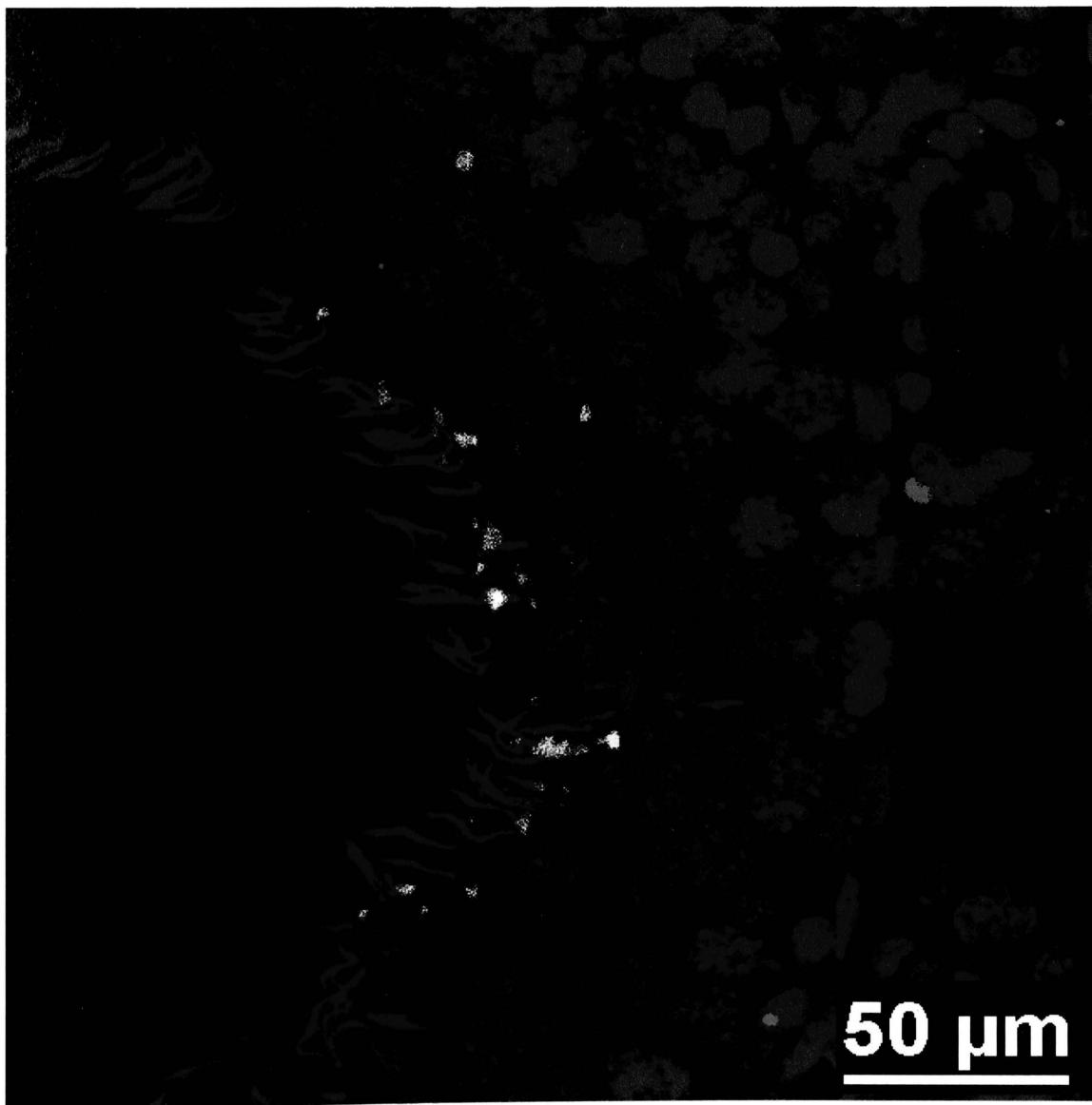
Figure 36: Confocal image of rat seminiferous tubule with co-localization of GZMK (green) and PRF (red) in cross-section of 7 day VEH-treated rat testis. Anti-rat polyclonal goat anti-GZMK antibody was detected by DyLight 649-conjugated donkey anti-goat polyclonal antibody (green) and anti-rat polyclonal mouse anti-PRF antibody was detected by DyLight 594-conjugated donkey anti-mouse polyclonal antibody (red) and nuclei were stained by DAPI (blue).
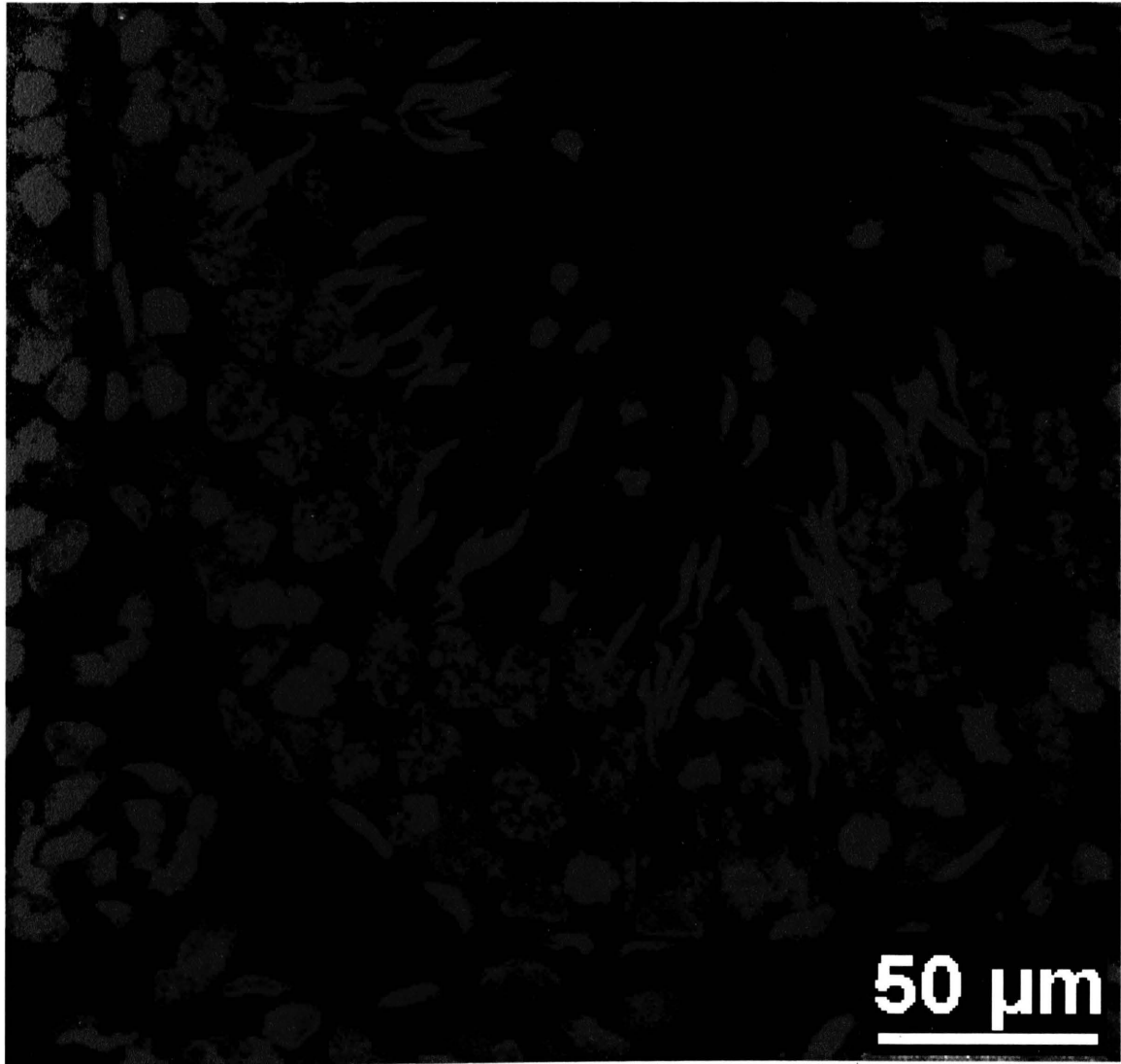
Figure 37: Confocal image of negative control for GZMK and PRF in rat seminiferous tubule cross-section of 7 day EDS-treated rat testis. The primary antibodies anti-rat polyclonal goat anti-GZMK antibody (for GZMK) and anti-rat polyclonal mouse anti-PRF antibody (for PRF) were omitted. Staining was performed by only the secondary antibodies DyLight 649-conjugated donkey anti-goat polyclonal antibody and DyLight 594-conjugated donkey anti-mouse polyclonal antibody. Nuclei were stained by DAPI (blue).

CHAPTER IV

DISCUSSION

The loss of *Lhr* and *Insl3* mRNAs after 5 and 7 days post-EDS treatment suggest elimination of most adult Leydig cells. With mature Leydig cells gone, there was depletion of testosterone to an undetectable level, progressive loss of testes weight and a time-dependent increase in germ cell apoptosis. Although testosterone replacement had no effect on *Lhr* and *Insl3* mRNA levels, testicular weights and viability of germ cells was maintained at the control levels. Thus, testosterone is vital for germ cell survival, and testosterone may act as a suppressor for apoptotic genes in testes.

Since effects of testosterone depletion on expression of BCL-2 family of proteins in testes (Woolveridge *et al.* 1999, Woolveridge *et al.* 2001, Show *et al.* 2004, O'Shaughnessy *et al.* 2008, Show *et al.* 2008) and the TNF family of proteins (Nandi *et al.* 1999, Taylor *et al.* 1999) have already been reported, we evaluated the response of GZM and PRF. Although granzyme members are present in testes (Hirst *et al.* 2001, Takano *et al.* 2004, Bhat *et al.* 2006, Chowdhury & Lieberman 2008), their comparative abundance, testosterone-responsiveness and association with germ cell apoptosis are not known. Moreover, PRF was not reported to be present in testes (Hirst *et al.* 2001). In this study, we evaluated testosterone-responsiveness on expression of *Prf*, four *Gzm* variants (*GzmA*, *GzmB*, *GzmK* and *GzmN*), along with localization of GZMK, PRF, CD4^{+} and CD8^{+} T cells in rat testes.

In normal rat testes, expression of *GzmN* is highest compared to *GzmA*, *GzmB* and *GzmK*, which is in agreement with an earlier report (Takano *et al*. 2004). Although *GzmK* had the least mRNA level than the other *Gzm* variants that were evaluated, it was the most testosterone-responsive *Gzm* variant followed by *GzmN*. The mRNA level of *GzmK* post-EDS treatment was 2- to 2.5-fold higher than controls. Moreover, testosterone supplementation reversed this effect after 7 days. A similar trend was observed regarding the mRNA levels of *Prf* and *Cd8*. Therefore, it was hypothesized that, in the absence of testosterone, the integrity of the blood-testis barrier may have been compromised resulting in infiltration and recruitment of CD8$^+$ T cells inside the seminiferous tubule. After coming in contact with germ cells, CD8$^+$ T cells release PRF and GZMK to induce apoptosis of germ cells. Therefore, using immunohistochemistry, we performed localization of CD8, GZMK and PRF in EDS-treated rat testes. Interestingly, CD8 staining was observed in the interstitium only and never inside the seminiferous tubule, which is in agreement with previous reports (Wang *et al*. 1994, Hedger *et al*. 1998). On the other hand, GZMK and PRF were co-localized inside the seminiferous tubule, but not on or around germ cells. This indicates that, although there is an increase in *GzmK* and *Prf* mRNAs, their expression may not be associated with CD8$^+$ T cells in testes, and GZMK and PRF, like other granzyme variants, may be involved in some non-apoptotic mechanism regulating spermatogenesis. For example, GZMB and GZMN are not associated with CD8$^+$ T cells in testes and GZMB is expressed in Sertoli cells (Hirst *et al*. 2001), and GZMN in primary spermatocytes, round spermatids and elongated spermatids (Takano *et al*. 2004). Both these granzyme variants

74

in testes were hypothesized to be involved in some non-apoptotic function during spermatogenesis (Takano *et al.* 2004), including a role in facilitation of migration of developing germ cells through the blood-testis barrier (Hirst *et al.* 2001).

Although granzymes are generally cytolytic, and are mostly associated with CD8^{+} T cells, they can be expressed in other non-immune cells as well (granulosa cells and chondrocytes) (Amsterdam *et al.* 2003, Chowdhury & Lieberman 2008). Moreover, granzymes are also involved in non-apoptotic extracellular activities such as remodeling of extracellular matrix, inducing inflammation and signal transduction (Buzza & Bird 2006, Romero & Andrade 2008, Anthony *et al.* 2010). Here, our results also indicated non-apoptotic functions of GZMK and PRF in testes.

Granzyme K, also known as *Gzm3* was originally discovered as the second tryptase granzyme member other than *GzmA* (Chowdhury & Lieberman 2008) and is closely located to *GzmA* on the same chromosome (human 5q11.2, mouse 13 13 and rat 2q14) (Zhao *et al.* 2007a). In various models *GzmK* induces apoptosis in a caspase-independent manner (Guo *et al.* 2008) by cleaving components of SET complex APEI, HMG2 and SET to allow DNase NM23H1 to generate single strand DNA breaks (Zhao *et al.* 2007b, Guo *et al.* 2008). GZMK also processes pro-apoptotic BID and produces reactive oxygen species from mitochondria during the initial stages of apoptosis (Zhao *et al.* 2007a). However, GZMK may also have a non-apoptotic function. Besides being in CTLs and natural killer cells, *GzmK* is also present in mouse brain (Suemoto *et al.* 1999). Using *in situ* hybridization *GzmK* mRNA was detected in the cerebral cortex, hippocampus, hypothalamus and diencephalon but not in glial cells of the mouse brain

(Suemoto et al. 1999). Therefore, it was suggested that GZMK in brain may process or degrade neuropeptides and β-amyloid precursor protein, since tryptase-like activity was seen during degradation of β-amyloid precursor protein in brain (Wiegand et al. 1993). Similarly, in testes GZMK and PRF may have such a non-apoptotic function and play a role during spermatogenesis.

Previous studies have shown that testosterone is essential to complete the process of elongation of round spermatids to elongated spermatids (O'Donnell et al. 1994, O'Donnell et al. 2006), and during release of spermatozoa (spermiation) from the Sertoli cell (Kerr et al. 2006, O'Donnell et al. 2006). During spermiation, spermatozoa disengage from the ectoplasmic specialization and progressively move towards the lumen (Kerr et al. 2006), and the Sertoli cell selectively retain the excess residual cytoplasm as residual bodies and release the sperm (Kerr et al. 2006). The exact mechanisms of spermatozoa release from ectoplasmic specialization, however, remain elusive (Kerr et al. 2006). It is suggested that when spematids begin to lose their relationship to the ectoplasmic specialization, structures rich in filaments and microtubules, called tubulobule, start to appear (Kerr et al. 2006) and these structures are retained until sperm are released (Kerr et al. 2006). These tubulobular structures indirectly help in the formation of residual bodies by pulling the excess cytoplasm from the lumen to the apical trunk of the Sertoli cell (Kerr et al. 2006). Just after the release of sperm, the spermatid cytoplasm in the residual bodies is reduced by 70% concurrently with successive degradation and reformation of the tubulobular structures (Kerr et al. 2006). Granzyme K and PRF may play a crucial role in this process and facilitate the degradation of the

tubulobular structures. Since, tubulobular structures are made of microtubules (Vogl *et al*. 2000) and β-tubulin is a specific target of GZMK (Bovenschen *et al*. 2009), GZMK may have a role in degradation of the tubulobular structures. Moreover, microtubules are also abundant in the Sertoli cell cytoplasm and surround the cisterns in which spermatids remain embedded (Vogl *et al*. 2000), therefore, GZMK may modulate the structural rearrangement of ectoplasmic specialization and movement of spermatids during spermiogenesis. Indeed, Guttman *et al*. (2004) reported that tubulobular complexes are responsible for internalization and disassembly of ectoplasmic specialization at the time of spermiation. Therefore our results indicated that, due to testosterone depletion there was an overexpression of *GzmK* and *Prf* which may have led to an increased degradation of tubulobular structures and ectoplasmic specialization. With premature degradation of the tubulobular structures, germ cells detached from Sertoli cell and became apoptotic. A comprehensive model for the localization of CD8^{+} T cells, GZMK and PRF with relation to various cells in the seminiferous tubule is depicted in figure 38.

In conclusion, at least four granzyme variants are expressed in rat testes, of which *GzmN* is the most abundant and *GzmK* is the least abundant variant. Both *GzmK* and *GzmN* in rat testes are testosterone-responsive. The expression of *GzmK* in EDS-treated rat testes was similar to the expression of *Prf*. There was an increase in mRNAs for *Cd4* and *Cd8*, however, both CD4^{+} T cells and CD8^{+} T cells were located in the interstitium, whereas GZMK and PRF were detected inside the seminiferous tubule. This showed that, in testes, testosterone-dependent expression of *GzmK*, *GzmN* and *Prf* are not associated with CD8^{+} T cells. Since, GZMK and PRF were not detected inside or in

proximity of germ cells, their direct role in inducing germ cell apoptosis in the absence of testosterone could not be proved. However, detection of GZMK and PRF by the residual bodies in the seminiferous tubule suggests their possible role in degradation of microtubules during spermiation.
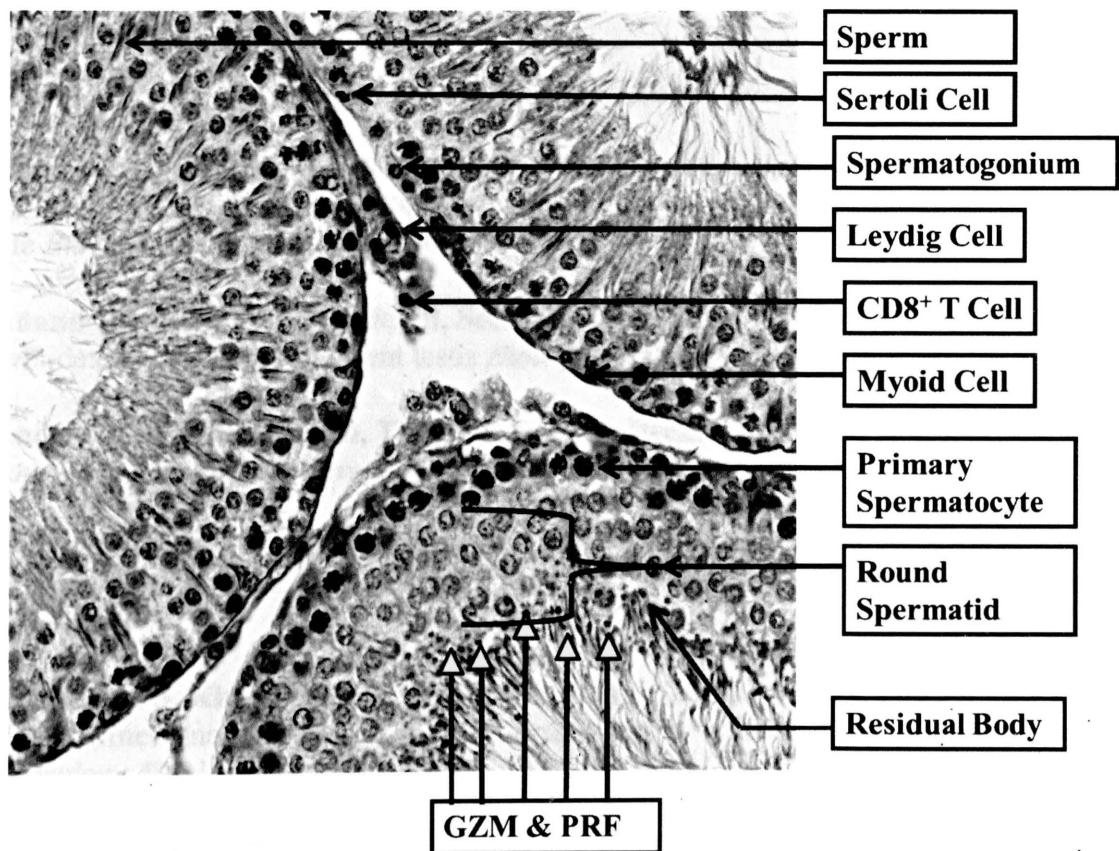
Figure 38: Localization of specific cell types in the cross-section of rat seminiferous tubule. Residual bodies containing GZMK and PRF (shown in yellow arrows) are localized to stripped cytoplasm of round spermatids. Cell types (CD8$^+$ T cells) containing GZMK and PRF are also localized in the interstitium, indicated by arrow. Magnification of photograph is 400X.

REFERENCES

Amsterdam A, Sasson R, Keren-Tal I, Aharoni D, Dantes A, Rimon E, Land A, Cohen T, Dor Y & Hirsh L 2003 Alternative pathways of ovarian apoptosis: death for life *Biochemical pharmacology* **66** 1355-1362.

Anand-Ivell R, Heng K, Hafen B, Setchell B & Ivell R 2009 Dynamics of INSL3 peptide expression in the rodent testis *Biology of reproduction* **81** 480-487.

Andersen MH, Schrama D, Thor Straten P & Becker JC 2006 Cytotoxic T cells *The Journal of investigative dermatology* **126** 32-41.

Anthony DA, Andrews DM, Watt SV, Trapani JA & Smyth MJ 2010 Functional dissection of the granzyme family: cell death and inflammation *Immunological reviews* **235** 73-92.

Ariyaratne S, Kim I, Mills N, Mason I & Mendis-Handagama C 2003 Effects of ethane dimethane sulfonate on the functional structure of the adult rat testis *Archives of Andrology* **49** 313-326.

Bhat GK, Sea TL, Olatinwo MO, Simorangkir D, Ford GD, Ford BD & Mann DR 2006 Influence of a leptin deficiency on testicular morphology, germ cell apoptosis, and expression levels of apoptosis-related genes in the mouse *Journal of andrology* **27** 302-310.

Boisen KA, Main KM, Rajpert-De Meyts E & Skakkebaek NE 2001 Are male reproductive disorders a common entity? The testicular dysgenesis syndrome *Annals of the New York Academy of Sciences* **948** 90-99.

Bovenschen N & Kummer JA 2010 Orphan granzymes find a home *Immunological reviews* **235** 117-127.

Bovenschen N, Quadir R, van den Berg AL, Brenkman AB, Vandenberghe I, Devreese B, Joore J & Kummer JA 2009 Granzyme K displays highly restricted substrate specificity that only partially overlaps with granzyme A *The Journal of biological chemistry* **284** 3504-3512.

Buzza MS & Bird PI 2006 Extracellular granzymes: current perspectives *Biological chemistry* **387** 827-837.

Chavez-Galan L, Arenas-Del Angel MC, Zenteno E, Chavez R & Lascurain R 2009 Cell death mechanisms induced by cytotoxic lymphocytes *Cellular & molecular immunology* **6** 15-25.

Chowdhury D &Lieberman J 2008 Death by a thousand cuts: granzyme pathways of programmed cell death *Annual Review of Immunology* **26** 389-420.

de Rooij DG 2001 Proliferation and differentiation of spermatogonial stem cells *Reproduction (Cambridge, England)* **121** 347-354.

Diamanti-Kandarakis E, Bourguignon JP, Giudice LC, Hauser R, Prins GS, Soto AM, Zoeller RT & Gore AC 2009 Endocrine-disrupting chemicals: an Endocrine Society scientific statement *Endocrine reviews* **30** 293-342.

Dym M &Romrell LJ 1975 Intraepithelial lymphocytes in the male reproductive tract of rats and rhesus monkeys *Journal of reproduction and fertility* **42** 1-7.

Eddy EM 2002 Male germ cell gene expression *Recent progress in hormone research* **57** 103-128.

Ferlin A, Garolla A, Rigon F, Rasi Caldogno L, Lenzi A & Foresta C 2006 Changes in serum insulin-like factor 3 during normal male puberty *The Journal of clinical endocrinology and metabolism* **91** 3426-3431.

Free MJ &Tillson SA 1973 Secretion rate of testicular steroids in the conscious and halothane-anesthetized rat *Endocrinology* **93** 874-879.

Froelich CJ, Metkar SS & Raja SM 2004 Granzyme B-mediated apoptosis--the elephant and the blind men? *Cell death and differentiation* **11** 369-371.

Garrity MM, Burgart LJ, Riehle DL, Hill EM, Sebo TJ & Witzig T 2003 Identifying and quantifying apoptosis: navigating technical pitfalls *Modern pathology : an official journal of the United States and Canadian Academy of Pathology, Inc* **16** 389-394.

Goldsby RA, Kindt TJ & Osborne BA 2000 Cell-Mediated Effector Responses. In *Kuby Immunology,* edn 4th, pp 351-370. Anonymous , New York, USA: W. H. Freeman and Company.

Griffin JE 2004 Male reproductive function. In *Textbook of Endocrine Physiology* edn 5th, pp 226-248. Eds JE Griffin and SR Ojeda, New York, USA: Oxford University Press.

Griswold MD 1998 The central role of Sertoli cells in spermatogenesis *Seminars in cell & developmental biology* **9** 411-416.

Grossman WJ, Revell PA, Lu ZH, Johnson H, Bredemeyer AJ & Ley TJ 2003 The orphan granzymes of humans and mice *Current opinion in immunology* **15** 544-552.

Guo Y, Chen J, Zhao T & Fan Z 2008 Granzyme K degrades the redox/DNA repair enzyme Ape1 to trigger oxidative stress of target cells leading to cytotoxicity *Molecular immunology* **45** 2225-2235.

Guttman JA, Takai Y & Vogl AW 2004 Evidence that tubulobulbar complexes in the seminiferous epithelium are involved with internalization of adhesion junctions *Biology of reproduction* **71** 548-559.

Hedger MP &Hales DB 2006 Immunology of the Male Reproductive Tract. In *Knobil and Neill's Physiology of Reproduction,* edn 3rd, pp 1195-1286. Ed. JD Neill, USA: Academic Press.

Hedger MP 2002 Macrophages and the immune responsiveness of the testis *Journal of reproductive immunology* **57** 19-34.

Hedger MP, Wang J, Lan HY, Atkins RC & Wreford NG 1998 Immunoregulatory activity in adult rat testicular interstitial fluid: relationship with intratesticular CD8+ lymphocytes following treatment with ethane dimethane sulfonate and testosterone implants *Biology of reproduction* **58** 935-942.

Henriksen K, Hakovirta H & Parvinen M 1995 Testosterone inhibits and induces apoptosis in rat seminiferous tubules in a stage-specific manner: in situ quantification in squash preparations after administration of ethane dimethane sulfonate *Endocrinology* **136** 3285-3291.

Hirst CE, Buzza MS, Sutton VR, Trapani JA, Loveland KL & Bird PI 2001 Perforin-independent expression of granzyme B and proteinase inhibitor 9 in human testis and placenta suggests a role for granzyme B-mediated proteolysis in reproduction *Molecular human reproduction* **7** 1133-1142.

Hutson JC 2006 Physiologic interactions between macrophages and Leydig cells *Experimental biology and medicine (Maywood, N.J.)* **231** 1-7.

Jackson CM &Jackson H 1984 Comparative protective actions of gonadotrophins and testosterone against the antispermatogenic action of ethane dimethanesulphonate *Journal of reproduction and fertility* **71** 393-401.

Kerr JB, Loveland KL, O'Bryan MK & de Kretser DM 2006 Cytology of the Testis and Intrinsic Control Mechanisms. In *Knobil and Neill's Physiology of Reproduction,* edn 3rd, pp 837-947. Ed. JD Neill, USA: Academic Press.

Kiernan JA 1990 Fixation. In *Histological and Histochemical Methods: Theory and Practices,* edn 2nd, pp 10-31. Anonymous , Great Britain: Pergamon Press.

Koeva YA, Bakalska MV, Atanassova NN & Davidoff MS 2008 INSLF3-LGR8 ligand-receptor system in testes of mature rats after exposure to ethane dimethanesulphonate (short communication) *Folia medica* **50** 37-42.

Kubista M, Andrade JM, Bengtsson M, Forootan A, Jonak J, Lind K, Sindelka R, Sjoback R, Sjogreen B, Strombom L, Stahlberg A & Zoric N 2006 The real-time polymerase chain reaction *Molecular aspects of medicine* **27** 95-125.

Lanning LL, Creasy DM, Chapin RE, Mann PC, Barlow NJ, Regan KS & Goodman DG 2002 Recommended approaches for the evaluation of testicular and epididymal toxicity *Toxicologic pathology* **30** 507-520.

Latendresse JR, Warbrittion AR, Jonassen H & Creasy DM 2002 Fixation of testes and eyes using a modified Davidson's fluid: comparison with Bouin's fluid and conventional Davidson's fluid *Toxicologic pathology* **30** 524-533.

Marsden VS &Strasser A 2003 Control of apoptosis in the immune system: Bcl-2, BH3-only proteins and more *Annual Review of Immunology* **21** 71-105.

McCabe MJ, Tarulli GA, Meachem SJ, Robertson DM, Smooker PM & Stanton PG 2010 Gonadotropins regulate rat testicular tight junctions in vivo *Endocrinology* **151** 2911-2922.

Mendis-Handagama SM, Ariyaratne HB, Mrkonjich L & Ivell R 2007 Expression of insulin-like peptide 3 in the postnatal rat Leydig cell lineage: timing and effects of triiodothyronine-treatment *Reproduction (Cambridge, England)* **133** 479-485.

Mori H &Christensen AK 1980 Morphometric analysis of Leydig cells in the normal rat testis *The Journal of cell biology* **84** 340-354.

Morris AJ, Taylor MF & Morris ID 1997 Leydig cell apoptosis in response to ethane dimethanesulphonate after both in vivo and in vitro treatment *Journal of andrology* **18** 274-280.

Mruk DD &Cheng CY 2004 Sertoli-Sertoli and Sertoli-germ cell interactions and their significance in germ cell movement in the seminiferous epithelium during spermatogenesis *Endocrine reviews* **25** 747-806.

Nandi S, Banerjee PP & Zirkin BR 1999 Germ cell apoptosis in the testes of Sprague Dawley rats following testosterone withdrawal by ethane 1,2-dimethanesulfonate administration: relationship to Fas? *Biology of reproduction* **61** 70-75.

O'Donnell L, McLachlan RI, Wreford NG, de Kretser DM & Robertson DM 1996 Testosterone withdrawal promotes stage-specific detachment of round spermatids from the rat seminiferous epithelium *Biology of reproduction* **55** 895-901.

O'Donnell L, McLachlan RI, Wreford NG & Robertson DM 1994 Testosterone promotes the conversion of round spermatids between stages VII and VIII of the rat spermatogenic cycle *Endocrinology* **135** 2608-2614.

O'Donnell L, Meachem SJ, Stanton PG & McLachlan RI 2006 Endocrine Regulation of Spermatogenesis. In *Knobil and Neill's Physiology of Reproduction,* edn 3rd, pp 1017-1070. Ed. JD Neill, USA: Academic Press.

O'Shaughnessy PJ, Morris ID & Baker PJ 2008 Leydig cell re-generation and expression of cell signaling molecules in the germ cell-free testis *Reproduction (Cambridge, England)* **135** 851-858.

O'Shaughnessy PJ, Morris ID & Baker PJ 2008 Leydig cell re-generation and expression of cell signaling molecules in the germ cell-free testis *Reproduction (Cambridge, England)* **135** 851-858.

Pelletier RM 1986 Cyclic formation and decay of the blood-testis barrier in the mink (Mustela vison), a seasonal breeder *The American Journal of Anatomy* **175** 91-117.

Romero V &Andrade F 2008 Non-apoptotic functions of granzymes *Tissue antigens* **71** 409-416.

Russell LD 1993 Morphological and functional evidence for Sertoli-germ cell relationships. In *The Sertoli Cell,* pp 365-390. Eds LD Russell and MD Griswold, Clearwater, FL, USA: Cache River Press.

Sasi N, Hwang M, Jaboin J, Csiki I & Lu B 2009 Regulated cell death pathways: new twists in modulation of BCL2 family function *Molecular cancer therapeutics* **8** 1421-1429.

Schwartzman RA &Cidlowski JA 1993 Apoptosis: the biochemistry and molecular biology of programmed cell death *Endocrine reviews* **14** 133-151.

Setchell BP &Breed WG 2006 Anatomy, Vasculature and Innervation of the Male Reproductive Tract. In *Knobil and Neill's Physiology of Reproduction,* edn 3rd, pp 771-826. Ed. JD Neill, USA: Academic Press.

Sharpe RM 1994 Regulation of Spermatogenesis. In *The Physiology of Reproduction,* edn 2nd, pp 1363-1434. Eds E Knobil and JD Neill, New York, USA: Raven Press.

Show MD, Folmer JS, Anway MD & Zirkin BR 2004 Testicular expression and distribution of the rat bcl2 modifying factor in response to reduced intratesticular testosterone *Biology of reproduction* **70** 1153-1161.

Show MD, Hill CM, Anway MD, Wright WW & Zirkin BR 2008 Phosphorylation of mitogen-activated protein kinase 8 (MAPK8) is associated with germ cell apoptosis and redistribution of the Bcl2-modifying factor (BMF) *Journal of andrology* **29** 338-344.

Shuttlesworth GA &Mills N 1995 Section adherence to glass slides from polyester wax-embedded tissue for in situ hybridization *BioTechniques* **18** 948-950.

Sircar S 2008 Puberty and Gametogenesis. In *Principles of Medical Physiology,* edn 1st, pp 552-561. Anonymous , India: Thieme Medical Publishers.

Skakkebaek NE, Rajpert-De Meyts E & Main KM 2001 Testicular dysgenesis syndrome: an increasingly common developmental disorder with environmental aspects *Human reproduction (Oxford, England)* **16** 972-978.

Stahelin BJ, Marti U, Solioz M, Zimmermann H & Reichen J 1998 False positive staining in the TUNEL assay to detect apoptosis in liver and intestine is caused by endogenous nucleases and inhibited by diethyl pyrocarbonate *Molecular pathology : MP* **51** 204-208.

Steinberger E &Steinberger A 1975 Spermatogenic function of the testis. In *Handbook of Physiology,* pp 1-19. Eds RO Greep and EB Astwood, Baltimore, USA: William and Wilkins.

Stocco DM &McPhaul MJ 2006 Physiology of Testicular Steroidogenesis. In *Knobil and Neill's Physiology of Reproduction,* edn 3rd, pp 977-1016. Ed. JD Neill, USA: Academic Press.

Suemoto T, Taniguchi M, Shiosaka S & Yoshida S 1999 cDNA cloning and expression of a novel serine protease in the mouse brain *Brain research. Molecular brain research* **70** 273-281.

Takano N, Matusi H & Takahashi T 2004 Granzyme N, a novel granzyme, is expressed in spermatocytes and spermatids of the mouse testis *Biology of reproduction* **71** 1785-1795.

Taylor MF, de Boer-Brouwer M, Woolveridge I, Teerds KJ & Morris ID 1999 Leydig cell apoptosis after the administration of ethane dimethanesulfonate to the adult male rat is a Fas-mediated process *Endocrinology* **140** 3797-3804.

Taylor MF, Woolveridge I, Metcalfe AD, Streuli CH, Hickman JA & Morris ID 1998 Leydig cell apoptosis in the rat testes after administration of the cytotoxin ethane dimethanesulphonate: role of the Bcl-2 family members *The Journal of endocrinology* **157** 317-326.

Tornusciolo DR, Schmidt RE & Roth KA 1995 Simultaneous detection of TDT-mediated dUTP-biotin nick end-labeling (TUNEL)-positive cells and multiple immunohistochemical markers in single tissue sections *BioTechniques* **19** 800-805.

Trapani JA & Bird PI 2008 A renaissance in understanding the multiple and diverse functions of granzymes? *Immunity* **29** 665-667.

Vogl AW, Pfeiffer DC, Mulholland D, Kimel G & Guttman J 2000 Unique and multifunctional adhesion junctions in the testis: ectoplasmic specializations *Archives of Histology and Cytology* **63** 1-15.

Wallach D, Kang TB & Kovalenko A 2008 The extrinsic cell death pathway and the elan mortel *Cell death and differentiation* **15** 1533-1541.

Wang J, Wreford NG, Lan HY, Atkins R & Hedger MP 1994 Leukocyte populations of the adult rat testis following removal of the Leydig cells by treatment with ethane dimethane sulfonate and subcutaneous testosterone implants *Biology of reproduction* **51** 551-561.

Woolveridge I, de Boer-Brouwer M, Taylor MF, Teerds KJ, Wu FC & Morris ID 1999 Apoptosis in the rat spermatogenic epithelium following androgen withdrawal: changes in apoptosis-related genes *Biology of reproduction* **60** 461-470.

Woolveridge I, Taylor MF, Rommerts FF & Morris ID 2001 Apoptosis related gene products in differentiated and tumorigenic rat Leydig cells and following regression

induced by the cytotoxin ethane dimethanesulphonate *International journal of andrology* **24** 56-64.

Yang ZW, Kong LS, Guo Y, Yin JQ & Mills N 2006 Histological changes of the testis and epididymis in adult rats as a result of Leydig cell destruction after ethane dimethane sulfonate treatment: a morphometric study *Asian Journal of Andrology* **8** 289-299.

Zar JH 1999 Biostatistical analysis.

Zhao T, Zhang H, Guo Y & Fan Z 2007 Granzyme K directly processes bid to release cytochrome c and endonuclease G leading to mitochondria-dependent cell death *The Journal of biological chemistry* **282** 12104-12111.

Zhao T, Zhang H, Guo Y, Zhang Q, Hua G, Lu H, Hou Q, Liu H & Fan Z 2007 Granzyme K cleaves the nucleosome assembly protein SET to induce single-stranded DNA nicks of target cells *Cell death and differentiation* **14** 489-499.

APPENDIX A

List of Abbreviations

LIST OF ABBREVIATIONS

Abbreviation	Full name
ANOVA	Analysis of variance
BCL-2	B-cell lymphoma-2
BID	BH3 interacting domain death agonist
BSA	Bovine serum albumin
BTB	Blood-testis barrier
CD	Cluster of differentiation
CDC	Centers for Disease Control and Prevention
cDNA	Complementary deoxyribonucleic acid
$C_{(t)}$	Cycle threshold
CTL	Cytotoxic T Lymphocyte
DAB	3,3'- diaminobenzidine
DAPI	4',6-diamidino-2-phenylindole
DMSO	Dimethyl sulfoxide
dNTP	Deoxyribonucleotide triphosphate
EDS	Ethylene dimethane sulfonate
EDS + TES	Testosterone-replaced
EDTA	Ethylenediaminetetraacetic acid

FSH	Follicle stimulating hormone
GAPDH	Glyceraldehyde 3-phosphate dehydrogenase
GnRH	Gonadotropin releasing hormone
GZMA[1]	Granzyme A
GZMB	Granzyme B
GZMK	Granzyme K
GZMN	Granzyme N
H&E	Hematoxylin and Eosin
HCl	Hydrochloric acid
IgG	Immunoglobulin G
IHC	Immunohistochemistry
IL	Interleukin
INSL3	Insulin-like peptide 3
ip	Intraperitoneal
ITT	Intratesticular testosterone
LH	Luteinizing hormone
LHR	Luteinizing hormone receptor
mDF	Modified Davidson's fixative
MHC	Major histocompatibility complex
mRNA	Messenger ribonucleic acid

---

[1] Name of genes are *italicized* and their protein forms are in CAPITAL letters

ND	Not detected
NT	No treatment
PBS	Phosphate buffered saline
PRF	Perforin
qPCR	Quantitative polymerase chain reaction
RIA	Radioimmunoassay
RT-PCR	Reverse transcriptase polymerase chain reaction
sc	Subcutaneous
SEM	Standard error of mean
SSO	Sesame seed oil
TdT	Terminal deoxynucleotidyl transferase
TES	Testosterone-supplemented
TGF	Transforming growth factor
T_m	Melting temperature
TNF	Tumor necrosis factor
TP	Testosterone propionate
TUNEL	Terminal deoxynucleotidyl transferase dUTP nick end-labeling
VEH	Vehicle treatment